BSC

Engineering Change Notice

Complete only applicable items.

1. QA: QA
2. Page 1 of 1

000-00C-DSU0-01000-000-00B-ECN1

3. Document Identifier:	4. Rev.:	5. Title:	6. ECN:
000-00C-DSU0-01000-000-00B	00B	21-PWR Waste Package Side and End Impacts	1

ENG.20050829.0004

7. Reason for Change:

Per LP-3.12Q-BSC, Design Calculations and Analyses, Section 5.1 [2]c,

"The decision of the DEM, PCSA Manager, Criticality Manager, or PCA Manager to issue calcualtions or analyses with a "committed" status will be based on an experienced assessment of the likelihood that the results of the calculation or analysis will change, and the degree of impact those changes will have on designs that support the regulatory submittals or procurement activities, based on the design bounding conservatism."

The status designation of *21-PWR Waste Package Side and End Impacts* (000-00C-DSU0-01000-000-00B) can be changed to "Committed" as the results are not expected to change in such a manner that will affect support of regulatory submittals.

Per LP-3.12Q-BSC, Design Calculations and Analyses, attachment 3, Design Calculation Analysis Cover Sheet, blocks 5 and 9 are not applicable.

DTN: MO0010SPASIL02.002 (Silica Adjusted General Corrosion Rates of Alloy 22 and Titanium Grade 7. Submittal date: 10/10/2000) has been replaced and is not to be used in LA products.

8. Supersedes Change Document:	☐ Yes	If, Yes, Change Doc.: _____	☒ No

9. Change Impact:

Inputs Changed:	☐ Yes	☒ No	Results Impacted:	☐ Yes	☒ No
Assumptions Changed:	☐ Yes	☒ No	Design Impacted:	☐ Yes	☒ No

10. Description of Change: (Address any "Yes" answers)

Add a "Committed" option in Block 8. On the cover sheet and change the "Document Status Designation" from Preliminary to "Committed". Block 8 on the cover sheet should read as follows:

8. Document Status Designation:

☐ Preliminary ☒ Committed ☐ Final ☐ Cancelled

Remove blocks 5 and 9 of the Cover Sheet. Per LP-3.12Q-BSC, Design Calculations and Analyses, attachment 3 - Design Calculation Analysis Cover Sheet, blocks 5 and 9 are not applicable.

Replace Section 3.14 on page 10, with "The thickness of the WP OS is reduced by 2 *mm*. The rationale for this assumption is the following: The OS will degrade due to general corrosion 2 *mm* over 10,000 years (see Reference 27, Table Corrosion, Closure Weld, and Heat Treatment). This assumption is used in Sections 1 and 5.2."

Replace reference 27 on page 32 with "BSC (Bechtel SAIC Company) 2005. *IED Waste Package Processes, Ground Motion Time Histories, and Testing and Materials [Sheet 1 of 1]*. 800-IED-WIS0-00501-000-00A. Las Vegas, Nevada: Bechtel SAIC Company. ACC: ENG.20050406.0004."

11. Originator: (Print/Sign/Date) Tim Schmitt	Tim Schmitt	8/29/05
Checker: (Print/Sign/Date) Michael Mullin		8/29/05
Approved: (Print/Sign/Date) Michael J. Anderson		8/29/05

OFFICE OF CIVILIAN RADIOACTIVE WASTE MANAGEMENT
DESIGN CALCULATION OR ANALYSIS COVER SHEET

1. QA: QA
2. Page 1

3. System: Uncanistered Spent Nuclear Fuel	4. Document Identifier: 000-00C-DSU0-01000-000-00B	5. Verified: ☐ Yes ☒ No

6. Title: 21-PWR Waste Package Side and End Impacts

7. Group: Specialty Analyses and Waste Package Design

8. Document Status Designation:
☒ Preliminary ☐ Final ☐ Superseded ☐ Cancelled

9.

T	F	
☒	☐	1. This product contains no potentially sensitive information.
☐	☒	2. This product contains information that could define a target.
☐	☒	3. This product contains information that could define a specific location.
☐	☒	4. This product contains information that identifies vulnerabilities.

10. Notes/Comments:
N/A

NOTICE OF OPEN CHANGE DOCUMENTS - THIS DOCUMENT IS IMPACTED BY THE LISTED CHANGE DOCUMENTS AND CANNOT BE USED WITHOUT THEM.
----
1) ECN-001, DATED 08/29/2005

Attachments	Total Number of Pages
See Section 8	

RECORD OF REVISIONS

11. No.	12. Reason for Revision	13. Total No. of Pages	14. Last Page No.	15. Originator (Print/Sign)	16. Checker (Print/Sign)	17. Quality Engineering Representative (Print/Sign)	18. Approved/ Accepted (Print/Sign)	19. Date
A	Initial Issue	76	VI-6	V. de la Brosse	S. Mastilovic	D. J. Tunney	M. J. Anderson	01/10/03
B	Added Assumption 3.14 (which was already taken into account in rev A, but not stated). Pages 1, 7, 10, 20 and 32 were affected.	76	VI-6	V. de la Brosse V. dela Brosse	S. Mastilovic	D. Tunney D. Tunney 2/26/2003	M. Anderson M. Anderson	2/26/03

CONTENTS

Page

FIGURES

Page

TABLES

Page

1. PURPOSE

The objective of this calculation is to determine the structural response of a 21-Pressurized Water Reactor (PWR) spent nuclear fuel waste package impacting an unyielding surface. A range of initial velocities and initial angles between the waste package and the unyielding surface is studied. The scope of this calculation is limited to estimating the area of the outer shell (OS) where the residual stress exceeds a given limit (hereafter "damaged area"). The stress limit is defined as a fraction of the yield strength of the OS material, Alloy 22 (SB-575 N06022), at the appropriate temperature.

The design of the 21-PWR waste package used in this calculation is that defined in Reference 8. However, a value of 4 *mm* (Ref. 23, Section 8.1.8) was used for the gap between the inner shell and the OS, and the thickness of the OS was reduced by 2 *mm* (See Assumption 3.14). The sketch in Attachment I provides additional information not included in Reference 8. All obtained results are valid for this design only.

This calculation is associated with the waste package design and was performed by the Specialty Analyses and Waste Package Design Section. The waste package (i.e. uncanistered spent nuclear fuel disposal container) is classified as Quality Level 1 (Ref. 13, page 7). Therefore, the preparation of this document is subject to the *Quality Assurance Requirements and Description* (Ref. 16). AP-3.12Q, *Design Calculations and Analyses* (Ref. 25), was used to perform the calculation and develop the document.

2. METHOD

The finite element calculations were performed using the commercially available ANSYS version (V) 5.4 (Ref. 12) and LS-DYNA finite element codes. ANSYS V5.4 was used for preprocessing, i.e., to create a finite element representation (FER) used subsequently in LS-DYNA V950 (Ref. 14) or LS-DYNA V960.1106 (Ref. 10) to obtain solutions. Hereafter, both versions of LS-DYNA will be referred to as "LS-DYNA", unless the distinction is relevant. The results of these calculations are provided in terms of damaged area in the OS.

3. ASSUMPTIONS

In the course of developing this document, the following assumptions were made regarding the structural calculations for the waste package. These assumptions do not require confirmation.

3.1 Some of the temperature-dependent material properties are not available for Alloy 22, SA-240 S31600 (316 stainless steel [SS]), SA-516 K02700 (A 516 Grade 70 carbon steel [CS]), and SA-240 S30400 (304 SS). Therefore, room-temperature (RT) (20 ℃) density and RT Poisson's ratio are assumed for all materials used. The impact of using RT density and RT Poisson's ratio is anticipated to be small. The rationale for this assumption is that these material properties do not change significantly at the temperatures relevant in this calculation and do not have a significant effect on the results. This assumption is used in Section 5.1 and corresponds to paragraph 5.2.8.4 of Ref. 20.

3.2 Strain-rate dependent material properties are not available for the materials used. Therefore, the material properties obtained under static loading conditions are assumed for all materials used. The impact of using material properties obtained under static loading conditions is anticipated to be small. The rationale for this assumption is that the mechanical properties of subject materials do not significantly change at the peak strain rates reached in the course of the impacts (See Figure 1, peak effective plastic strain rate = 0.25/0.005 = 50 s^{-1}. [The presented elements are characterized by the highest effective plastic strain at the end of the simulation.] For this value of strain rate, Reference 22, figures 27 through 31, pages 42 through 46, shows no significant change of the tensile strength of materials.). This assumption is used in Section 5.1 and corresponds to paragraph 5.2.5 of Ref. 20.

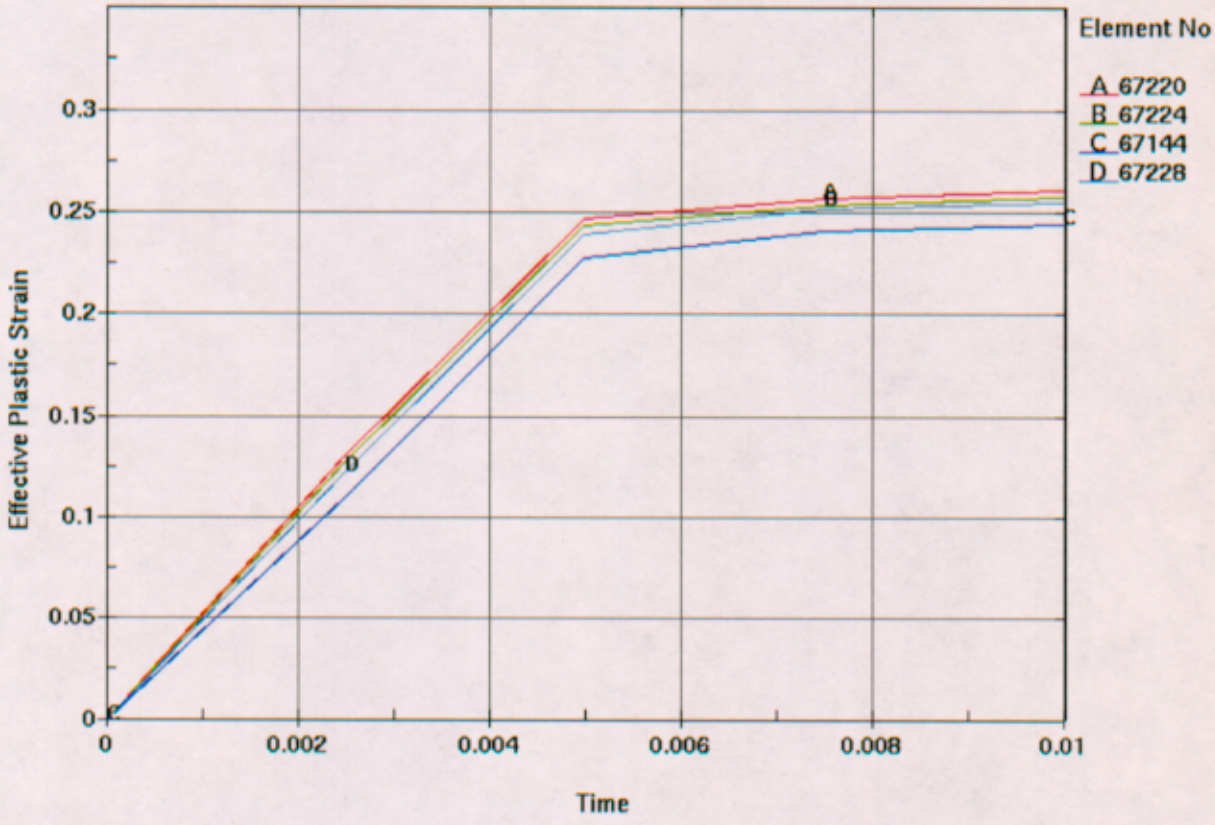

Figure 1: Strain Rate in the Outer Shell during the Impact (150 °C, α=8°, v=20 *m/s*)

3.3 The Poisson's ratio of Alloy 22 is not available in literature. Therefore, the Poisson's ratio of Alloy 625 (SB-443 N06625) is assumed for Alloy 22. The impact of this assumption is anticipated to be negligible. The rationale for this assumption is that the chemical compositions of Alloy 22 and Alloy 625 are similar (Ref. 4, Section II, Part B, SB-575, Table 1 and Ref. 2, page 143, respectively). This assumption is used in Section 5.1.1 and corresponds to paragraph 5.2.8.2 of Ref. 20.

3.4 The uniform strain of Alloy 22 and 316 SS are not available in literature. Therefore it is conservatively assumed that the uniform strain is 90% of the elongation. The rationale for this assumption is the character of the stress-strain curve for Alloy 22 and 316 SS (Ref. 19

and Ref. 7, page 304, respectively). This assumption is used in Section 5.1.2 and corresponds to paragraph 5.2.8.6 of Ref. 20.

3.5 The uniform strain of 304 SS is not available in literature. Therefore it is conservatively assumed that the uniform strain is 75% of the elongation. The rationale for this assumption is the character of the stress-strain curve for 304 SS (Ref. 7, page 295). This assumption is used in Section 5.1.2 and corresponds to paragraph 5.2.14.1 of Ref. 20.

3.6 The uniform strain of A 516 Grade 70 CS is not available in literature. Therefore it is conservatively assumed that the uniform strain is 50% of the elongation. The rationale for this assumption is the character of the stress-strain curve for A 36 CS (Ref. 7, page 189) that has similar chemical composition to A 516 Grade 70 CS (see Ref. 4, Section II, Part A, SA-516/SA-516M, Table 1 and SA-36/SA-36M, Table 2 for chemical compositions of A 516 Grade 70 CS and A 36 CS, respectively). This assumption is used in Section 5.1.2 and corresponds to paragraph 5.2.11.1 of Ref. 20.

3.7 The change of minimum elongation with increase of temperature for 316 SS is not available in literature. Therefore, the magnitude of this change at elevated temperature is assumed, based on the relative change of typical elongation for said materials available in vendor catalogues (Ref. 1, page 8). The rationale for this assumption is that the relative change of typical elongation should be bounding for the relative change of minimum elongation. This assumption is used in Section 5.1.1 and corresponds to paragraph 5.2.8.5 of Ref. 20.

3.8 The exact geometry of the PWR fuel assemblies is simplified for the purpose of this calculation in such a way that its total mass is assumed to be distributed within a bar of square cross section with uniform mass density. The rationale for this assumption is to simplify the FER, while providing a set of bounding results. This assumption is used in Section 5.3.1 and corresponds to paragraph 5.2.9.1 of Ref. 20.

3.9 The material used to represent the fuel assemblies is 304 SS. The rationale for this assumption is that the end fittings are made of 304 SS (Ref. 24, Section 2.1, page 2-4) and they are the parts that will come in contact with other components. This assumption is used in Sections 5.1.1 and 5.3.1 and corresponds to paragraph 5.2.9.2 of Ref. 20.

3.10 The following design parameters are assumed for the PWR spent nuclear fuel assemblies to be loaded into a 21-PWR waste package: mass = 773.4 *kg*, width = 216.9 *mm*, and length = 4407 *mm*. The rationale for this assumption is that these parameters correspond to the B&W (Babcock & Wilcox) 15x15 fuel assembly, which is the heaviest PWR fuel assembly available (Ref. 9, Table 2). The mass of the B&W fuel assembly has been increased by 25 *lbs* (11.4 *kg*) to account for variations in fuel assembly mass. It should be noted that South Texas PWR fuel assemblies will not be disposed in the 21-PWR waste package, and are therefore excluded from this assumption. This assumption is used in Section 5.3.1 and corresponds to paragraph 5.2.9.5 of Ref. 20.

3.11 The target surface was assumed to be unyielding (i.e. elastic), and A 36 CS was used to represent it in the FER. The rationale for this assumption was that this material has a high modulus of elasticity compared to concrete and it is known that the use of an unyielding surface with high modulus of elasticity would ensure conservative results in terms of stresses in the waste package. This assumption is used in Section 5.1.1 and 5.3.1 and corresponds to paragraph 5.2.8.1 of Ref. 20.

3.12 The friction coefficients for contacts occurring between the materials used in this calculation are not available in literature. It is, therefore, assumed that the dynamic (sliding) friction coefficient is 0.5 for all contacts. The rationale for this assumption is that this friction coefficient represents the reasonable typical value for most metal-on-metal contacts (see Ref. 6, Table 3.2.1, p. 3-26). This assumption is used in Section 5.3.1.

3.13 The variation of functional friction coefficient between the static and dynamic value as a function of relative velocity of the surfaces in contact (see Ref. 18, p. 6.9) is not available in literature for the materials used in this calculation. Therefore, the effect of relative velocity of the surfaces in contact is neglected in this calculation by assuming that the functional friction coefficient and static friction coefficient are both equal to the dynamic friction coefficient. The impact of this assumption on results presented in this document is anticipated to be negligible. The rationale for this conservative assumption is that it provides a bounding set of results by minimizing the friction coefficient within the given finite element analysis framework. This assumption is used in Section 5.3.1 and corresponds to paragraph 5.2.14.4 of Ref. 20.

3.14 The thickness of the WP OS is reduced by 2 *mm*. The rationale for this assumption is the following: The OS will degrade due to general corrosion during the regulatory period. The thickness reduction of 2 mm over the regulatory period of 10,000 years corresponds to a general corrosion rate of $2 \cdot 10^{-4}$ *mm/yr*. According to Reference 27 (See file WDgA22Sand_all), the general corrosion rate of $2 \cdot 10^{-4}$ *mm/yr* exceeds the 97th percentile of general corrosion rate for Alloy 22. This assumption is used in Sections 1 and 5.2.

4. USE OF COMPUTER SOFTWARE

One of the finite element analysis (FEA) computer codes used for this calculation is ANSYS V5.4 (Ref. 12), which was obtained from Software Configuration Management in accordance with appropriate procedures, and is identified by the Computer Software Configuration Item number 30040 V5.4. ANSYS V5.4 is a qualified, commercially available FEA code and is appropriate for creating a mesh as performed in this calculation. The calculations using the ANSYS V5.4 software were executed on the Hewlett-Packard (HP) 9000 series UNIX workstation (operating system HP-UX B.10.20) identified with YMP (Yucca Mountain Project) tag number 117161 located in Las Vegas, NV. The ANSYS evaluation performed for this calculation is fully within the range of the validation performed for the ANSYS V5.4 code. Access to the code was granted by the Software Configuration Management in accordance with the appropriate procedures.

The input files (identified by .inp file extensions) and output files (identified by .out file extensions) for ANSYS V5.4 are provided in Attachment IV.

The other FEA computer code used for this calculation is Livermore Software Technology Corporation LS-DYNA V950 (Ref. 14) and V960.1106 (Ref. 10), which was obtained from the Software Configuration Management in accordance with appropriate procedures, and is identified by the Software Tracking Numbers 10300-950-00 and 10300-960.1106-00. LS-DYNA is a qualified, commercially available finite element code and both versions are appropriate for structural calculations of waste packages as performed in this calculation. These two versions of the LS-DYNA code perform the same way for the simulations run in this calculation, and both versions were used in order to take advantage of all the available computing resources. The calculations using LS-DYNA V950 were executed on the HP 9000 series UNIX workstations (operating system HP-UX B.10.20) identified with YMP tag numbers 114193, 114434, 700888, 117161 and 117162, located in Las Vegas, NV. The calculations using LS-DYNA V960.1106 were executed on the HP 9000 series UNIX workstation (operating system HP-UX 11.0) identified with YMP tag number 151325, 151324, 151664, 151665, 150690, 150691, 150688 and 150689 located in Las Vegas, NV. The LS-DYNA evaluations performed for this calculation are fully within the range of the validation performed for both versions of the LS-DYNA code. Access to the code was granted by the Software Configuration Management in accordance with the appropriate procedures.

LS-POST V2 was used to post-process the results. As per AP-SI.1Q, Section 2.1.2 (Ref. 26), this software is exempt from the requirements of this same procedure.

The input files (identified by .k and .inc file extensions) and output files (filenames starting with "d3hsp") for LS-DYNA are provided in Attachment IV. The geometry used in each run is defined in Attachment III, Table III-1. The binary graphic files (name similar to d3plot) containing the first and last time steps of each calculation are also provided, for information only. They can be viewed using LS-POST V2.

5. CALCULATION

5.1 MATERIAL PROPERTIES

Material properties used in this calculation are listed in this section. Some of the temperature-dependent material properties are not available for the materials used in this calculation. Therefore, RT density and RT Poisson's ratio are used for all materials (see Assumption 3.1). Furthermore, all material properties listed below were obtained under static loading conditions (see Assumption 3.2).

The values of each material property are needed at 100 ℃ (212 ℉), 150 ℃ (302 ℉) and 200 ℃ (392 ℉). The material properties at these temperatures are obtained by linear interpolation of the corresponding material properties presented in Table 1, by using the formula:

$$p = p(T) = p_l + \left(\frac{T - T_l}{T_u - T_l}\right) \cdot (p_u - p_l)$$

Subscripts u and l denote the upper and lower bounding values of generic material property p at the corresponding bounding temperatures.

Table 1. Material Properties Cited in References

		Temperature (℃ - ℉)	Value	Reference
Alloy 22	Yield Strength	93 - 200	338 *MPa*	Ref. 21, Values for Plates, ¼ - ¾ in. (6.4 – 19.1 mm) thick
		204 - 400	283 *MPa*	
	Tensile Strength	93 - 200	738 *MPa*	Ref. 21, Values for Plates, ¼ - ¾ in. (6.4 – 19.1 mm) thick
		204 - 400	676 *MPa*	
	Elongation	93 - 200	65 %	Ref. 21, Values for Plates, ¼ - ¾ in. (6.4 – 19.1 mm) thick
		204 - 400	66 %	
	Modulus of Elasticity	93 - 200	203 *GPa*	Ref. 21, Values for Sheets, 0.028 – 0.125 in. (0.713-3.2 mm) thick
		204 - 400	196 *GPa*	

		Temperature (°C - °F)	Value	Reference
316 SS	Yield Strength	93 - 200	25.9 *ksi*	Ref. 4, Section II, Part D, Table Y-1
		121 - 250	24.6 *ksi*	
		149 - 300	23.4 *ksi*	
		204 - 400	21.4 ksi	
	Tensile Strength	93 - 200	75.0 *ksi*	Ref. 4, Section II, Part D, Table U
		149 - 300	72.9 *ksi*	
		204 - 400	71.9 *ksi*	
	Typical Elongation	20 - 68	68.0 %	Ref. 1, page 8
		93 - 200	54.0 %	
		204 - 400	51.0 %	
	Modulus of Elasticity	93 - 200	27.6 e6 *psi*	Ref. 4, Section II, Part D, Table TM-1
		149 - 300	27.0 e6 *psi*	
		204 - 400	26.5 e6 *psi*	
304 SS	Yield Strength	93 - 200	25.0 *ksi*	Ref. 4, Section II, Part D, Table Y-1
		121 - 250	23.6 *ksi*	
		149 - 300	22.4 *ksi*	
		204 - 400	20.7 ksi	
	Tensile Strength	93 - 200	71.0 *ksi*	Ref. 4, Section II, Part D, Table U
		149 - 300	66.2 *ksi*	
		204 - 400	64.0 *ksi*	
	Modulus of Elasticity	93 - 200	27.6 e6 *psi*	Ref. 4, Section II, Part D, Table TM-1
		149 - 300	27.0 e6 *psi*	
		204 - 400	26.5 e6 *psi*	

		Temperature (°C - °F)	Value	Reference
516 CS	Yield Strength	93 - 200	34.8 *ksi*	Ref. 4, Section II, Part D, Table Y-1
		121 - 250	34.2 *ksi*	
		149 - 300	33.6 *ksi*	
		204 - 400	32.5 ksi	
	Tensile Strength	93 - 200	70.0 *ksi*	Ref. 4, Section II, Part D, Table U
		149 - 300	70.0 *ksi*	
		204 - 400	70.0 *ksi*	
	Modulus of Elasticity	93 - 200	28.8 e6 *psi*	Ref. 4, Section II, Part D, Table TM-1
		149 - 300	28.3 e6 *psi*	
		204 - 400	27.7 e6 *psi*	

5.1.1 Material properties at 100 °C, 150 °C and 200 °C

SB-575 N06022 (Alloy 22) (OS, OS lids, extended OS lid, upper and lower trunnion collar sleeves, and inner shell support ring):

- Density = 8690 kg/m^3 (0.314 lb/in^3) (at RT) (Ref. 21, Paragraph "Properties of Alloy 22")

- Yield strength = 335 *MPa* at 100 °C
  Yield strength = 310 *MPa* at 150 °C
  Yield strength = 285 *MPa* at 200 °C

- Tensile strength = 734 *MPa* at 100 °C
  Tensile strength = 706 *MPa* at 150 °C
  Tensile strength = 678 *MPa* at 200 °C

- Elongation = 0.65 at 100 °C
  Elongation = 0.66 at 150 °C
  Elongation = 0.66 at 200 °C

- Poisson's ratio = 0.278 (at RT) (Ref. 21, paragraph "Mechanical Properties"; See Assumption 3.3)

- Modulus of elasticity = 203 *GPa* at 100 °C
  Modulus of elasticity = 199 *GPa* at 150 °C
  Modulus of elasticity = 196 *GPa* at 200 °C

SA-240 S31600 (316 SS) (inner shell, inner shell lids, shear ring and shell interface ring):

- Density = 7980 *kg/m*^{3} (at RT) (Ref. 5, Table X1.1, p. 7)

- Yield strength = 177 *MPa* (25.6 *ksi*) at 100 ℃
  Yield strength = 161 *MPa* (23.4 *ksi*) at 150 ℃
  Yield strength = 149 *MPa* (21.6 *ksi*) at 200 ℃

- Tensile strength = 515 *MPa* (74.7 *ksi*) at 100 ℃
  Tensile strength = 503 *MPa* (72.9 *ksi*) at 150 ℃
  Tensile strength = 496 *MPa* (72.0 *ksi*) at 200 ℃

- Minimum elongation = 0.40 (at RT) (Ref. 4, Section II, Part A, SA-240, Table 2).
  The change of minimum elongation with increase of temperature for 316 SS is not available in literature. Therefore, the magnitude of this change is estimated based on the relative change of typical elongation (see Assumption 3.7 and Ref. 1) and applied to the value of the minimum elongation at RT (see Table 2).

Table 2. Change in Typical Elongation for 316 SS between RT and High Temperatures

Temperature (°C)	RT	100	150	200
Typical Elongation (%)	0.68	0.538	0.525	0.511
Change in Typical Elongation between RT and Higher Temperature (%)	N/A	-21	-23	-25

Minimum elongation for 316 SS at 100 ℃: 0.4 · (1-0.21) = 0.32
Minimum elongation for 316 SS at 150 ℃: 0.4 · (1-0.23) = 0.31
Minimum elongation for 316 SS at 200 ℃: 0.4 · (1-0.25) = 0.30

- Poisson's ratio = 0.30 (at RT) (Ref. 2, Figure 15, p. 755)

- Modulus of elasticity = 190 *GPa* (27.5·10^6 *psi*) at 100 ℃
  Modulus of elasticity = 186 *GPa* (27.0·10^6 *psi*) at 150 ℃
  Modulus of elasticity = 183 *GPa* (26.6·10^6 *psi*) at 200 ℃

SA-240 S30400 (304 SS) (PWR fuel assemblies, see Assumption 3.9):

- Yield strength = 170 *MPa* (24.7 *ksi*) at 100 ℃
  Yield strength = 154 *MPa* (22.4 *ksi*) at 150 ℃
  Yield strength = 143 *MPa* (20.8 *ksi*) at 200 ℃

- Tensile strength = 485 *MPa* (70.4 *ksi*) at 100 ℃
  Tensile strength = 456 *MPa* (66.2 *ksi*) at 150 ℃
  Tensile strength = 443 *MPa* (64.2 *ksi*) at 200 ℃

- Elongation = 0.40 (at RT) (Ref. 4, Section II, SA-240, Table 2)

- Poisson's ratio = 0.29 (at RT) (Ref. 2, Figure 15, p. 755)

- Modulus of elasticity = 190 *GPa* ($27.5 \cdot 10^6$ *psi*) at 100 ℃
  Modulus of elasticity = 186 *GPa* ($27.0 \cdot 10^6$ *psi*) at 150 ℃
  Modulus of elasticity = 183 *GPa* ($26.6 \cdot 10^6$ *psi*) at 200 ℃

SA-516 K02700 (A 516 Grade 70 CS) (basket guides and stiffeners, fuel basket plates and tubes):

- Density = 7850 kg/m^3 (at RT) (Ref. 4, Section II, Part A, SA-20/SA-20M, Section 14.1) (Material supplied to American Society for Testing and Materials [ASTM] A 516/A 516M-90 specification shall conform to specification ASTM A 20/A 20M [see Ref. 4, Section II, SA-516/SA-516M, section 3.1])

- Yield strength = 239 *MPa* (34.7 *ksi*) at 100 ℃
  Yield strength = 232 *MPa* (33.6 *ksi*) at 150 ℃
  Yield strength = 225 *MPa* (32.6 *ksi*) at 200 ℃

- Tensile strength = 483 *MPa* (70 *ksi*) at 100 ℃
  Tensile strength = 483 *MPa* (70 *ksi*) at 150 ℃
  Tensile strength = 483 *MPa* (70 *ksi*) at 200 ℃

- Elongation = 0.21 (at RT) (Ref. 4, Section II, Part A, SA-516/SA-516M, Table 2)

- Poisson's ratio = 0.3 (at RT) (Ref. 3, p. 374)

- Modulus of elasticity = 198 *GPa* ($28.7 \cdot 10^6$ *psi*) at 100 ℃
  Modulus of elasticity = 195 *GPa* ($28.3 \cdot 10^6$ *psi*) at 150 ℃
  Modulus of elasticity = 191 *GPa* ($27.7 \cdot 10^6$ *psi*) at 200 ℃

SA-36 K02600 (A 36 CS) (unyielding surface, see Assumption 0):

- Density = 7860 kg/m^3 (at RT) (Ref. 5, Table X1.1, p. 7)

- Poisson's ratio = 0.30 (at RT) (Ref. 3, p. 374)

- Modulus of elasticity = 203 *GPa* ($29.5 \cdot 10^6$ *psi*) (at RT) (Ref. 4, Section II, Part D, Table TM-1)

5.1.2 Calculations for True Measures of Ductility

The material properties in Section 5.1 refer to engineering stress and strain definitions: $s = P/A_0$ and $e = L/L_0 - 1$, where P stands for the force applied during static tensile test, L is the deformed-specimen length, and L_0 and A_0 are original length and cross-sectional area of specimen,

respectively. The engineering stress-strain curve does not give a true indication of the deformation characteristics of a material during plastic deformation since it is based entirely on the original dimensions of the specimen. In addition, ductile metal that is pulled in tension becomes unstable and necks down during the test. Hence, LS-DYNA FEA code requires input in terms of true stress and strain definition: $\sigma = P/A$ and $\varepsilon = \ln (L/L_0)$ (see Ref. 15, Chapter 9).

The relationships between the true stress and strain definitions and engineering stress and strain definitions, $\sigma = s\,(1+e)$ and $\varepsilon = \ln (1+e)$ (see Ref. 15, Chapter 9), can be readily derived based on constancy of volume ($A_0 \cdot L_0 = A \cdot L$) and strain homogeneity during plastic deformation. These expressions are applicable only in the hardening region of stress-strain curve that is limited by the onset of necking.

The following parameters are used in the subsequent calculations:

$s_y \approx \sigma_y$ = yield strength

s_u = engineering tensile strength

σ_u = true tensile strength

$e_y \approx \varepsilon_y$ = strain corresponding to yield strength ($=\frac{\sigma_y}{E}$)

E = modulus of elasticity

e_u = engineering strain corresponding to tensile strength (engineering uniform strain)

ε_u = true strain corresponding to tensile strength (true uniform strain)

In the absence of uniform strain data in available literature, it needs to be estimated based on the character of stress-strain curves and elongation (strain corresponding to rupture of the tensile specimen).

The stress-strain curves for Alloy 22 and 316 SS do not manifest pronounced softening phase (see Ref. 19 and Ref. 7, page 304). Therefore, the elongation, reduced by 10% to take into account the specimen-failure part of the stress-strain curve (see Assumption 3.4), can be used in place of uniform strain for these two materials.

For Alloy 22:

$e_u = 0.9 \cdot elongation = 0.9 \cdot 0.65 = 0.59, \varepsilon_u = \ln (1+e_u) = \ln (1+0.59) = 0.46$ and

$\sigma_u = s_u \cdot (1+e_u) = 734 \cdot (1+0.59) = 1170\ MPa$ at 100 °C

$e_u = 0.9 \cdot 0.66 = 0.59, \varepsilon_u = \ln (1+0.59) = 0.46$ and $\sigma_u = 706 \cdot (1+0.59) = 1120\ MPa$ at 150 °C

$e_u = 0.9 \cdot 0.66 = 0.59, \varepsilon_u = \ln (1+0.59) = 0.46$ and $\sigma_u = 678 \cdot (1+0.59) = 1080\ MPa$ at 200 °C

For 316 SS:

$e_u = 0.9 \cdot 0.4 \cdot (1-0.21) = 0.28, \varepsilon_u = \ln (1+0.28) = 0.25$ and $\sigma_u = 515 \cdot (1+0.28) = 659\ MPa$ at 100 °C

Originator: VB 02/26/03 Checker: JM 02/26/03

$e_u = 0.9 \cdot 0.4 \cdot (1 - 0.23) = 0.28, \varepsilon_u = \ln(1 + 0.28) = 0.25$ and $\sigma_u = 503 \cdot (1 + 0.28) = 644$ *MPa* at 150 ℃
$e_u = 0.9 \cdot 0.4 \cdot (1 - 0.25) = 0.27, \varepsilon_u = \ln(1 + 0.27) = 0.24$ and $\sigma_u = 496 \cdot (1 + 0.27) = 630$ *MPa* at 200 ℃

Contrary to the two previous cases, the stress-strain curve for 304 SS exhibits pronounced three-stage (elastic-hardening-softening) deformation character. The uniform strain is, therefore, estimated to be 75% of elongation based on the available stress-strain curves (see Assumption 3.5).

Hence $e_u = 0.75 \cdot \text{elongation} = 0.75 \cdot 0.40 = 0.30$. The true uniform strain is therefore

$$\varepsilon_u = \ln(1 + e_u) = \ln(1 + 0.30) = 0.26$$

The true tensile strength is

$\sigma_u = s_u \cdot (1 + e_u) = 485 \cdot (1 + 0.30) = 630\ MPa$ (at 100 ℃)
$\sigma_u = s_u \cdot (1 + e_u) = 456 \cdot (1 + 0.30) = 593\ MPa$ (at 150 ℃)
$\sigma_u = s_u \cdot (1 + e_u) = 443 \cdot (1 + 0.30) = 576\ MPa$ (at 200 ℃)

Finally, the stress-strain curve for A 516 Grade 70 CS exhibits stress-strain curve character typical for CS. The uniform strain is estimated to be 50 % of elongation based on the available stress-strain curves for A 36 CS (see Assumption 3.6).

Hence $e_u = 0.5 \cdot \text{elongation} = 0.5 \cdot 0.21 = 0.11$. The true uniform strain is therefore

$$\varepsilon_u = \ln(1 + e_u) = \ln(1 + 0.11) = 0.10$$

Since the engineering tensile strength of A 516 Grade 70 CS does not vary with temperature for the temperature range of interest, the true tensile strength is

$\sigma_u = s_u \cdot (1 + e_u) = 483 \cdot (1 + 0.11) = 536\ MPa$ (at 100 ℃, at 150 ℃, and at 200 ℃)

5.1.3 Calculations for Tangent Moduli

As previously discussed, the results of this simulation are required to include elastic and plastic deformations for Alloy 22, 316 SS, A 516 Grade 70 CS, and 304 SS. When the materials are driven into the plastic range, the slope of stress-strain curve continuously changes. A ductile failure is preceded by a protracted regime of hardening (and possibly softening) and substantial accumulation of inelastic strains. Thus, a simplification for this curve was needed to incorporate plasticity into the FER. A standard approximation commonly used in engineering is to use a straight line that connects the yield point and the ultimate tensile strength point of the material. The tangent modulus (E_t) is a parameter used in the subsequent calculations in addition to those defined in Section 5.1. The tangent modulus represents the slope of the stress-strain curve in the plastic region; it can be calculated using the following expression:

$E_t = (\sigma_u - \sigma_y)/(\varepsilon_u - \sigma_y/E)$

and the material properties given in Sections 5.1.1 and 5.1.2. For example, for Alloy 22 at RT, $E_t = (1.17 - 0.335) / (0.46 - 335 \cdot 10^6 / 203 \cdot 10^9) = 1.82$ *GPa*. The values of tangent moduli used in this calculation are presented in Table 3.

Table 3. Tangent Moduli at Three Different Temperatures

Material	Tangent Modulus (GPa)		
	100 °C	150 °C	200 °C
Alloy 22	1.82	1.77	1.73
316 SS	1.94	1.94	2.02
304 SS	1.77	1.69	1.67
A 516 CS	3.01	3.08	3.15

5.2 INITIAL CONDITIONS FOR THE DROPS

The initial conditions for the impacts are as follows:

End impacts: Initial velocity = 1, 2, 4, 6, 10 and 20 m/s
Angle between the axis of the waste package and the vertical (α, see Figure 2) = 0, 1, 5 and 8 degrees.

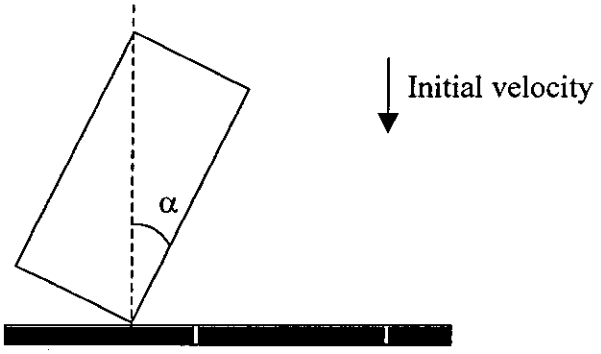

Figure 2: Initial Position of the Waste Package for the End Impacts

Side impacts: Initial velocity = 1, 2, 4, 6, 10 and 20 m/s
Angle between the axis of the waste package and the horizontal (α, see Figure 3) = 0, 1 and 8 degrees.

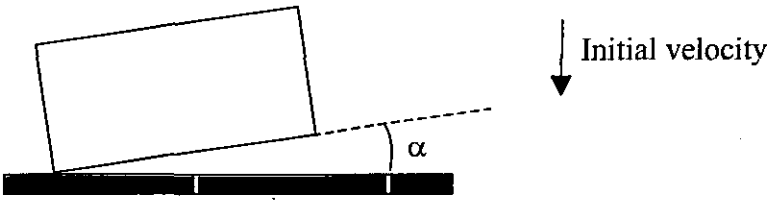

Figure 3: Initial Position of the Waste Package for the Side Impacts

5.3 FINITE ELEMENT REPRESENTATION

5.3.1 Description of the Finite Element Representation

A three-dimensional FER of the waste package was developed in ANSYS V5.4 using the dimensions provided in Attachment I. The internal structure of the waste package was simplified in several ways. The PWR fuel assemblies were reduced to bars of square cross section of uniform mass density, and assumed to be constructed of 304 SS (Assumptions 3.8 and 3.9). Also, the geometric dimensions of the fuel assemblies were modified to keep the value of the gap between the fuel assemblies and the nearest element consistent with the gap defined using the elements found in Attachment I and Assumption 3.10. Finally, the mass density of the fuel assemblies was modified so that the total mass of the loaded waste package equals the mass given in Attachment I. Furthermore, in the end impacts, the fuel basket tubes were not represented in the FER.

The thickness of the OS was reduced by 2 mm on its outer surface (see Assumption 3.14).

The target surface was conservatively assumed to be unyielding (Assumption 3.11), and its density was rounded up to 8000 kg/m^3.

A static and dynamic friction coefficient of 0.5 was taken into account between all parts (Assumptions 3.12 and 3.13).

5.3.2 Gap Between the Inner and the Outer Shell

Reference 8 indicates a tight fit between the inner shell and the OS. However, Reference 23 describes the fit between the two shells as "loose" (Section 8.1.8). In order to determine which configuration was more conservative for this study, two of the cases (end impacts, α=5°, v=4 *m/s* and α=1°, v=2 *m/s*, both at 150 ℃) were run with each geometry (tight fit and maximum loose fit). The results are presented in Attachment II, and show that the configuration with a 4-*mm* gap is conservative. Consequently, all other cases were run with a 4-*mm* gap between the inner shell and the OS.

5.3.3 Mesh Refinement Study

The mesh of the FER was generated and refined in the contact region according to standard engineering practice. This mesh was then further refined in the higher-stress region to verify that the

results are not mesh sensitive. The volume and stress for the element of highest stress (at the end of the calculation) were compared, according to the method described in Reference 20, Section 6.2.3. The results are presented in Attachment III. Since the criterion defined in Reference 20, Section 6.2.3, is met, the accuracy and representativeness of the mesh are deemed acceptable for this calculation.

5.3.4 System Damping for the Relaxation Period

In order to capture the residual stresses efficiently, system damping (see Ref. 17, Section 28.2) is applied after the first impact between the waste package and the unyielding surface (i.e. after 0.03 *s*), until the termination of the simulation (i.e. for 0.02 *s*). The value used for the damping coefficient is 200. This value was determined after running 3 test cases: one with a damping coefficient of 0 (no system damping), the second with a coefficient of 50, and the third with a coefficient of 200. The variation of maximum 1st principal stress with time is presented in Figure 4. Based on these results, a damping coefficient of 200 was considered adequate for this calculation.

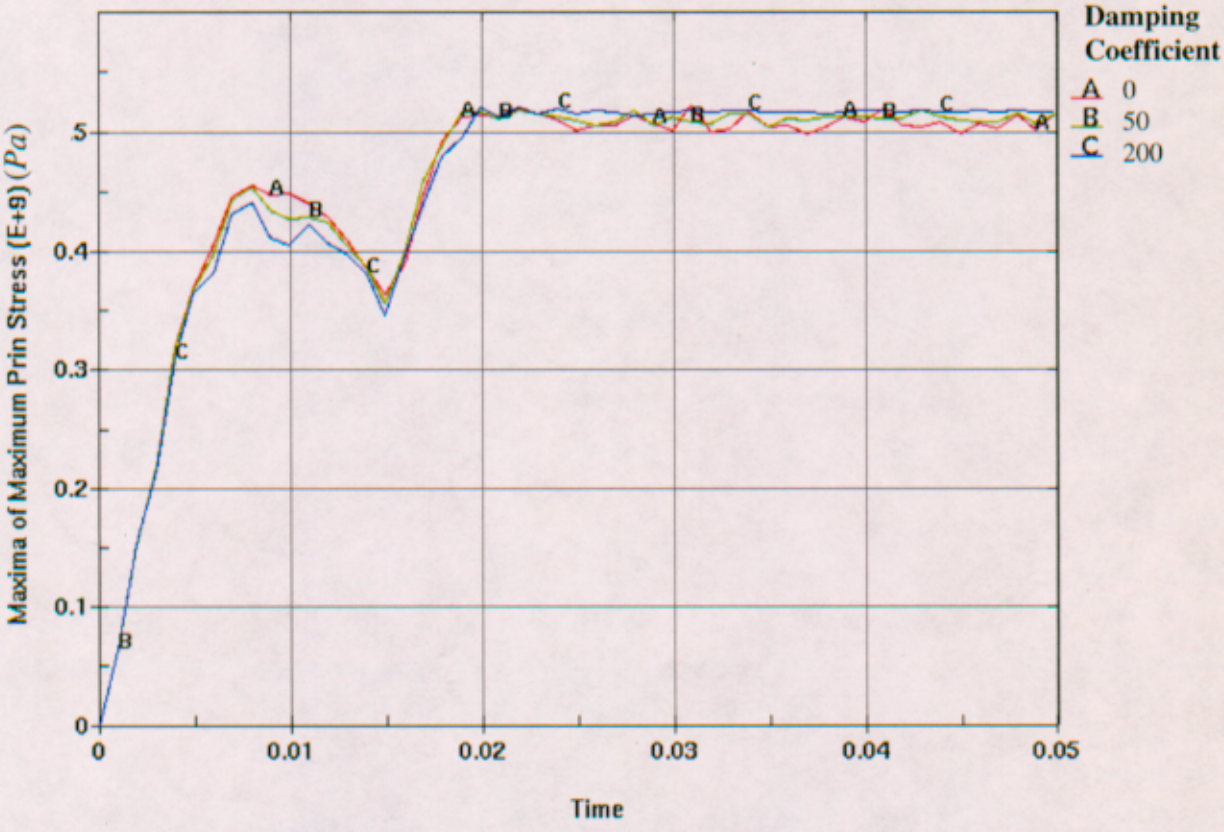

Figure 4: Variation of Maximum 1st Principal Stress with Time for Different Values of Damping Coefficient

5.4 POST-PROCESSING

For clarity, the "damaged area" is called "damage" throughout this section. Also, the elements where the residual 1st principal stress is above the limit are called damaged elements (if the stress is below the limit, they are called undamaged elements).

Originator: VB. 02/26/03 Checker: JM 02/26/03

In order to determine the damage, the results obtained in the last time step of each simulation are post-processed as follows: the undamaged elements of the OS are "blanked out" (dark blue color in Figure 5). The damage on the OS outer surface is estimated by calculating the area of each damaged element's face that coincides with the OS outer surface. Since the number of damaged elements can be very large, the area of neighboring elements is calculated as the area of a rectangle containing these elements. However, if the damaged elements do not form a perfect rectangle, outside elements can be accounted for as shown in Figure 5 (count these 2 elements/do not count these 2 elements).

Once the damage on the outer surface of the OS is calculated, the inner surface of the OS is treated in the same way. However, if the damage on the outer and inner surfaces overlap, the corresponding area is counted only once.

Finally, in the area where the OS and the OS bottom lid join, only the more damaged side of the junction is taken into account. For example, in Figure 6, the damage in the area A is larger than the damage in area B. Thus, only the damage in area A will be taken into account to avoid excessive conservatism.

The angle defining the maximum extension of the damage in the circumferential direction (see Figure 5) is also reported in Section 6.

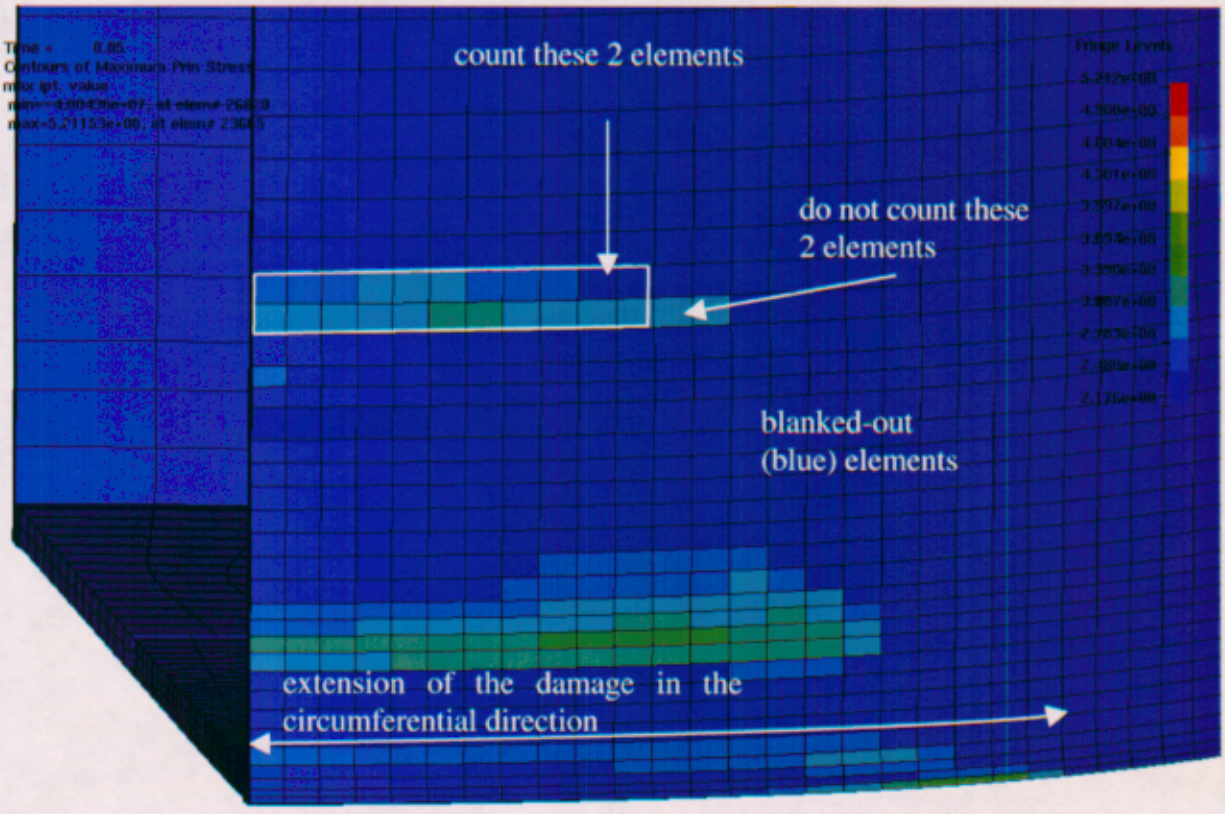

Figure 5: Determination of the damaged area (example)

Originator: VB. 02/26/03 Checker: JM 02/26/03

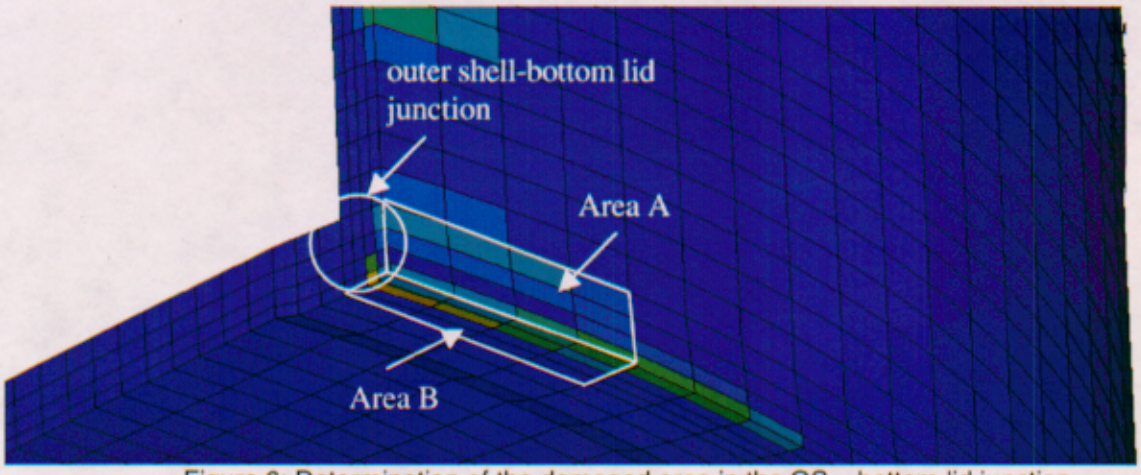

Figure 6: Determination of the damaged area in the OS – bottom lid junction

6. RESULTS

The running time (0.05 *s*) was chosen so that the waste package had enough time to bounce off the unyielding surface, and for the residual 1st principal stress to be established. At the end of the calculation, the damaged area in the OS was calculated for each configuration, using LS-POST V2 (see Section 5.4).

Tables 4 to 8 list the damaged area and the angle defining its circumferential extension for the different configurations studied and different limits of stress.

Table 4. Damaged Area (m^2) and Associated Angle (*degree*) at 150 °C, Stress Limit = 80% of Yield Strength

		End Impacts: Angle between the axis of the Waste Package and the Vertical (*degree*)				Side Impacts: Angle between the axis of the Waste Package and the Horizontal (*degree*)		
		0	1	5	8	0	1	8
Initial Velocity (*m/s*)	1	0	0.0033 ±17	0.0017 ±10	0.0011 ±8	0	0	0
	2	0	0.0221 ±41	0.0109 ±25	0.0113 ±23	0.0013 ±5	0.0020 ±5	0
	4	0.0244 ±180	0.0734 ±75	0.0850 ±42	0.0716 ±37	0.0156 ±15	0.0063 ±13	0.0068 ±15
	6	0.0276 ±180	0.1665 ±108	0.1556 ±53	0.1082 ±46	0.0379 ±20	0.0204 ±17	0.0153 ±22
	10	0.0254 ±180	0.0834 ±171	0.1280 ±75	0.1061 ±61	0.0715 ±32	0.0283 ±24	0.0508 ±26
	20	0.0542 ±180	0.0698 ±180	0.1916 ±62	0.2332 ±72	0.6232 ±90	0.1560 ±37	0.2193 ±90

Table 5. Damaged Area (m^2) and Associated Angle (*degree*) at 150 °C, Stress Limit = 90% of Yield Strength

		End Impacts: Angle between the axis of the Waste Package and the Vertical (*degree*)				Side Impacts: Angle between the axis of the Waste Package and the Horizontal (*degree*)		
		0	1	5	8	0	1	8
Initial Velocity (*m/s*)	1	0	0.0018 ±13	0.0011 ±8	0.0009 ±6	0	0	0
	2	0	0.0112 ±39	0.0056 ±25	0.0066 ±23	0.0004 ±3	0.0011 ±5	0
	4	0.0244 ±180	0.0212 ±75	0.0508 ±42	0.0367 ±37	0.0046 ±13	0.0015 ±11	0.0006 ±13
	6	0.0244 ±180	0.0549 ±103	0.0767 ±53	0.0501 ±44	0.0176 ±20	0.0092 ±17	0.0081 ±21
	10	0.0254 ±180	0.0264 ±164	0.0610 ±75	0.0379 ±61	0.0257 ±30	0.0157 ±22	0.0160 ±24
	20	0.0278 ±180	0.0403 ±180	0.1008 ±64	0.1279 ±68	0.3103 ±64	0.0404 ±30	0.1040 ±67

Table 6. Damaged Area (m^2) and Associated Angle (*degree*) at 150 °C, Stress Limit = 100% of Yield Strength

		End Impacts: Angle between the axis of the Waste Package and the Vertical (degree)			
		0	1	5	8
Initial Velocity (*m/s*)	1	0	0.0016 ±11	0.0009 ±6	0.0006 ±5
	2	0	0.0051 ±37	0.0037 ±23	0.0044 ±21
	4	0	0.0103 ±72	0.0217 ±39	0.0143 ±35
	6	0.0244 ±180	0.0185 ±101	0.0302 ±51	0.0273 ±44
	10	0.0254 ±180	0.0211 ±149	0.0227 ±73	0.0150 ±59
	20	0	0.0120 ±74	0.0444 ±55	0.0734 ±61

Table 7. Damaged Area (m^2) and Associated Angle (*degree*) at 200 °C, Stress Limit = 80% of Yield Strength

		End Impacts: Angle between the axis of the Waste Package and the Vertical (*degree*)				Side Impacts: Angle between the axis of the Waste Package and the Horizontal (*degree*)		
		0	1	5	8	0	1	8
Initial Velocity (*m/s*)	1	0	0.0038 ±17	0.0022 ±11	0.0017 ±10	0.0002 ±2	0	0
	2	0	0.0221 ±41	0.0123 ±26	0.0116 ±23	0.0034 ±5	0.0023 ±5	0
	4	0.0244 ±180	0.0885 ±78	0.0968 ±42	0.0714 ±37	0.0187 ±15	0.0072 ±13	0.0092 ±25
	6	0.0244 ±180	0.1822 ±108	0.1489 ±54	0.1038 ±46	0.0430 ±26	0.0238 ±17	0.0153 ±22
	10	0.0476 ±180	0.0846 ±180	0.1287 ±75	0.1163 ±64	0.0910 ±35	0.0409 ±30	0.0585 ±46
	20	0.0595 ±180	0.1219 ±180	0.2668 ±66	0.2525 ±72	0.7443 ±67	0.2351 ±54	0.2451 ±90

Table 8. Damaged Area (m^2) and Associated Angle (*degree*) at 200 °C, Stress Limit = 90% of Yield Strength

		End Impacts: Angle between the axis of the Waste Package and the Vertical (*degree*)				Side Impacts: Angle between the axis of the Waste Package and the Horizontal (*degree*)		
		0	1	5	8	0	1	8
Initial Velocity (*m/s*)	1	0	0.0021 ±15	0.0013 ±10	0.0011 ±8	0	0	0
	2	0	0.0138 ±42	0.0064 ±25	0.0057 ±23	0.0004 ±3	0.0010 ±5	0
	4	0.0244 ±180	0.0242 ±75	0.0571 ±42	0.0416 ±37	0.0051 ±25	0.0025 ±13	0.0006 ±24
	6	0.0244 ±180	0.0602 ±106	0.0815 ±54	0.0517 ±46	0.0205 ±21	0.0128 ±17	0.0089 ±20
	10	0.0254 ±180	0.0257 ±171	0.0594 ±75	0.0518 ±62	0.0373 ±30	0.0210 ±28	0.0202 ±39
	20	0.0262 ±180	0.0536 ±180	0.1707 ±90	0.1403 ±68	0.4153 ±64	0.0904 ±49	0.1283 ±50

Attachment VI presents stress fields in the OS for some of these cases. These stress fields illustrate the extension of damage in the axial direction, and present the 1st principal stress in the OS – bottom lid junction.

Originator: VB - 02/26/03 Checker: 02/26/03

Besides, some of the end impacts were run and post processed at 100 ℃. Tables 9 to 11 list the damaged area for these configurations.

Table 9. Damaged Area (m^2) and Associated Angle (*degree*) at 100 °C, Stress Limit = 80% of Yield Strength

		End Impacts: Angle between the axis of the Waste Package and the Vertical (*degree*)			
		0	**1**	**5**	**8**
Initial Velocity (*m/s*)	**1**	0	0.0027 ±15	0.0011 ±8	0.0009 ±6
	2	0	0.0203 ±39	0.0113 ±25	0.0102 ±21
	4	0.0300 ±180	0.0576 ±66	0.0770 ±42	0.0676 ±37
	6	0.0266 ±180	0.1466 ±99	0.1474 ±53	0.1021 ±46
	10	0.0251 ±180	0.0969 ±162	0.1262 ±72	0.0807 ±61

Table 10. Damaged Area (m^2) and Associated Angle (*degree*) at 100 °C, Stress Limit = 90% of Yield Strength

		End Impacts: Angle between the axis of the Waste Package and the Vertical (*degree*)			
		0	**1**	**5**	**8**
Initial Velocity (*m/s*)	**1**	0	0.0016 ±11	0.0009 ±6	0.0006 ±5
	2	0	0.0071 ±37	0.0069 ±23	0.0065 ±21
	4	0.0193 ±143	0.0173 ±72	0.0424 ±39	0.0349 ±35
	6	0.0244 ±180	0.0566 ±101	0.0737 ±51	0.0510 ±44
	10	0.0254 ±180	0.0254 ±158	0.0628 ±72	0.0413 ±59

Table 11. Damaged Area (m^2) and Associated Angle (*degree*) at 100 °C, Stress Limit = 100% of Yield Strength

		End Impacts: Angle between the axis of the Waste Package and the Vertical (*degree*)			
		0	**1**	**5**	**8**
Initial Velocity (*m/s*)	**1**	0	0.0011 ±8	0.0006 ±5	0.0004 ±3
	2	0	0.0051 ±37	0.0031 ±23	0.0037 ±19
	4	0	0.0112 ±69	0.0170 ±39	0.0171 ±35
	6	0.0244 ±180	0.0173 ±99	0.0346 ±51	0.0258 ±44
	10	0.0251 ±180	0.0220 ±151	0.0183 ±74	0.0180 ±59

Finally, Table 12 shows the damaged area for the OS at 150 °C, obtained by comparing the residual stress intensity to the damage threshold (= 80% of Yield Strength in this case).

The stress intensity is defined as $\sigma_D = \sigma_1 - \sigma_3 = 2 \cdot \tau_{max}$ where σ_1 and σ_3 are the 1st and the 3rd principal stress, respectively, and τ_{max} is the maximum shear stress (see Ref. 15, p. 82).

This table is added for information only. Its purpose is to illustrate the difference in damage induced by two different residual stress measures (1st principal stress vs. stress intensity, i.e. Table 4 vs. Table 12). The difference in results reflects the influence of the 3rd principal stress.

Table 12. Damaged Area (m^2) and Associated Angle (*degree*) at 150 °C, Stress Limit = 80% of Yield Strength, Damaged Area Calculated using the Residual Stress Intensity

		End Impacts: Angle between the axis of the Waste Package and the Vertical (*degree*)			
		0	1	5	8
Initial Velocity (*m/s*)	1	0	0.0044 ±21	0.0026 ±13	0.0022 ±11
	2	0.0075 ±180	0.0240 ±44	0.0155 ±26	0.0160 ±25
	4	0.0502 ±180	0.1238 ±78	0.1419 ±44	0.1089 ±39
	6	0.0445 ±180	0.2572 ±112	0.2763 ±59	0.2229 ±48
	10	0.0926 ±180	0.1944 ±180	0.6018 ±90	0.6126 ±72
	20	0.5711 ±180	0.8137 ±180	1.747 ±90	1.675 ±106

The output values are reasonable for the given inputs in this calculation. The uncertainties are taken into account by varying the most important input parameters such as the temperature and the stress limit. The results are suitable for use in assessing the damaged area in the OS due to the impact of the waste package on an unyielding surface.

7. REFERENCES

1. Allegheny Ludlum 1999. "Technical Data Blue Sheet, Stainless Steels, Chromium-Nickel-Molybdenum, Types 316 (S31600), 316L (S31603), 317 (S31700), 317L (S31703)." Pittsburgh, Pennsylvania: Allegheny Ludlum Corporation. Accessed July 31, 2000. TIC: 248631. http://www.alleghenytechnologies.com/ludlum/pages/products/t316_317.pdf

2. ASM (American Society for Metals) 1980. *Properties and Selection: Stainless Steels, Tool Materials and Special-Purpose Metals.* Volume 3 of *Metals Handbook.* 9th Edition. Benjamin, D., ed. Metals Park, Ohio: American Society for Metals. TIC: 209801.

3. ASM International 1990. *Properties and Selection: Irons, Steels, and High-Performance Alloys.* Volume 1 of *Metals Handbook* 10th Edition. Materials Park, Ohio: ASM International. TIC: 245666.

4. ASME (American Society of Mechanical Engineers) 2001. *2001 ASME Boiler and Pressure Vessel Code.* New York, New York: American Society of Mechanical Engineers. TIC: 251425

5. ASTM G 1-90 (Reapproved 1999). 1999. *Standard Practice for Preparing, Cleaning, and Evaluating Corrosion Test Specimens.* West Conshohocken, Pennsylvania: American Society for Testing and Materials. TIC: 238771.

6. Avallone, E.A. and Baumeister, T., III, eds. 1987. Marks' Standard Handbook for Mechanical Engineers. 9th Edition. New York, New York: McGraw-Hill. TIC: 206891.

7. Boyer, H.E., ed. 2000. *Atlas of Stress-Strain Curves.* Metals Park, Ohio: ASM International. TIC: 248901.

8. BSC (Bechtel SAIC Company) 2001. *Repository Design, Waste Package, Project 21-PWR Waste Package with Absorber Plates, Sheet 1 of 3, Sheet 2 of 3, and Sheet 3 of 3.* DWG-UDC-ME-000001 REV A. Las Vegas, Nevada: Bechtel SAIC Company. ACC: MOL.20020102.0174.

9. BSC (Bechtel SAIC Company) 2001. *Uncanistered Spent Nuclear Fuel Disposal Container System Description Document* SDD-UDC-SE-000001 REV 01 ICN 01 Las Vegas, Nevada: Bechtel SAIC Company ACC: MOL.20010927.0070.

10. BSC (Bechtel SAIC Company) 2002. *Software Code: LS-DYNA.* V960.1106. HP9000. 10300-960.1106-00.

11. CRWMS M&O 1997. *Waste Container Cavity Size Determination.* BBAA00000-01717-0200-00026 REV 00. Las Vegas, Nevada: CRWMS M&O. ACC: MOL.19980106.0061.

12. CRWMS M&O 1998. *ANSYS.* V5.4. HP-UX 10.20. 30040 5.4.

13. CRWMS M&O 1999. *Classification of the MGR Uncanistered Spent Nuclear Fuel Disposal Container System.* ANL-UDC-SE-000001 REV 00. Las Vegas, Nevada: CRWMS M&O. ACC: MOL.19990928.0216.

14. CRWMS M&O 2000. *Software Code: LS-DYNA.* V950. HP 9000. 10300-950-00.

15. Dieter, G.E 1976 *Mechanical Metallurgy* 2nd Edition. Materials Science and Engineering Series New York, New York McGraw-Hill Book Company. TIC: 247879.

16. DOE (U.S. Department of Energy) 2002. *Quality Assurance Requirements and Description.* DOE/RW-0333P, Rev. 12. Washington, D.C.: U.S. Department of Energy, Office of Civilian Radioactive Waste Management. ACC: MOL.20020819.0387.

17. Hallquist, J.O. 1998. *LS-DYNA, Theoretical Manual.* Livermore, California: Livermore Software Technology Corporation. TIC: 238997.

18. Livermore Software Technology Corporation 2001. LS-DYNA Keyword User's Manual, Version 960. Livermore, California: Livermore Software Technology Corporation. TIC: 252119.

19. LL020603612251.015. Slow Strain Rate Test Generated Stress Corrosion Cracking Data. Submittal date: 08/27/2002.

20. McKenzie, D.G., IV. 2002. *Waste Package Design Methodology Report.* TDR-MGR-MD-000006 REV 02. Las Vegas, Nevada: Bechtel SAIC Company. ACC: MOL.20020404.0085.

21. MO0003RIB00071.000. Physical and Chemical Characteristics of Alloy 22. Submittal date: 03/13/2000.

22. Nicholas, T. 1980. *Dynamic Tensile Testing of Structural Materials Using A Split Hopkinson Bar Apparatus.* AFWAL-TR-80-4053. Wright-Patterson Air Force Base, Ohio: Air Force Wright Aeronautical Laboratories. TIC: 249469.

23. Plinski, M.J. 2001. *Waste Package Operations Fabrication Process Report.* TDR-EBS-ND-000003 REV 02. Las Vegas, Nevada: Bechtel SAIC Company. ACC: MOL.20011003.0025.

24. Punatar, M.K. 2001. *Summary Report of Commercial Reactor Criticality Data for Crystal River Unit 3.* TDR-UDC-NU-000001 REV 02. Las Vegas, Nevada: Bechtel SAIC Company. ACC: MOL.20010702.0087.

25. AP-3.12Q, Rev. 1, ICN 2. *Design Calculations and Analyses.* Washington, D.C. U.S. Department of Energy, Office of Civilian Radioactive Waste Management. ACC: MOL.20020607.0013.

Originator: VB. 02/26/03 Checker: 02/26/03

26. AP-SI.1Q, Rev. 3, ICN 4. *Software Management.* Washington, D.C.: U.S. Department of Energy, Office of Civilian Radioactive Waste Management. ACC: MOL.20020520.0283.

27. MO0010SPASIL02.002. Silica Adjusted General Corrosion Rates of Alloy 22 and Titanium Grade 7. Submittal date: 10/10/2000.

8. ATTACHMENTS

Attachment I (2 pages): Design sketch (*21-PWR Waste Package Configurations for Site Recommendation* [SK-0175 REV 02]. This attachment uses Ref. 11.)

Attachment II (5 pages): Gap between the inner and outer shell

Attachment III (24 pages): Mesh refinement study

Attachment IV (2 Compact Discs):
ANSYS V5.4 and LS-DYNA electronic files for the side and end impacts of the 21-PWR waste package. The LS-DYNA input files can be run using either LS-DYNA V950 or LS-DYNA V960.1106. The files were compressed using "WinZip V8.1 (WinZip Computing, Inc)".

Attachment V (7 pages): Name, size, date and time of creation of the files in Attachment IV

Attachment VI (6 pages): Selected Stress Field Plots

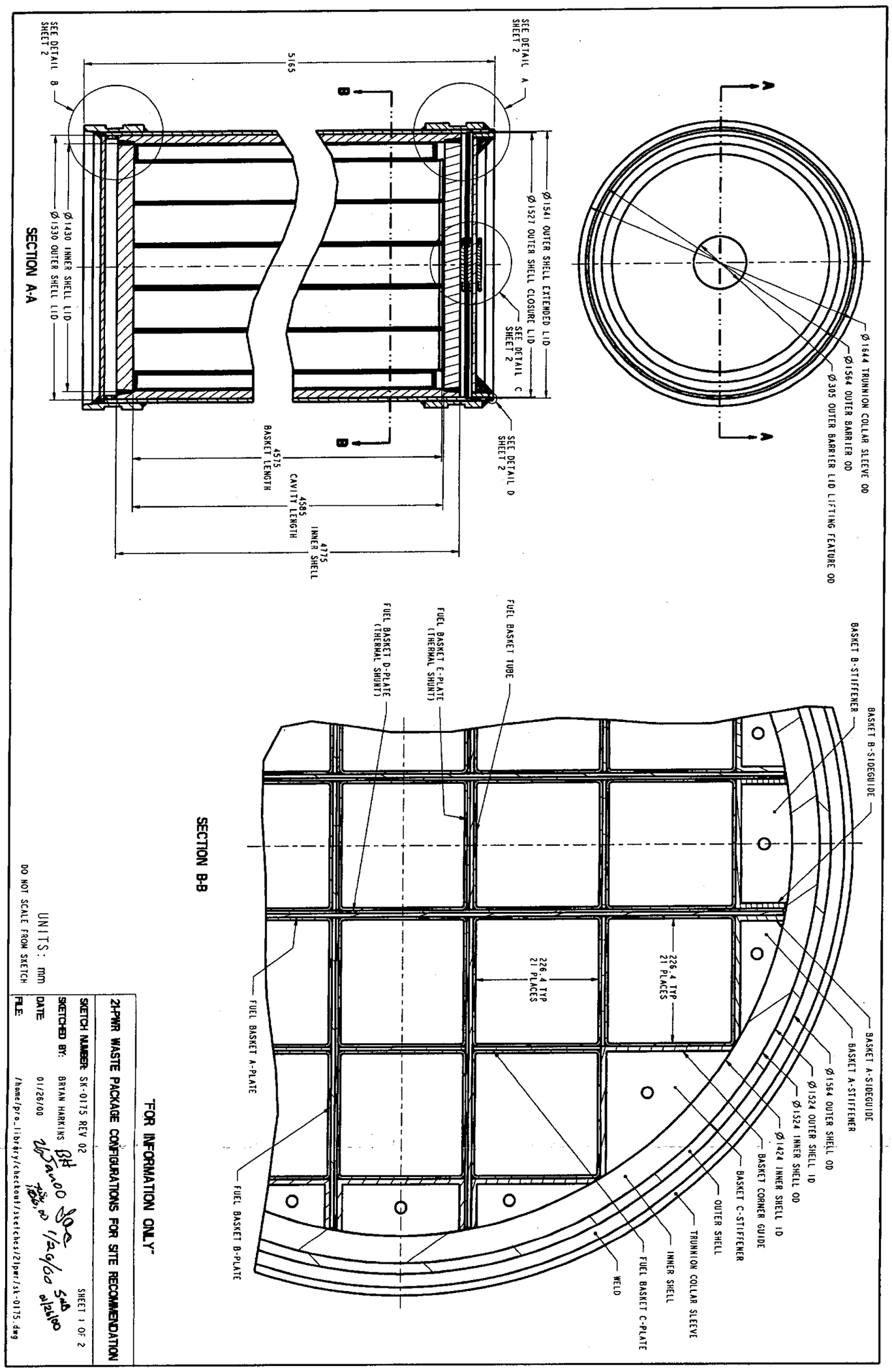
SECTION A-A
SEE DETAIL A SHEET 2
SEE DETAIL B SHEET 2
SEE DETAIL C SHEET 2
SEE DETAIL D SHEET 2
5165
Ø1541 OUTER SHELL EXTENDED LID
Ø1527 OUTER SHELL CLOSURE LID
Ø1430 INNER SHELL LID
Ø1530 OUTER SHELL LID
4575 BASKET LENGTH
4585 CAVITY LENGTH
4715 INNER SHELL
Ø1644 TRUNNION COLLAR SLEEVE OD
Ø1564 OUTER BARRIER OD
Ø305 OUTER BARRIER LID LIFTING FEATURE OD
SECTION B-B
FUEL BASKET D-PLATE (THERMAL SHUNT)
FUEL BASKET E-PLATE (THERMAL SHUNT)
FUEL BASKET TUBE
BASKET B-STIFFENER
BASKET B-SIDEGUIDE
226.4 TYP 21 PLACES
FUEL BASKET A-PLATE
FUEL BASKET B-PLATE
BASKET A-SIDEGUIDE
BASKET A-STIFFENER
Ø1564 OUTER SHELL OD
Ø1524 OUTER SHELL ID
Ø1524 INNER SHELL OD
Ø1424 INNER SHELL ID
BASKET CORNER GUIDE
BASKET C-STIFFENER
OUTER SHELL
TRUNNION COLLAR SLEEVE
INNER SHELL
FUEL BASKET C-PLATE
WELD
UNITS: mm
DO NOT SCALE FROM SKETCH
"FOR INFORMATION ONLY"
21-PWR WASTE PACKAGE CONFIGURATIONS FOR SITE RECOMMENDATION
SKETCH NUMBER: SK-0175 REV 02
SHEET 1 OF 2
SKETCHED BY: BRYAN HARKINS
DATE: 01/26/00
FILE: /home/pro_library/checkout/sketches/21pwr/sk-0175.dwg

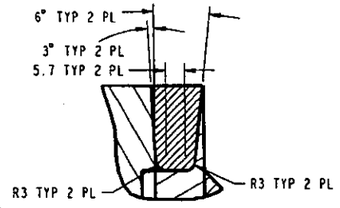

DETAIL D

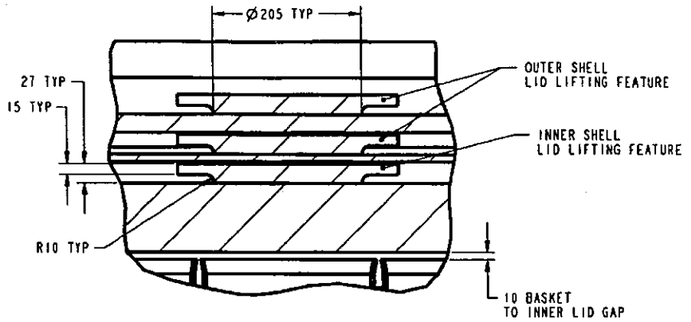

DETAIL C

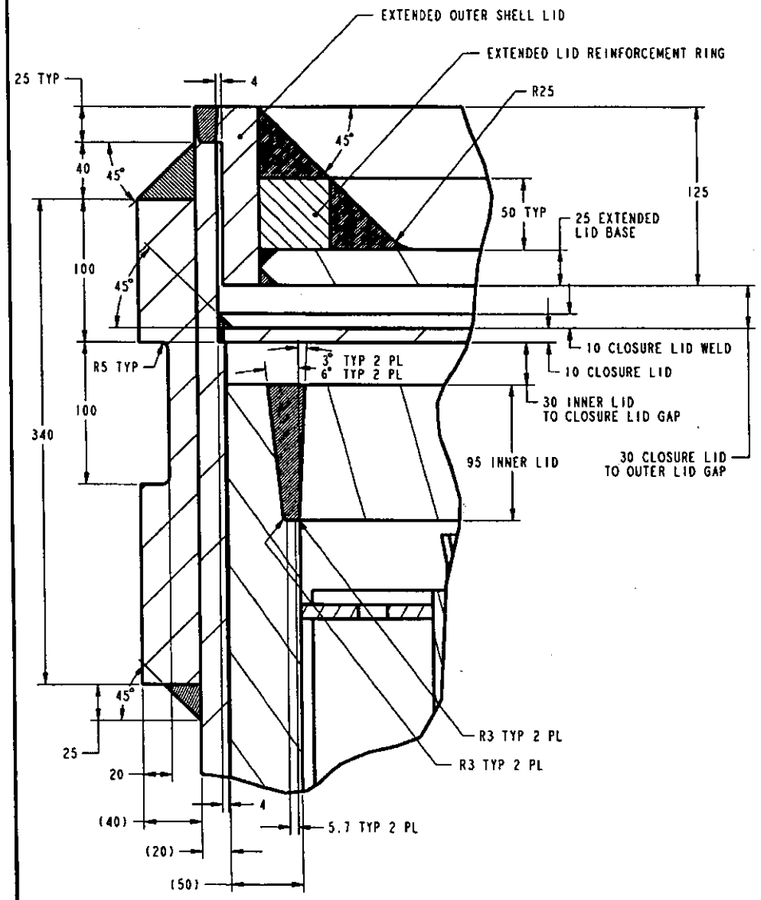

DETAIL A

21-PWR WASTE PACKAGE ASSEMBLY WITH STAINLESS STEEL/BORON PLATES

& 21-PWR CONTROL ROD WASTE PACKAGE ASSEMBLY WITH CARBON STEEL PLATES

COMPONENT NAME	MATERIAL	THICKNESS	MASS (KG)	QTY ROD
BASKET A-SIDEGUIDE	SA-516 K02700	10	27	32
BASKET A-STIFFENER	SA-516 K02700	10	0.72	64
BASKET B-SIDEGUIDE	SA-516 K02700	10	36	16
BASKET B-STIFFENER	SA-516 K02700	10	1.5	32
BASKET C-STIFFENER	SA-516 K02700	10	2.3	32
BASKET CORNERGUIDE	SA-516 K02700	10	42	16
FUEL BASKET A-PLATE	NEUTRONIT A 978	7	85	8
	&SA-516 K02700	&7	&86	&8
FUEL BASKET B-PLATE	NEUTRONIT A 978	7	85	8
	&SA-516 K02700	&7	&86	&8
FUEL BASKET C-PLATE	NEUTRONIT A 978	7	44	16
	&SA-516 K02700	&7	&45	&16
FUEL BASKET D-PLATE	SB-209 A96061 T4	5	21	8
FUEL BASKET E-PLATE	SB-209 A96061 T4	5	21	8
FUEL BASKET TUBE	SA-516 K02700	5	164	21
INNER SHELL	SA-240 S31600	50	8709	1
INNER SHELL LID	SA-240 S31600	95	1200	2
INNER LID LIFTING FEATURE	SA-240 S31600	27	12	1
OUTER SHELL	SB-575 N06022	20	4193	1
EXTENDED OUTER SHELL LID	SB-575 N06022	25	132	1
EXTENDED OUTER SHELL LID BASE	SB-575 N06022	25	366	1
OUTER LID LIFTING FEATURE	SB-575 N06022	27	13	2
EXTENDED LID REINFORCEMENT RING	SB-575 N06022	50	97	1
OUTER SHELL FLAT CLOSURE LID	SB-575 N06022	10	159	1
OUTER SHELL FLAT BOTTOM LID	SB-575 N0-6022	25	396	1
UPPER TRUNNION COLLAR SLEEVE	SB-575 N06022	40	507	1
LOWER TRUNNION COLLAR SLEEVE	SB-575 N06022	40	497	1
INNER SHELL SUPPORT RING	SB-575 N06022	20	41	1
TOTAL ALLOY 22 WELDS	SFA-5.14 N06022	-	249	**
TOTAL 316 WELDS	SFA-5.9 S31680	-	128	**
WASTE PACKAGE ASSEMBLY	-	-	26035	1
	-	-	&26059	&1
PWR FUEL ASSEMBLY	-	-	773.4*	21
WP ASSEMBLY WITH SNF	-	-	42277	1
	-	-	&42301	&1

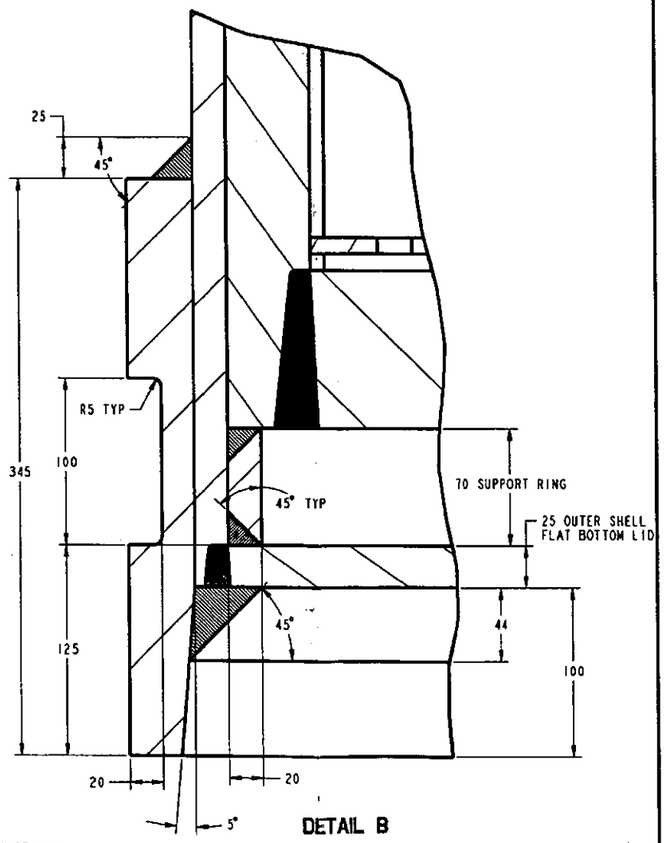

DETAIL B

* CRWMS M&O 1997. WASTE CONTAINER CAVITY SIZE DETERMINATION. BBAA00000-01717-0200-00026 REV 00. LAS VEGAS, NV: CRWMS M&O. ACC: MOL.19980106.0061

** REFER TO SK-0191 REV 00 "21-PWR WASTE PACKAGE WELD CONFIGURATION"

02 SMB 01/27/00

SK-0175 REV 01	SHEET 2 OF 2

Attachment I: SK-0175 rev 02 – 21-PWR Waste Package Configurations for Site Recommendation
Originator: VB. 01/16/03 Checker: DU 02/26/03

ATTACHMENT II
GAP BETWEEN THE INNER AND OUTER SHELL

The drawing used to create the geometry of the 21-PWR WP in this calculation specifies a tight fit (0-mm nominal gap) between the IS and the OS in the radial direction. However, Reference 23 (Section 8.1.8) specifies a 4-*mm* nominal gap between the IS and OS in the radial direction. In order to determine which geometry would be the more conservative, two cases (end impacts, α=1 °, v=2 *m/s* and α=5 °, v=4 *m/s*) were run with the tight fit and the maximum loose fit (4-*mm* gap) and the results are compared. The cases were run at 150 °C.

Table II-1: Comparison of two Geometries (With and Without Gap between the Inner and Outer Shell)

		Without Gap	With a 4-*mm* Gap	Difference (%)
α=1 °, v=2 *m/s*	Maxi Residual 1st Principal Stress (*MPa*)	361.5 (See Figure II-1)	360.3 (See Figure II-2)	<1
	Damaged Area (m^2) - 80% of Yield Stress	0.0212	0.0221	4.2
	Damaged Area (m^2) - 90% of Yield Stress	0.0110	0.0112	1.8
	Damaged Area (m^2) - 100% of Yield Stress	0.0054	0.0051	-5.5
α=5 °, v=4 *m/s*	Maxi Residual 1st Principal Stress (*MPa*)	514.4 (See Figure II-3)	521.2 (See Figure II-4)	1.3
	Damaged Area (m^2) - 80% of Yield Stress	0.0719	0.0850	18
	Damaged Area (m^2) - 90% of Yield Stress	0.0390	0.0508	38
	Damaged Area (m^2) - 100% of Yield Stress	0.0154	0.0217	40.9

In all the cases but one, the geometry including a 4-*mm* radial gap yielded more conservative results. This geometry was used for the remainder of the runs.

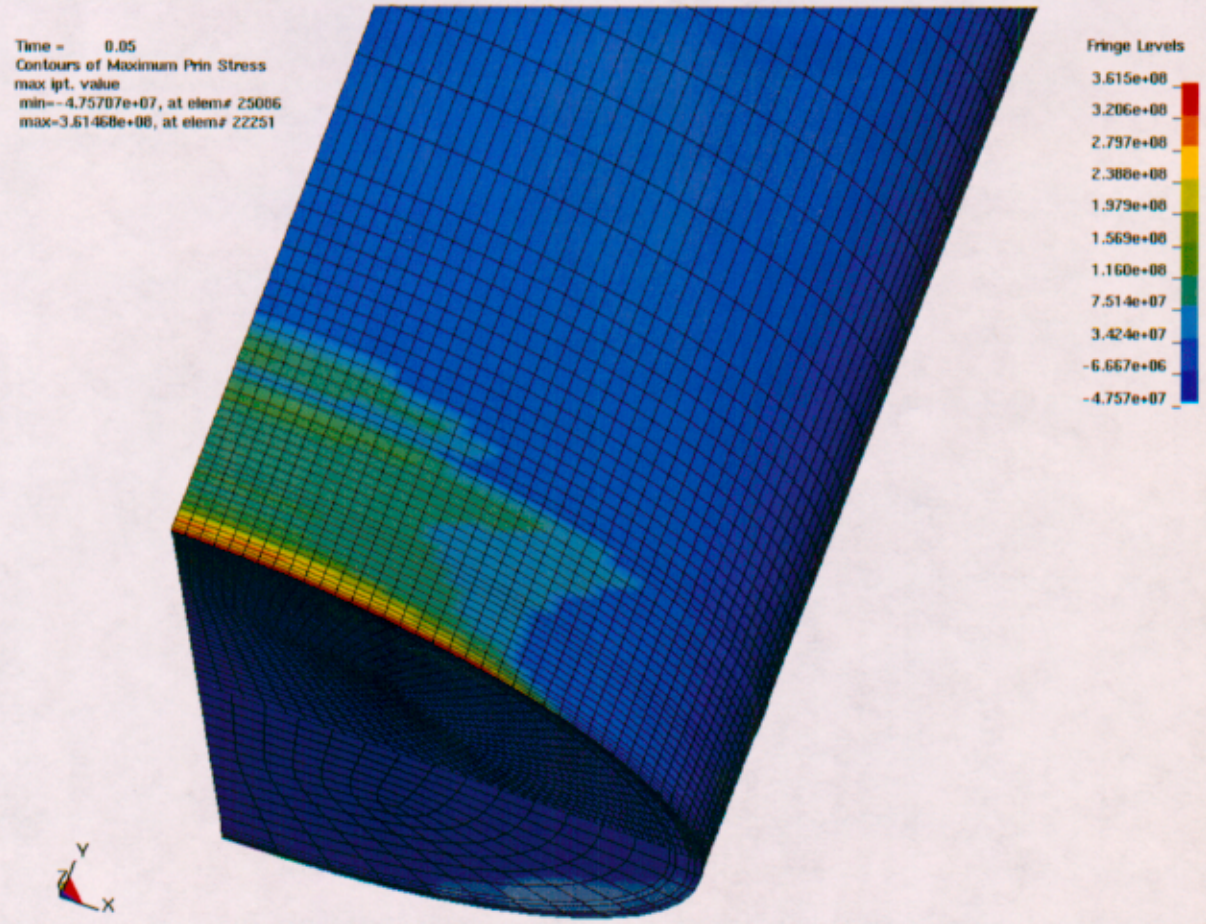

Figure II-1: Maximum Residual 1st Principal Stress (*Pa*), no Gap, α=1 °, v=2 *m/s*

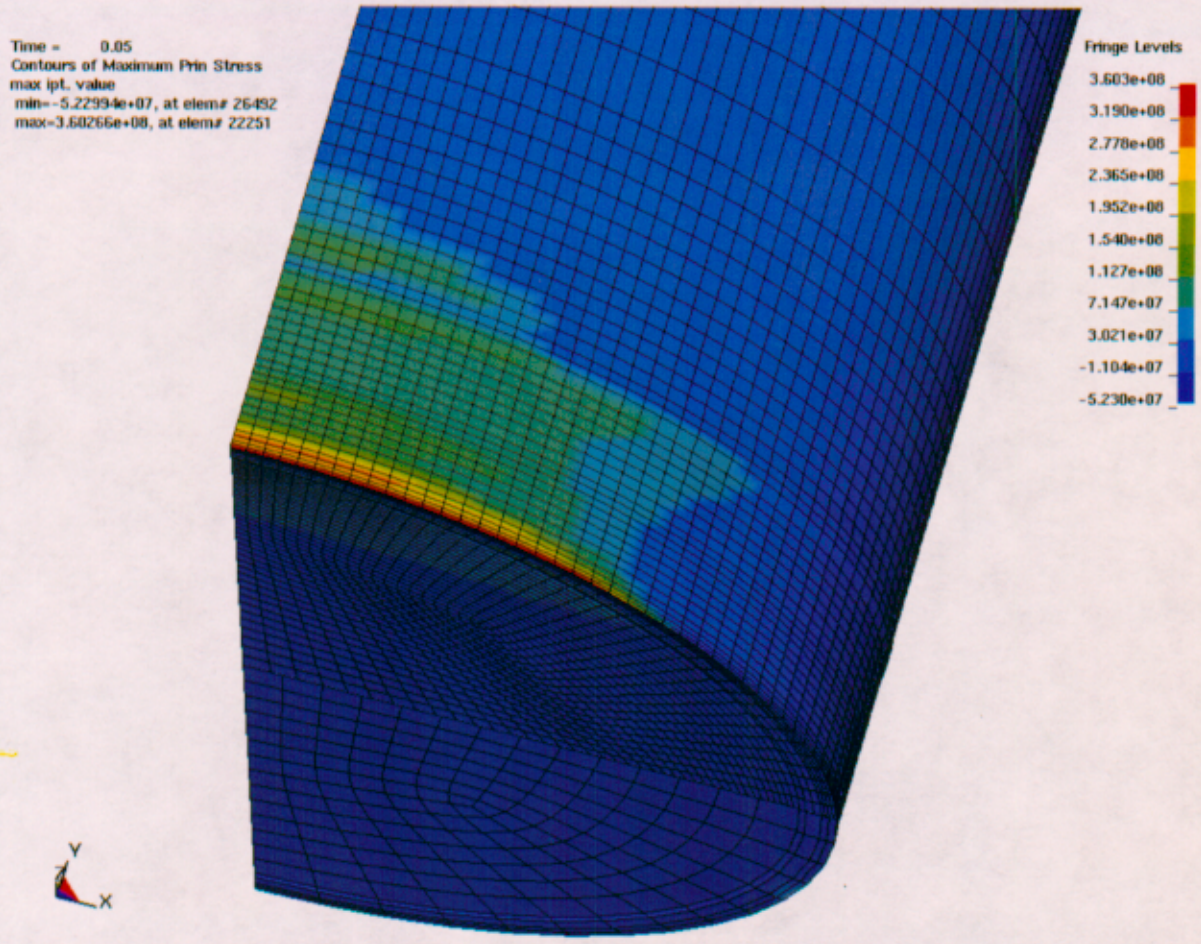

Figure II-2: Maximum Residual 1st Principal Stress (*Pa*), 4-*mm* Gap, α=1 °, v=2 *m/s*

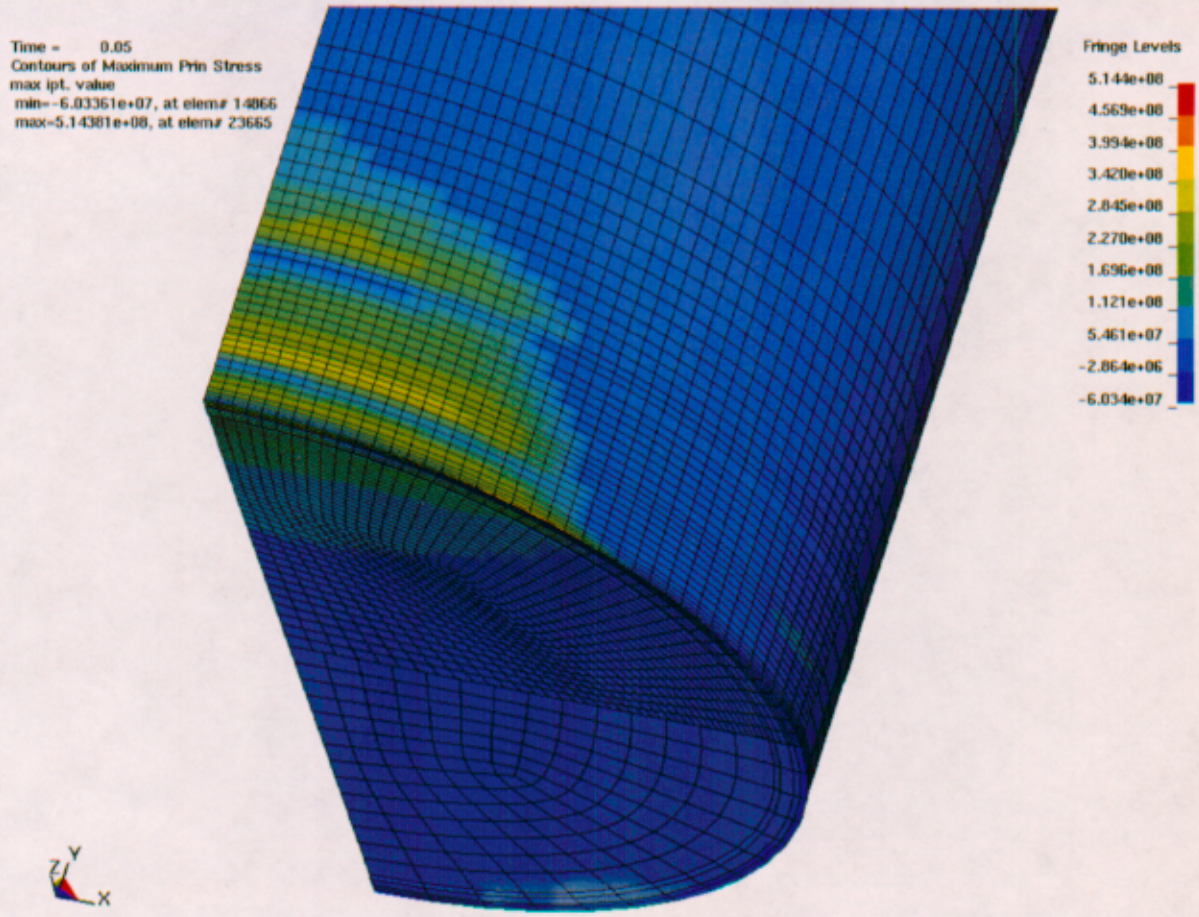

Figure II-3: Maximum Residual 1st Principal Stress (*Pa*), no Gap, α=5°, v=4 *m/s*

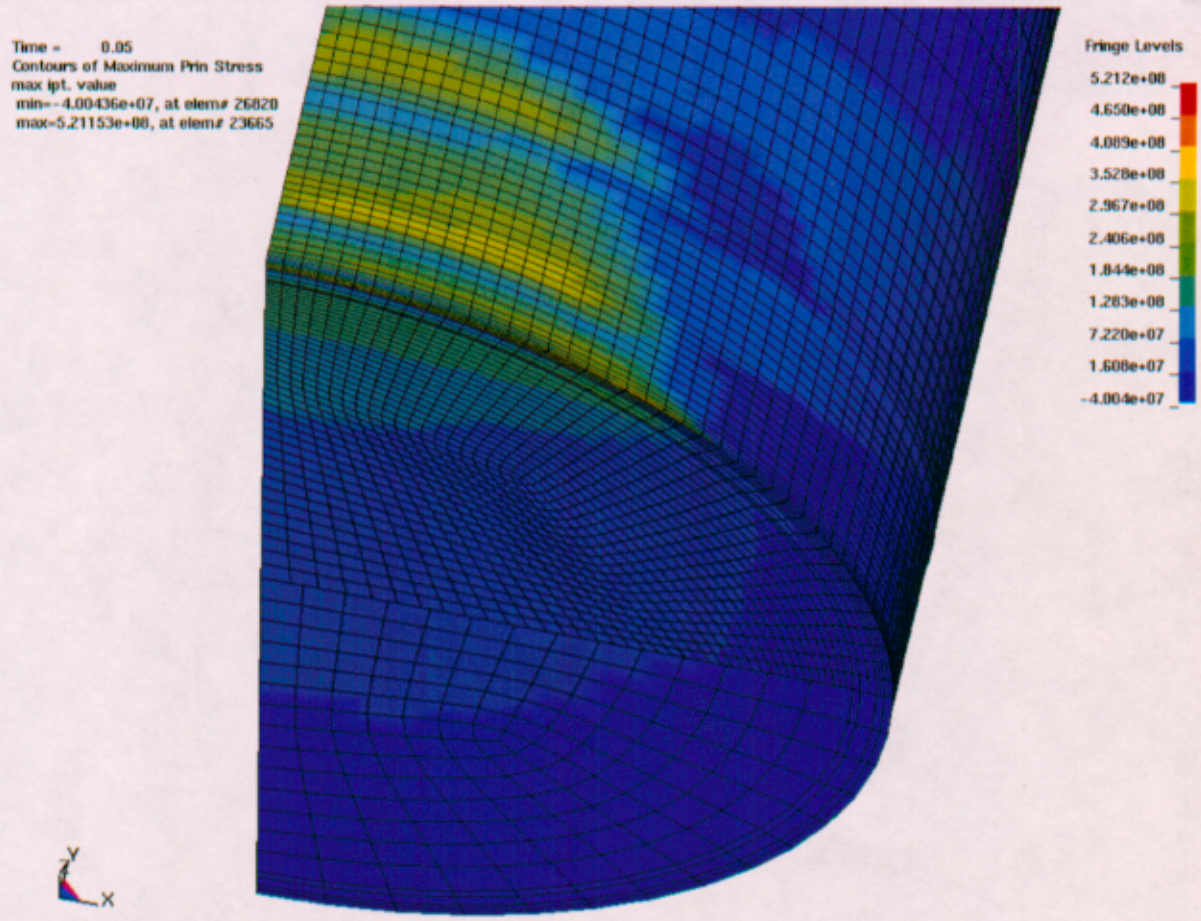

Figure II-4: Maximum Residual 1st Principal Stress (*Pa*), 4-*mm* Gap, α=5°, v=4 *m/s*

ATTACHMENT III
MESH REFINEMENT STUDY

For each type of impact (end impact, side impact, inclined end impact, inclined side impact), the following mesh refinement study was conducted to verify the objectivity of the mesh (i.e. that the calculation results are not mesh-sensitive). A mesh was generated and refined in the contact region according to standard engineering practice. The mesh was then further refined in the higher-stress region. The difference in maximum stress was compared to the variation in volume of an element representative of the mesh according to the method described in Reference 20, Section 6.2.3. The results are presented in Table III-2 to III-6.

For example, in Table III-2, the values of maximum residual stresses are presented for two different meshes. The average OS element volume in the impact region (characterized by the highest stresses; see Figure III-1) of the first mesh is 260% larger than the corresponding element in the second mesh ($(4.4969.10^{-7}-1.2482.10^{-7})/1.2482.10^{-7}=2.60$). Note that the volumes of each element can be directly verified by using LS-POST V2. For this very large difference in element volume, the variation in maximum residual 1st principal stress is 18% and the variation in maximum residual shear stress is smaller than 5 %. These results indicate that a large reduction of the element volume in the contact region results in very mild sensitivity of the maximum residual stresses. The original FE mesh is, therefore, deemed acceptable, and all remaining calculations are performed with the coarser mesh.

In this study, 10 different meshes were used. Table III-1 presents which mesh was used for each run. The larger, bold letters indicate the runs that were used in the mesh refinement study. Meshes B and E are strictly identical to mesh D, except for the angle between the axis of the waste package and the unyielding surface. Therefore, the mesh refinement study conducted for mesh D is considered to be representative for meshes B and E. Similarly, mesh G was considered to be representative of mesh F, and mesh C representative of meshes J and K for the purpose of this attachment.

Table III-1: Identification of the Mesh used in each Run

		Angle (deg)						
		End Impacts				Side Impacts		
		0	1	5	8	82	89	90
Initial Velocity (m/s)	1	A	B	D	E	F	G	H
	2	A	B	D	E	F	G	H
	4	**A**	B	**D**	E	F	**G**	H
	6	A	**C**	D	E	F	G	**H**
	10	A	C	D	E	F	G	H
	20	A	C	J	K	F	G	H

Table III-2: Mesh Verification for Mesh A

	Standard Mesh	Refined Mesh	Variation Between Standard and Refined Mesh (%)
Maxi Residual 1st Principal Stress	309.9 (see Figure III-1)	377.9 (see Figure III-2)	18
Element #	15526	32563	
Maxi Residual Shear Stress	154.3 (see Figure III-3)	147.7 (see Figure III-4)	-4.5
Element #	15545	34883	
Representative Element Volume	4.4969 e-7	1.2482 e-7	-260
Element #	14156	30290	

Table III-3: Mesh Verification for Mesh D

	Standard Mesh	Refined Mesh	Variation Between Standard and Refined Mesh (%)
Maxi Residual 1st Principal Stress	521.2 (see Figure III-5)	536.1 (see Figure III-6)	2.8
Element #	23665	28662	
Maxi Residual Shear Stress	179.4 (see Figure III-7)	180.8 (see Figure III-8)	< 1
Element #	14575	15177	
Representative Element Volume	4.4936 e-7	2.5161 e-7	-79
Element #	22266	26684	

Table III-4: Mesh Verification for Mesh C

	Standard Mesh	Refined Mesh	Variation Between Standard and Refined Mesh (%)
Maxi Residual 1st Principal Stress	507.0 (see Figure III-9)	554.8 (see Figure III-10)	8.6
Element #	17971	22293	
Maxi Residual Shear Stress	173.0 (see Figure III-11)	173.0 (see Figure III-12)	0
Element #	8879	9033	
Representative Element Volume	6.4855 e-7	3.6313 e-7	-79
Element #	16582	13143	

Table III-5: Mesh Verification for Mesh F

	Standard Mesh	Refined Mesh	Variation Between Standard and Refined Mesh (%)
Maxi Residual 1st Principal Stress	293.0 (see Figure III-13)	338.4 (see Figure III-14)	13
Element #	29691	47050	
Maxi Residual Shear Stress	172.3 (see Figure III-15)	172.0 (see Figure III-16)	< 1
Element #	30296	47050	
Representative Element Volume	4.4931 e-7	1.9978 e-7	-129
Element #	29536	45718	

Table III-6: Mesh Verification for Mesh G

	Standard Mesh	Refined Mesh	Variation Between Standard and Refined Mesh (%)
Maxi Residual 1st Principal Stress	442.0 (see Figure III-17)	525.8 (see Figure III-18)	16
Element #	16013	16598	
Maxi Residual Shear Stress	173.1 (see Figure III-19)	172.0 (see Figure III-20)	< 1
Element #	29575	27968	
Representative Element Volume (Location A)	4.4969 e-7	1.9948 e-7	-125
Element #	29536	45718	
Representative Element Volume (Location B)	4.6946 e-7	1.2686 e-7	-270
Element #	16136	16834	

In this case, the location where the maximum residual shear stress occurs varies between the refined and the standard mesh. The comparison of volume is then done at the two locations where it occurs: Location A is at the junction of the OS and its bottom lid, location B is at the junction of the closure lid and the OS.

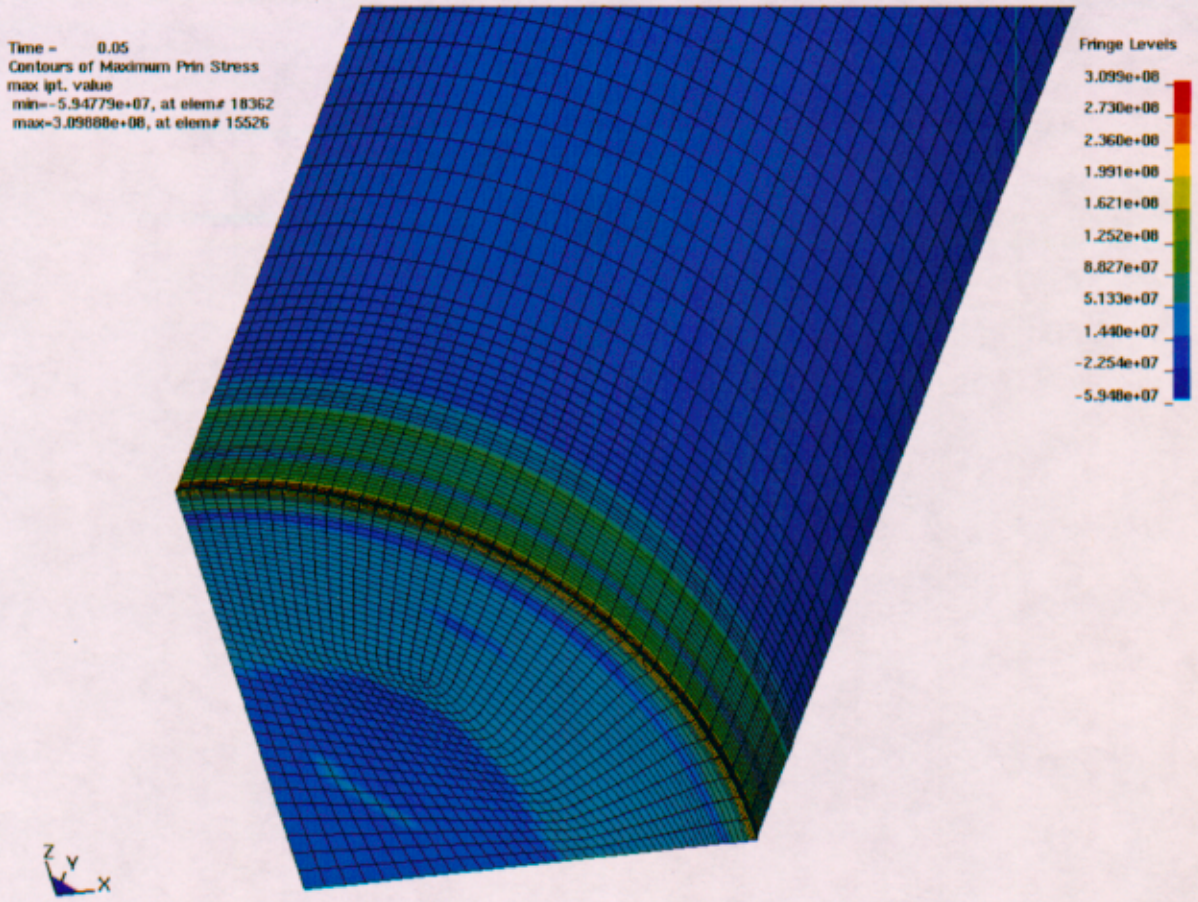

Figure III-1: Mesh A - Maximum Residual 1st Principal Stress, Standard Mesh (*Pa*)

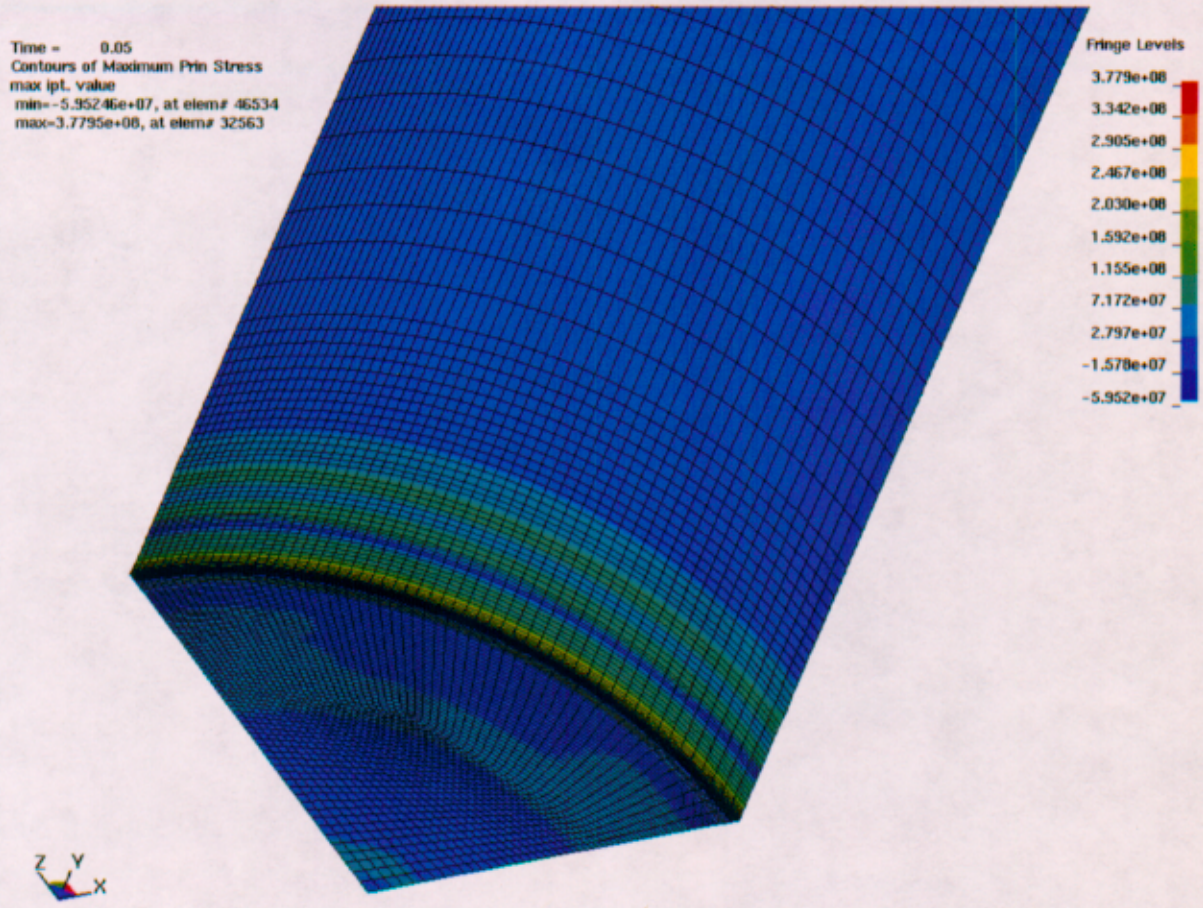

Figure III-2: Mesh A - Maximum Residual 1st Principal Stress, Refined Mesh (*Pa*)

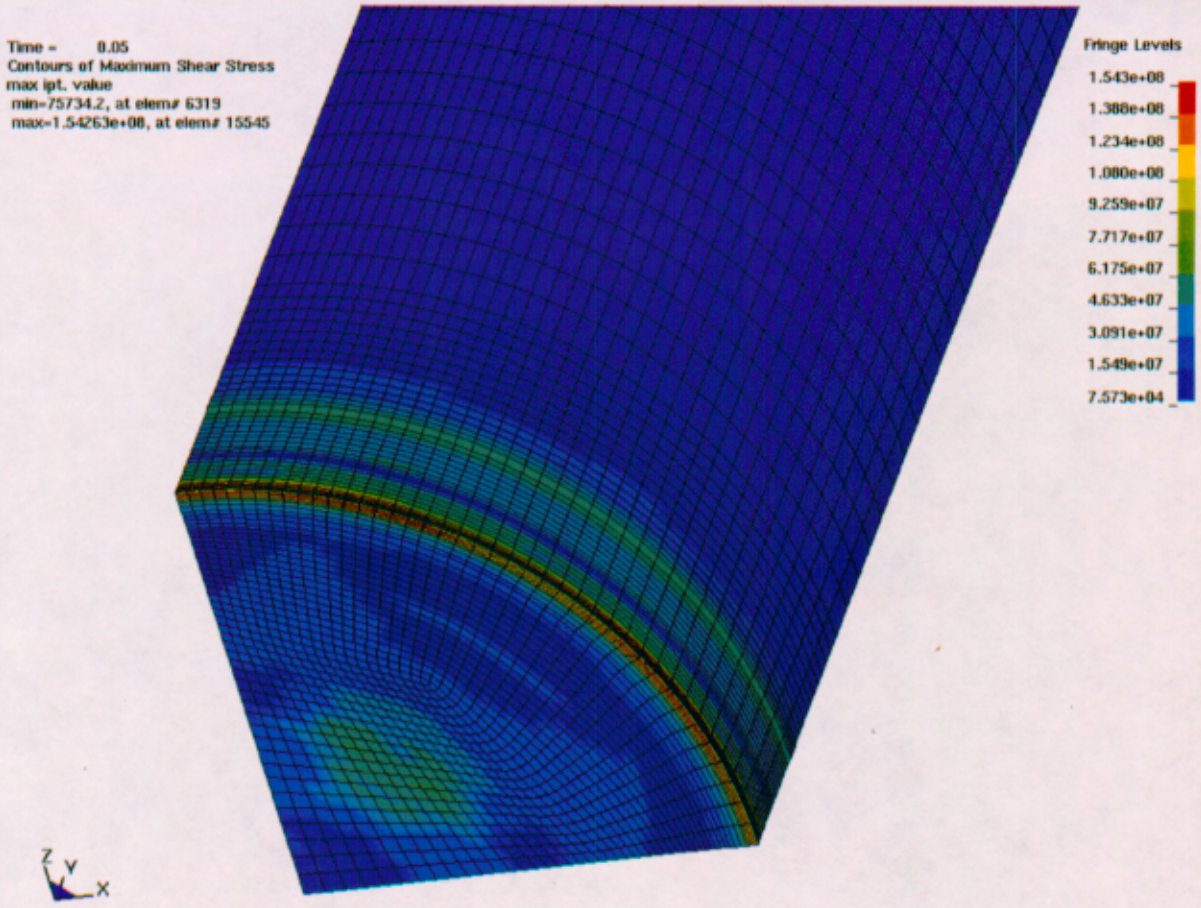

Figure III-3: Mesh A - Maximum Residual Shear Stress, Standard Mesh (*Pa*)

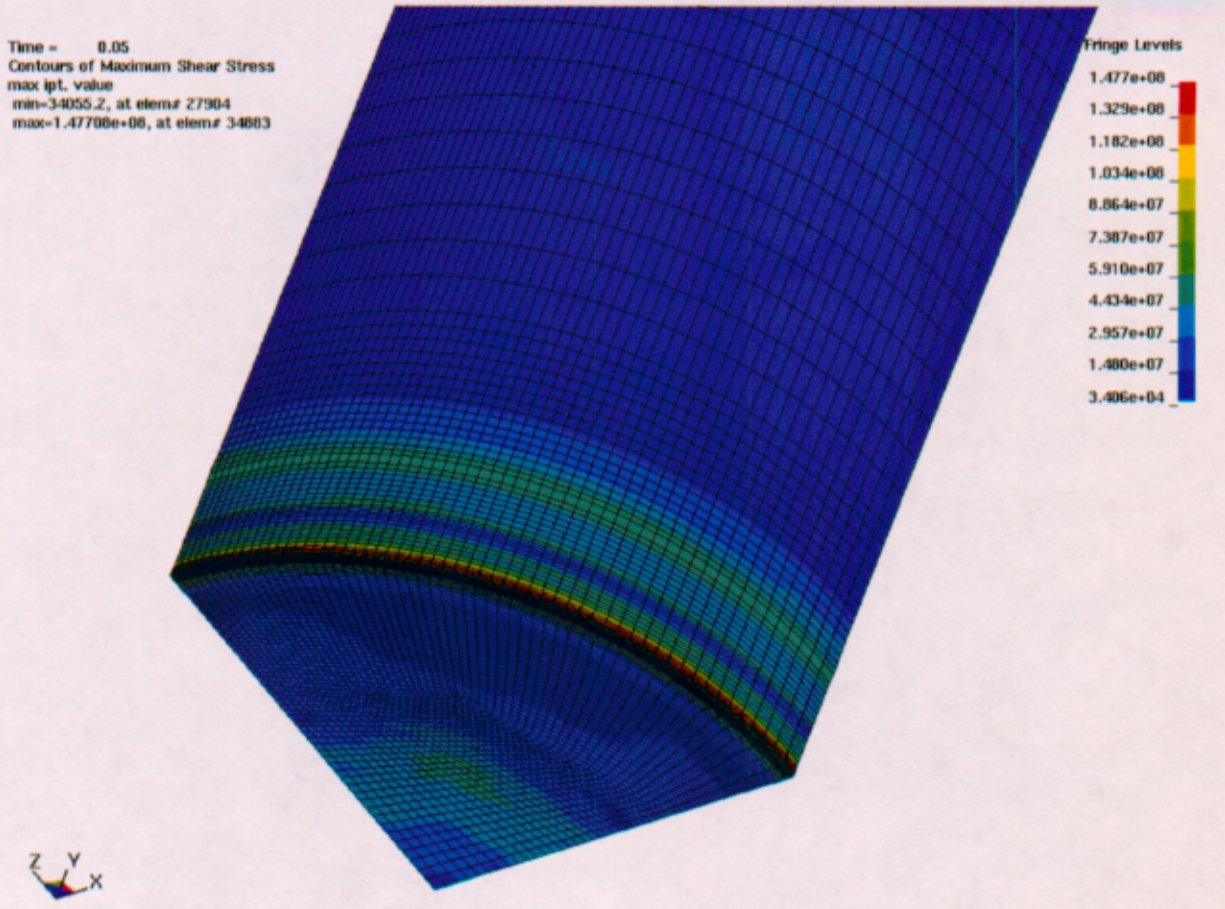

Figure III-4: Mesh A - Maximum Residual Shear Stress, Refined Mesh (*Pa*)

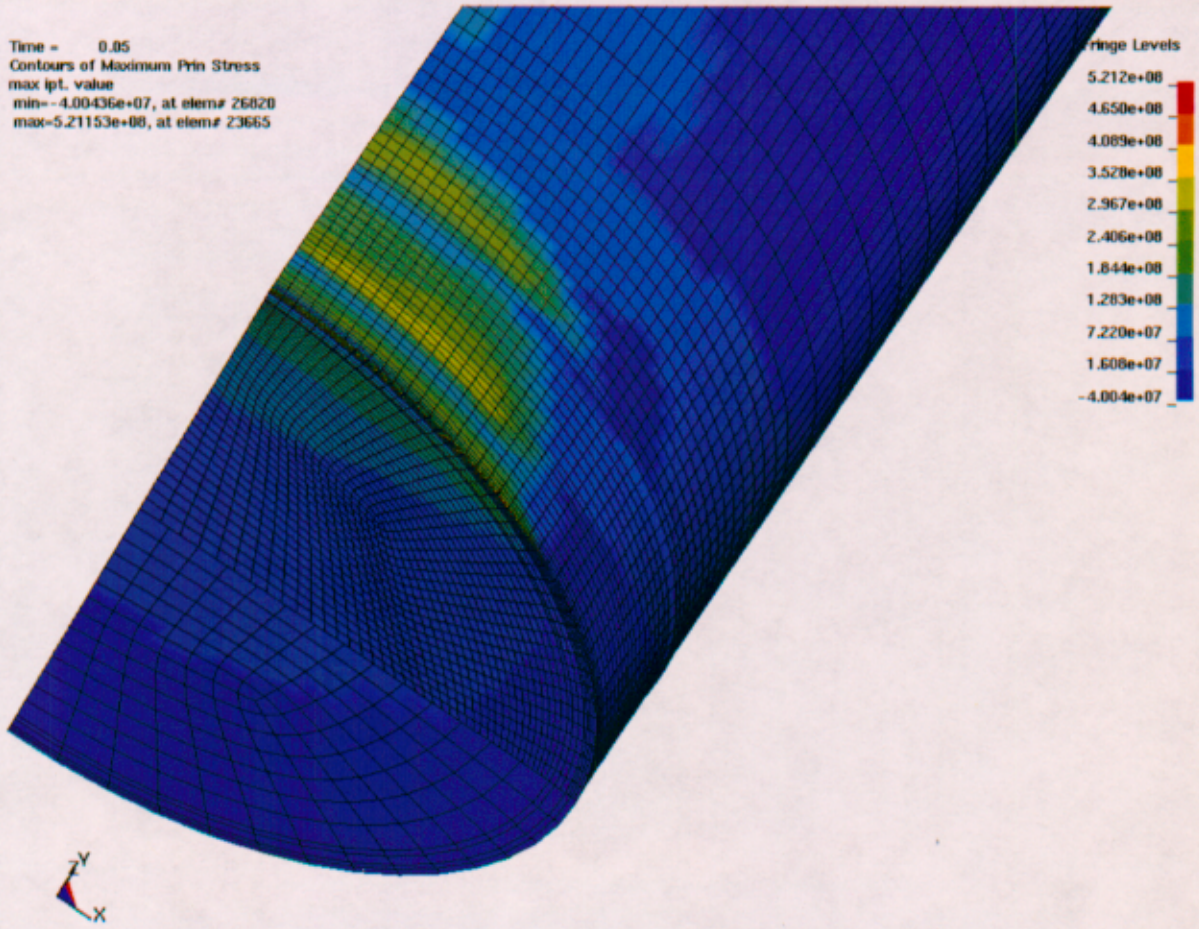

Figure III-5: Mesh D - Maximum Residual 1st Principal Stress, Standard Mesh (*Pa*)

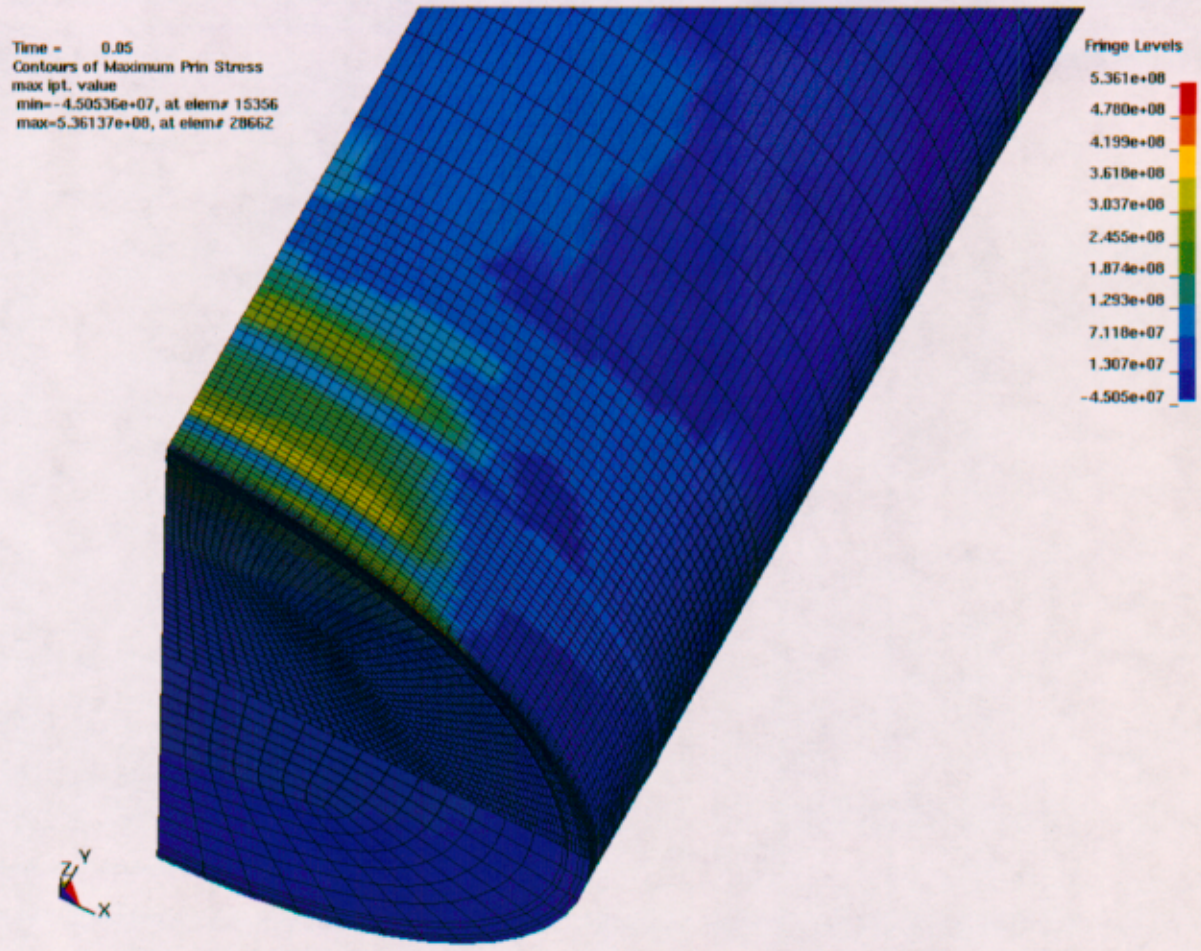

Figure III-6: Mesh D - Maximum Residual 1st Principal Stress, Refined Mesh (*Pa*)

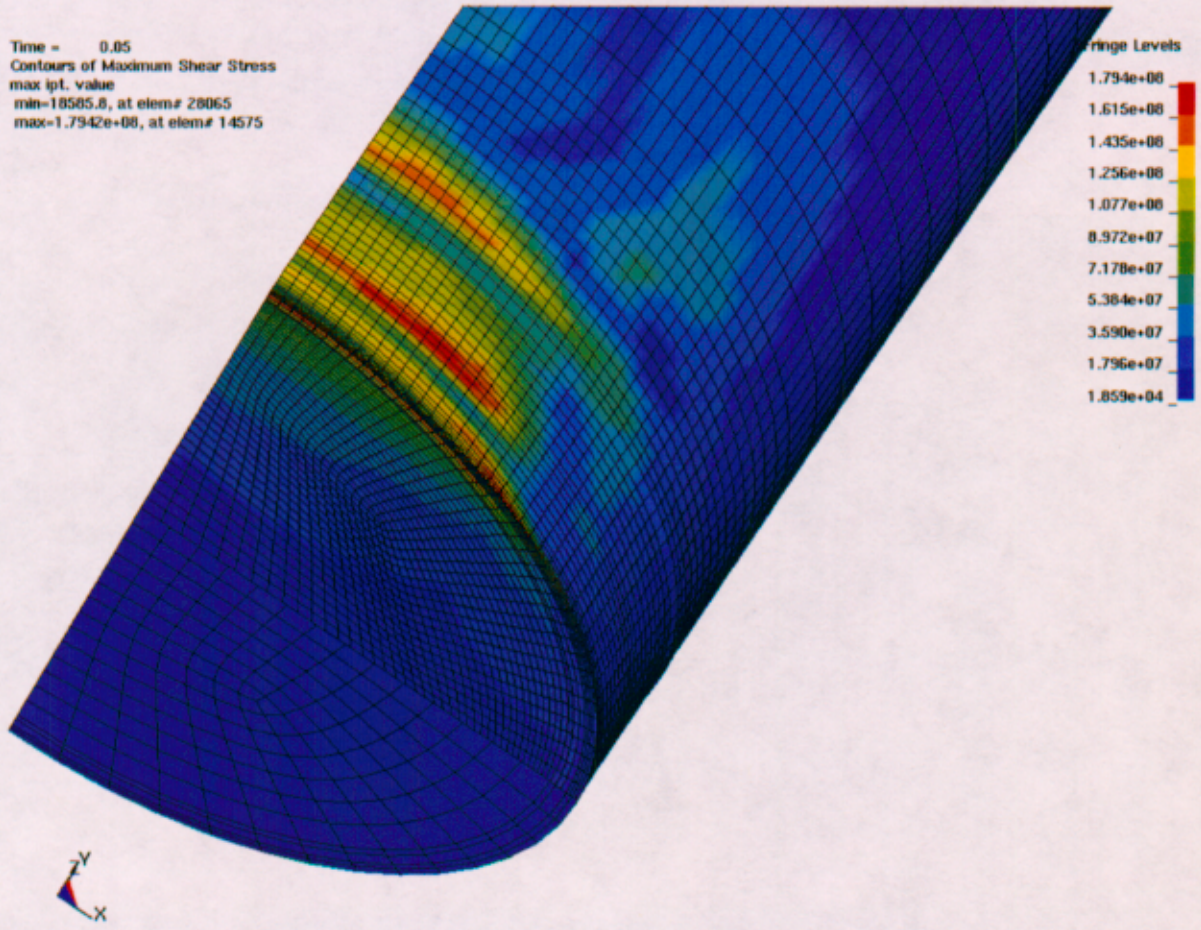

Figure III-7: Mesh D - Maximum Residual Shear Stress, Standard Mesh (*Pa*)

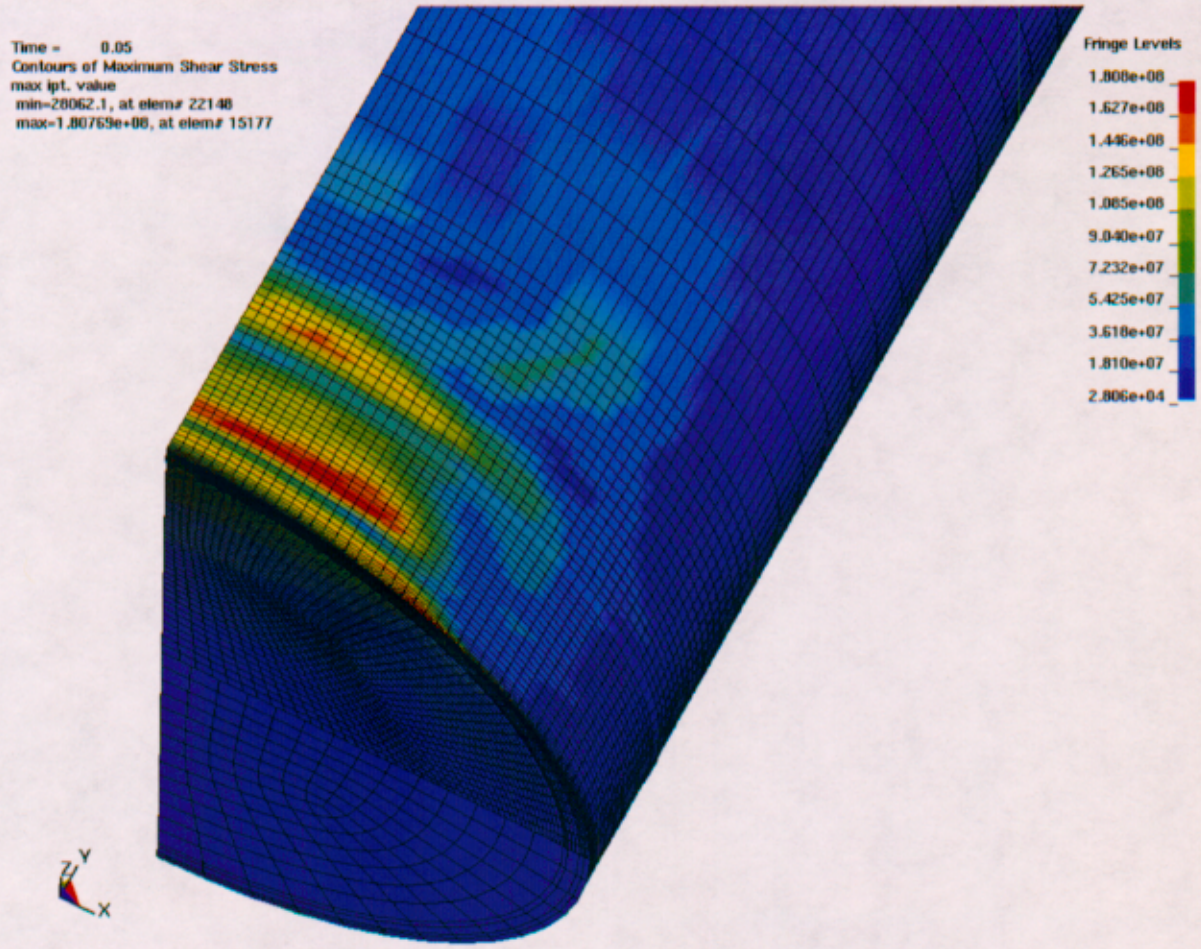

Figure III-8: Mesh D - Maximum Residual Shear Stress, Refined Mesh (*Pa*)

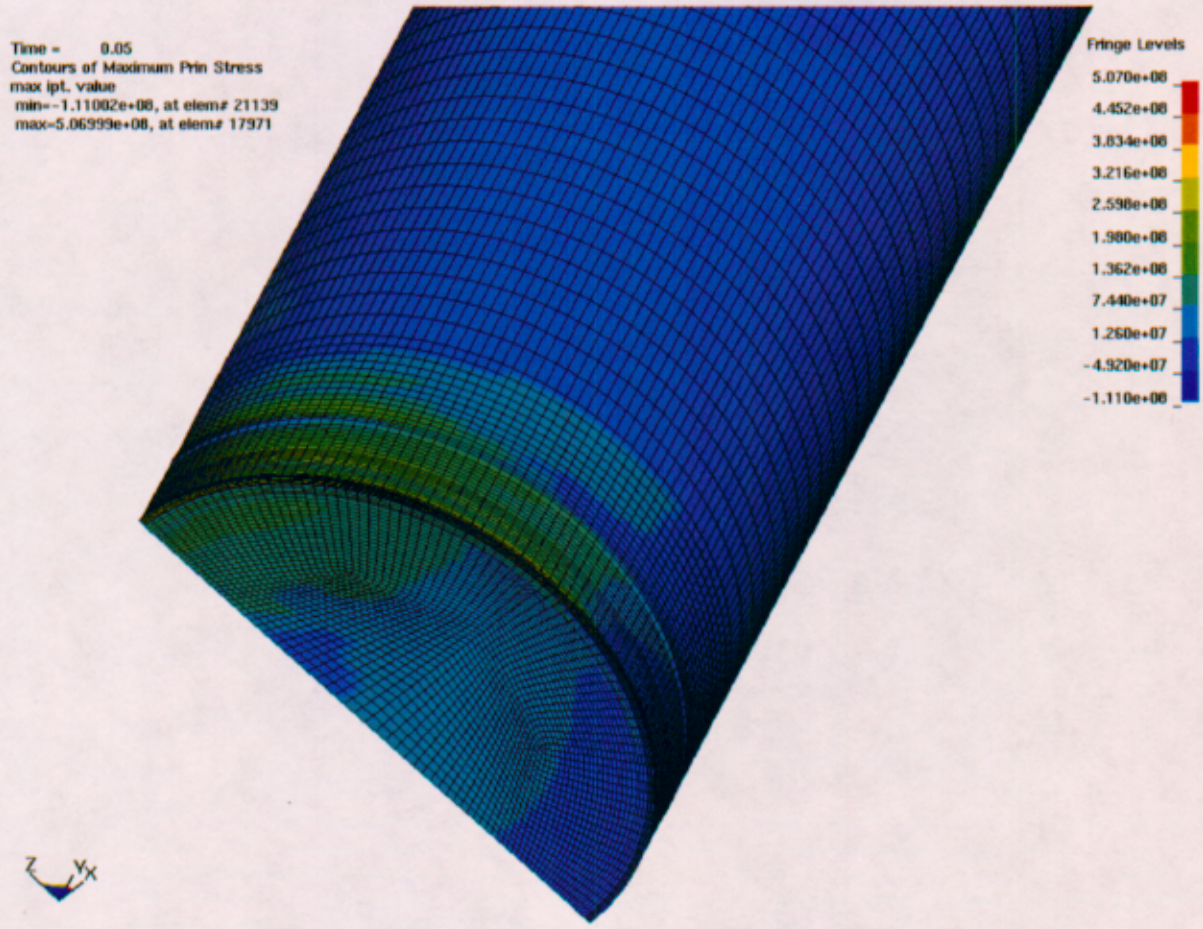

Figure III-9: Mesh C - Maximum Residual 1st Principal Stress, Standard Mesh (*Pa*)

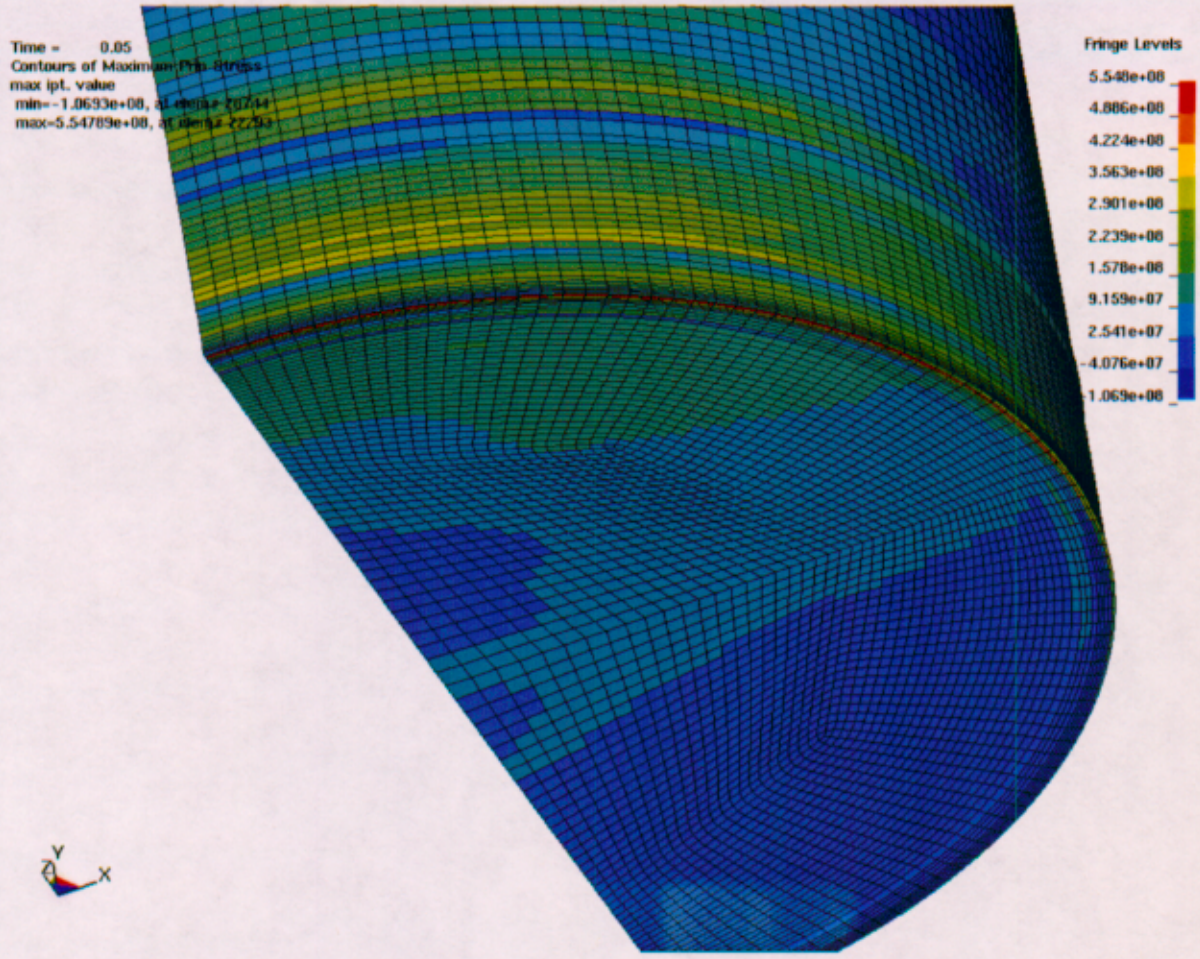

Figure III-10: Mesh C - Maximum Residual 1st Principal Stress, Refined Mesh (*Pa*)

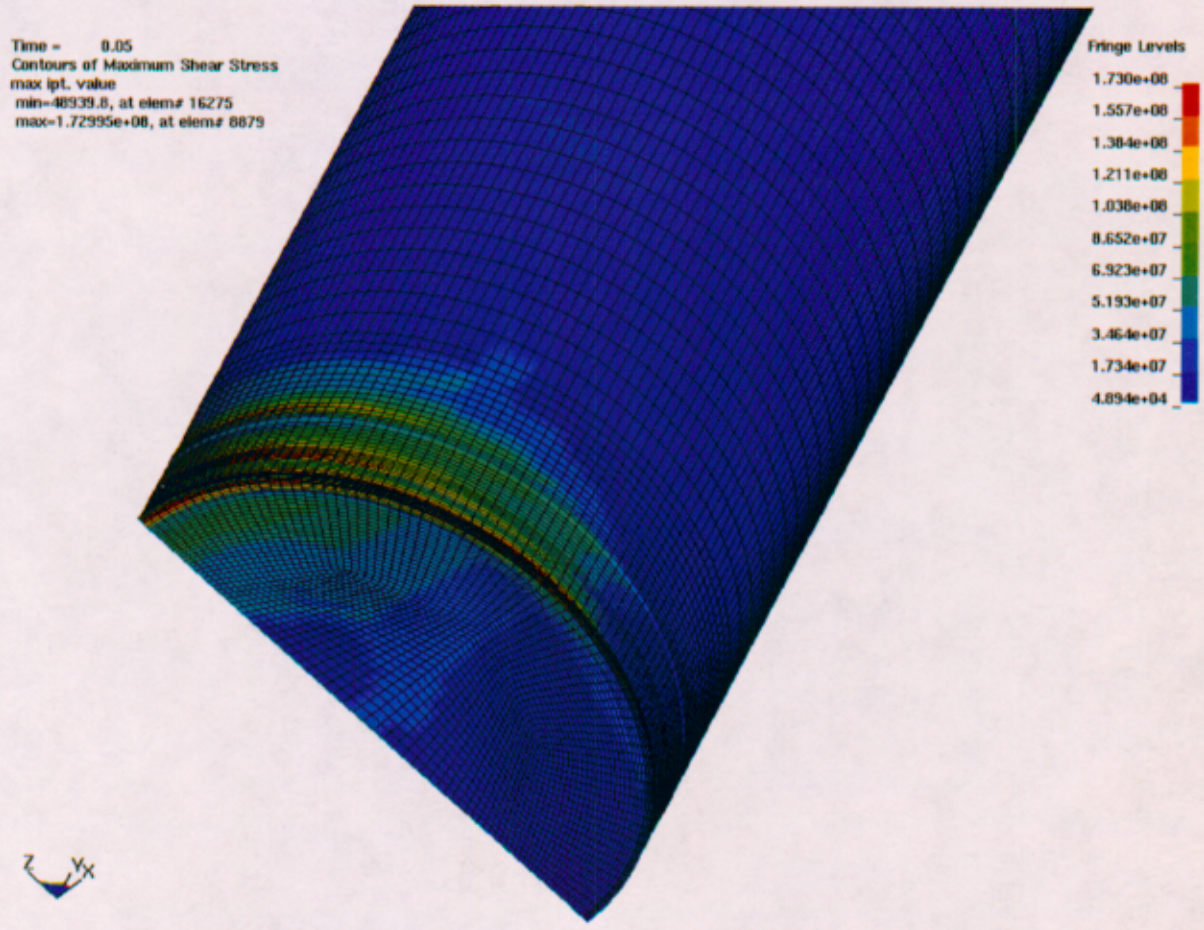

Figure III-11: Mesh C - Maximum Residual Shear Stress, Standard Mesh (*Pa*)

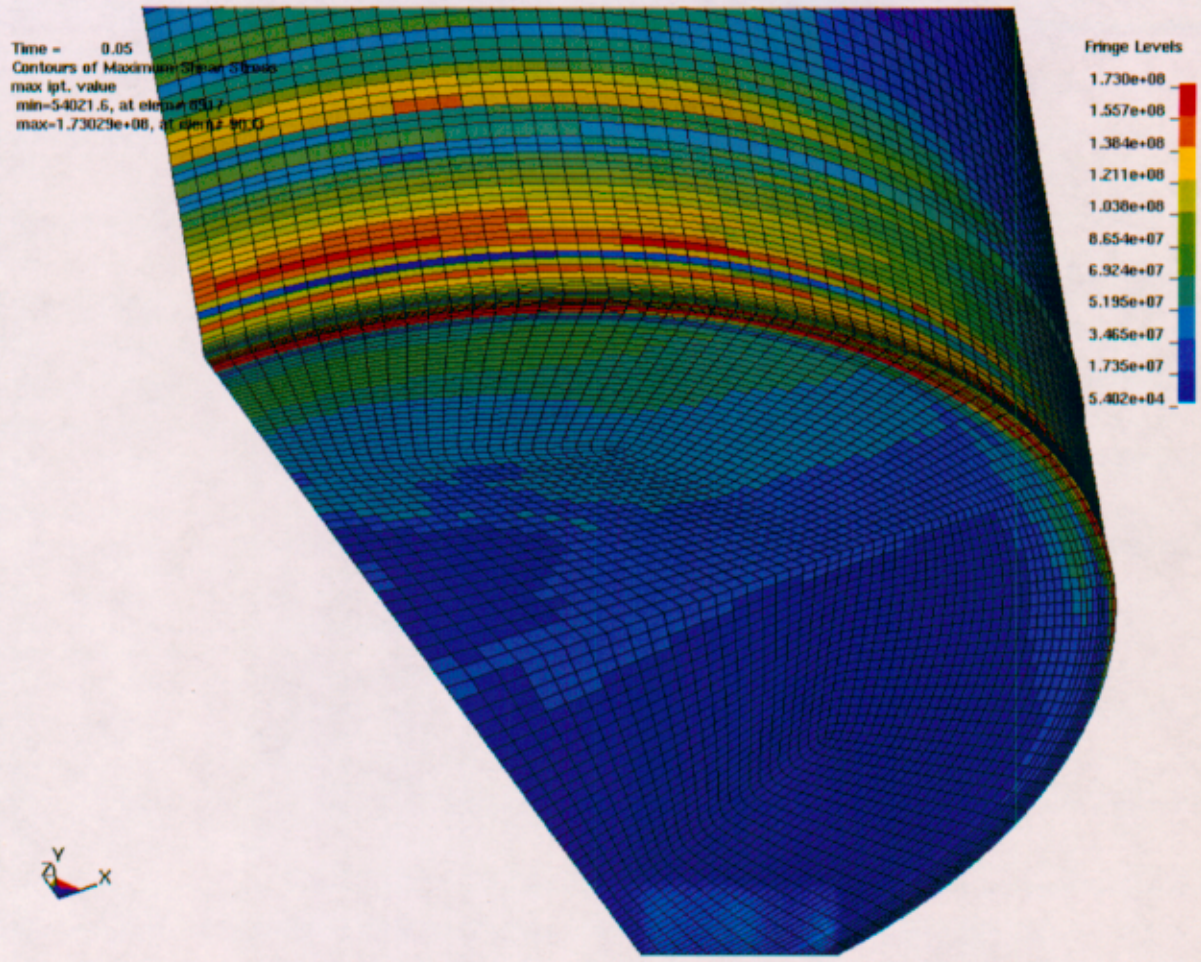

Figure III-12: Mesh C - Maximum Residual Shear Stress, Refined Mesh (*Pa*)

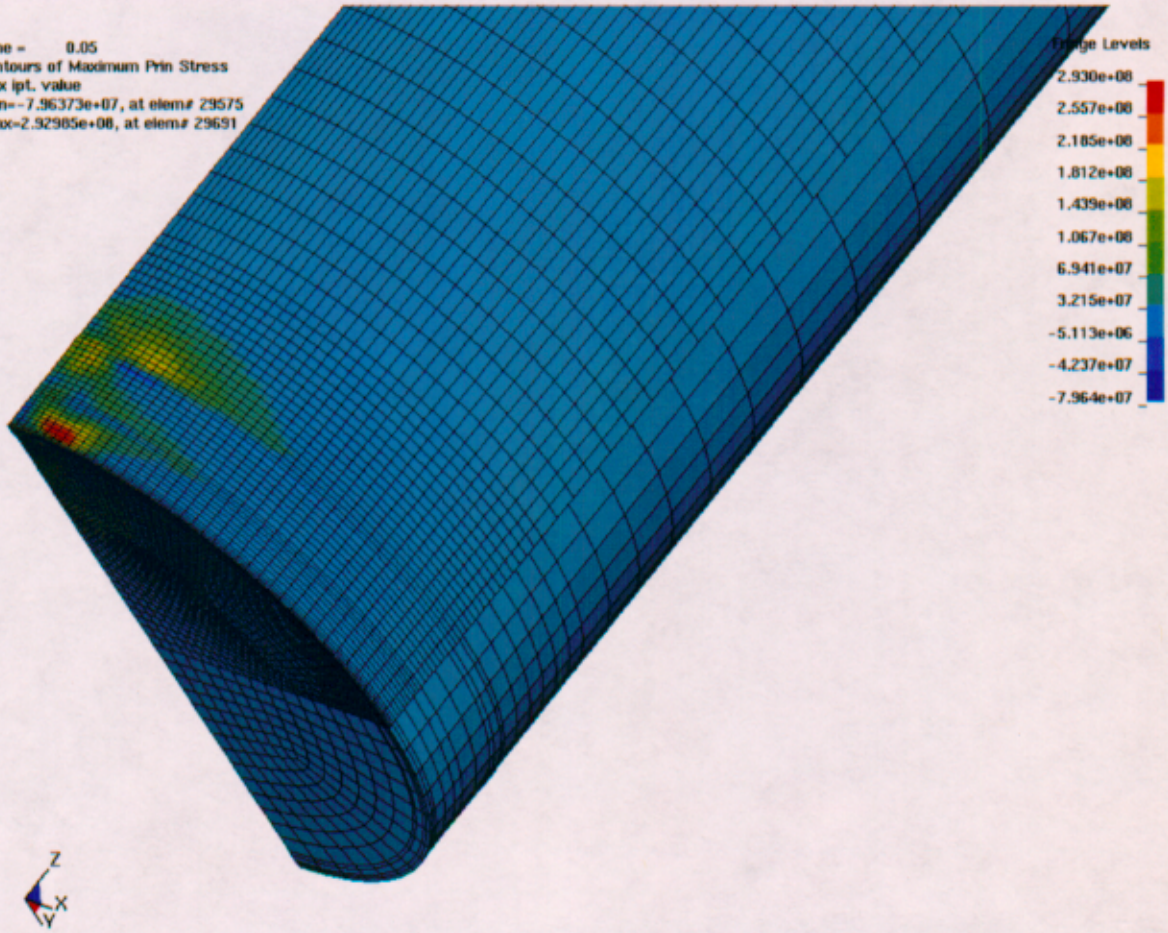

Figure III-13: Mesh F - Maximum Residual 1st Principal Stress, Standard Mesh (*Pa*)

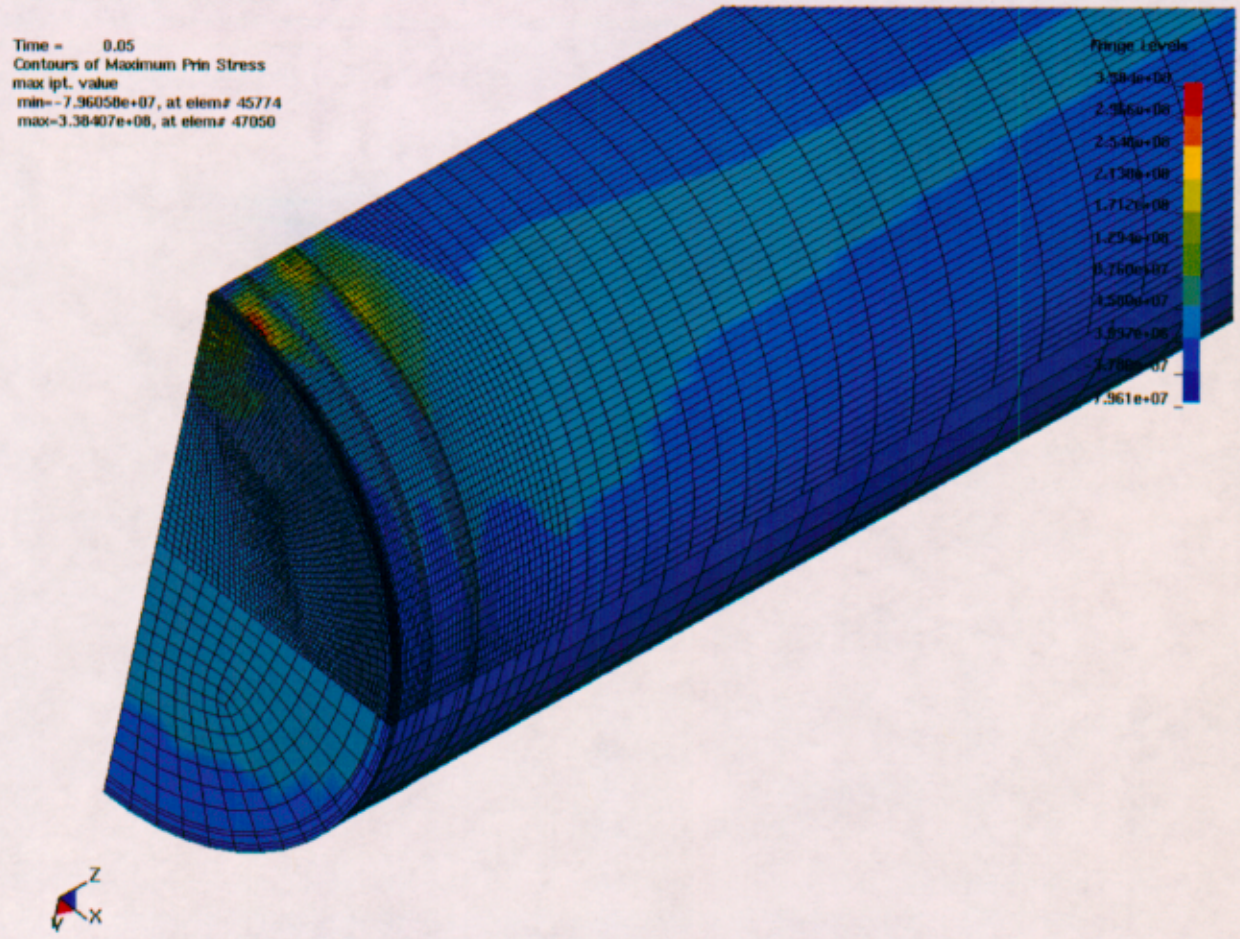

Figure III-14: Mesh F - Maximum Residual 1st Principal Stress, Refined Mesh (*Pa*)

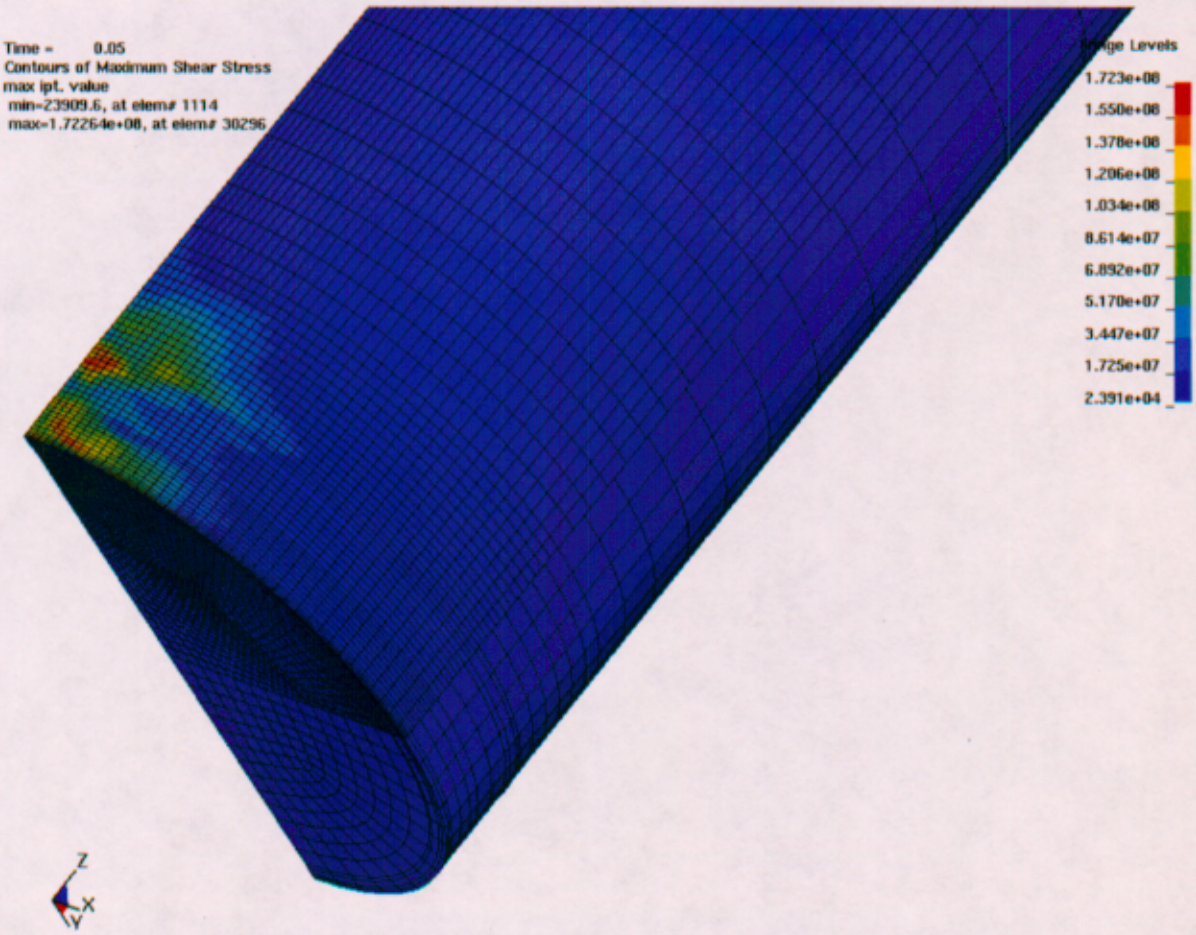

Figure III-15: Mesh F - Maximum Residual Shear Stress, Standard Mesh (*Pa*)

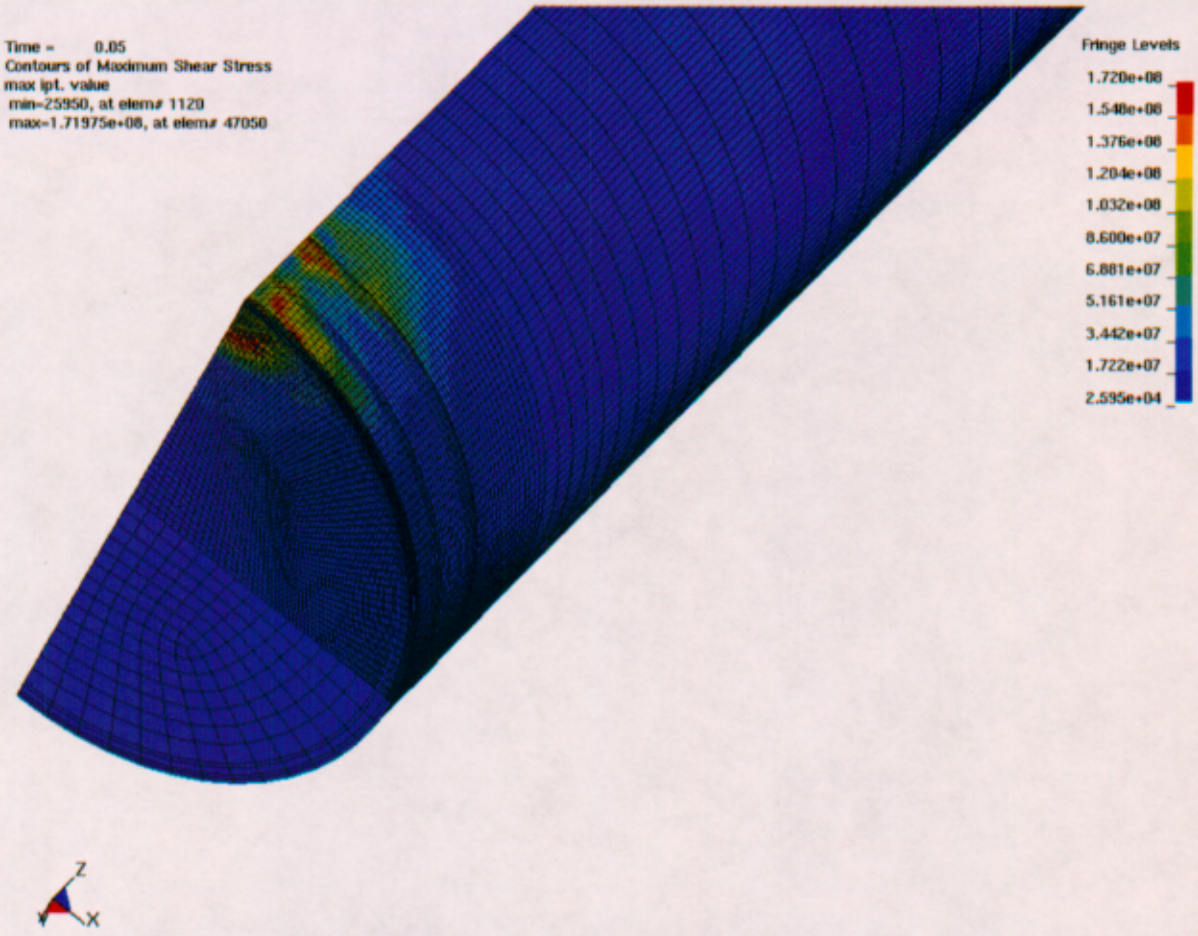

Figure III-16: Mesh F - Maximum Residual Shear Stress, Refined Mesh (*Pa*)

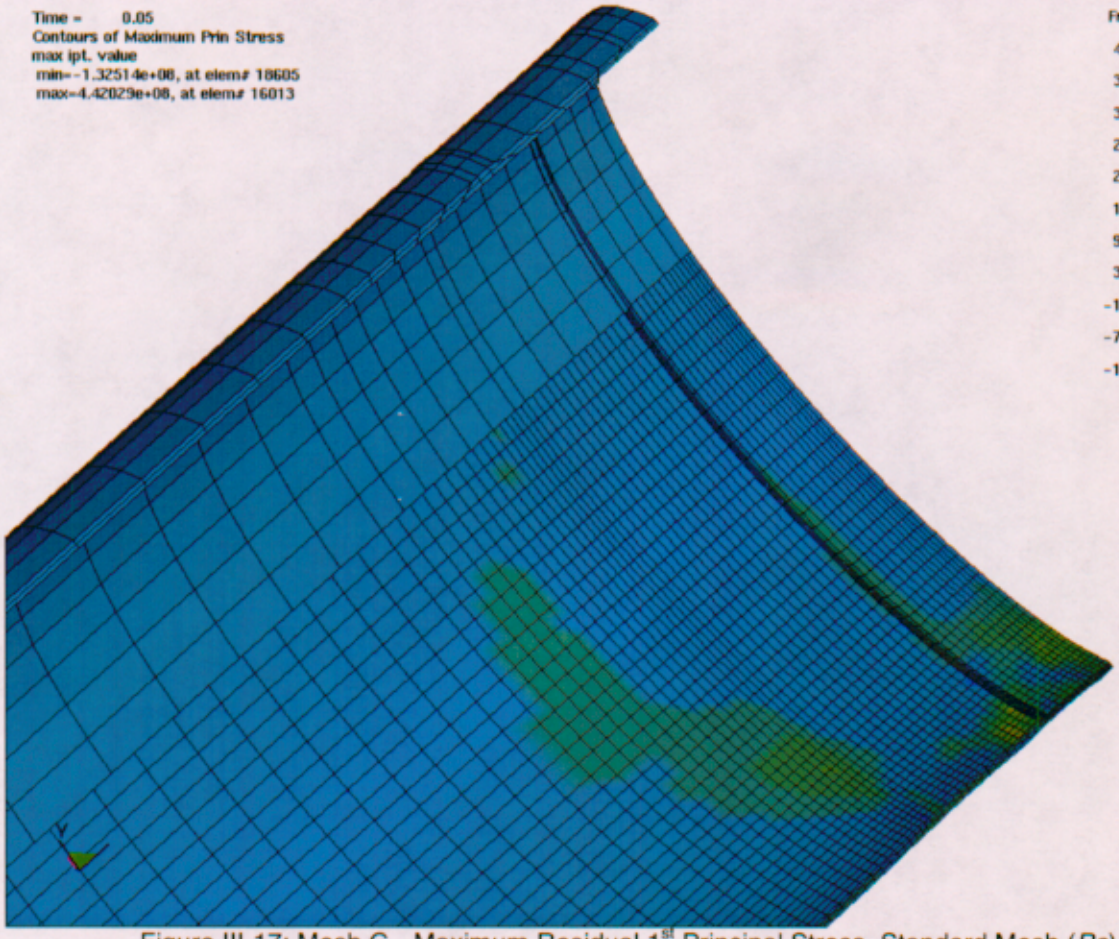

Figure III-17: Mesh G - Maximum Residual 1st Principal Stress, Standard Mesh (*Pa*)

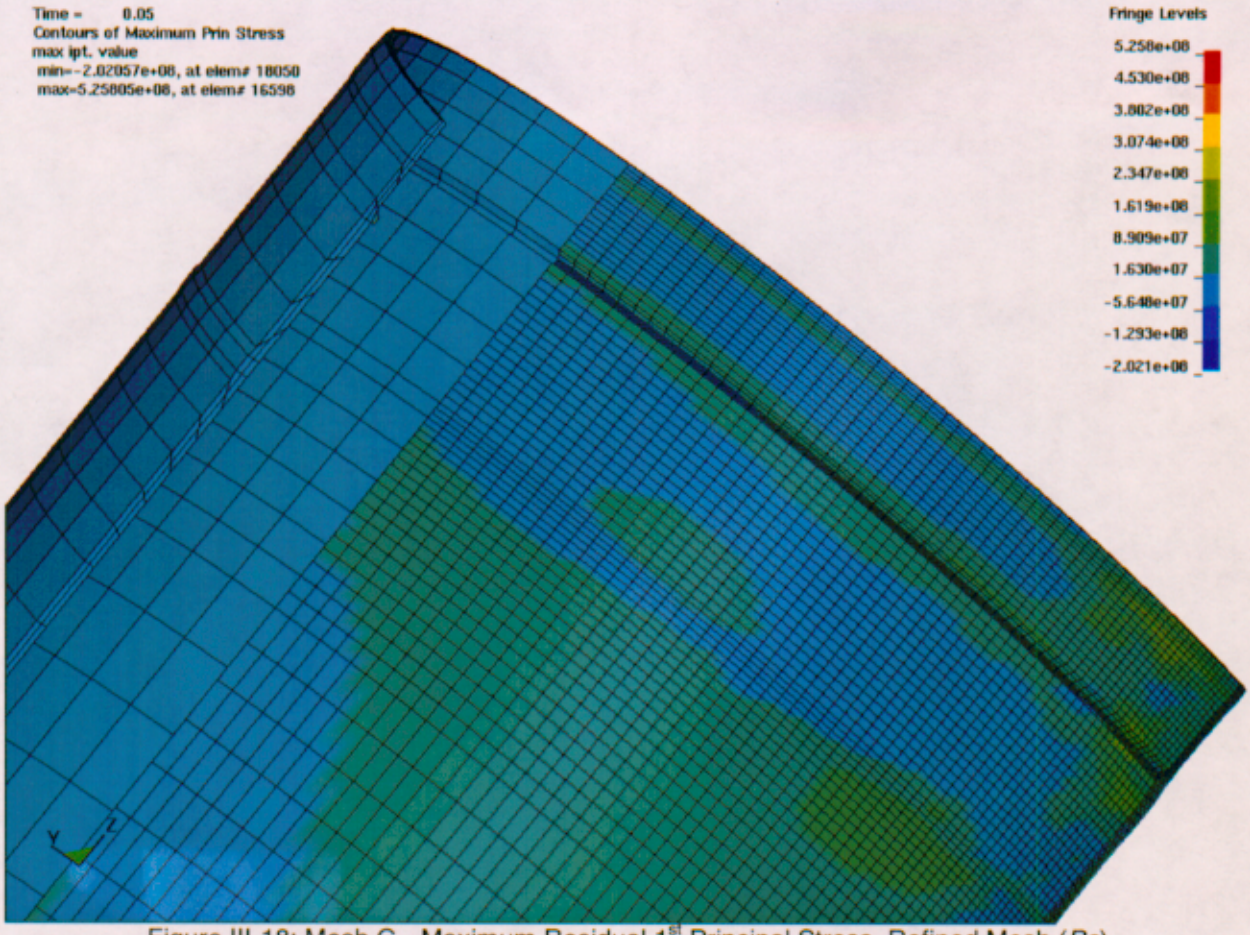

Figure III-18: Mesh G - Maximum Residual 1st Principal Stress, Refined Mesh (*Pa*)

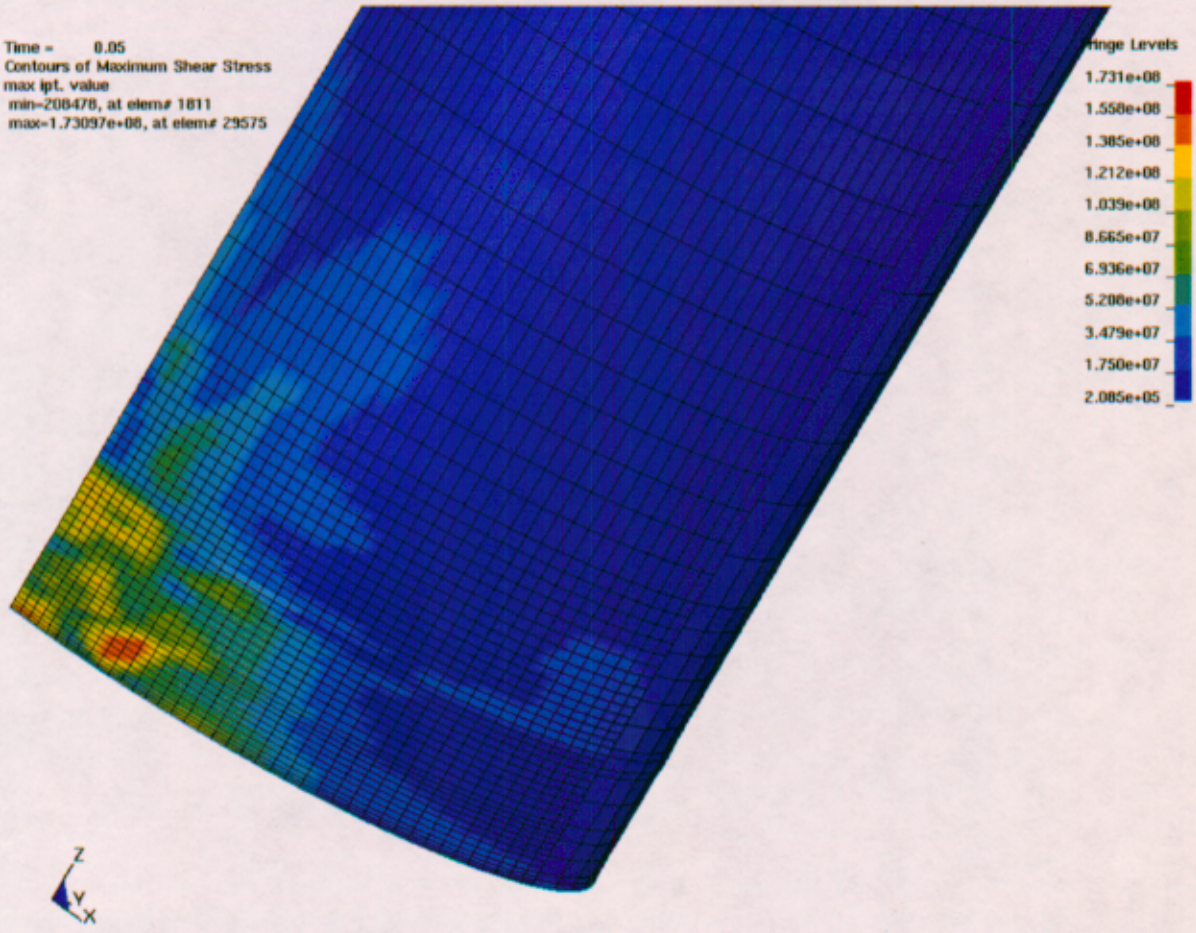

Figure III-19: Mesh G - Maximum Residual Shear Stress, Standard Mesh (*Pa*)

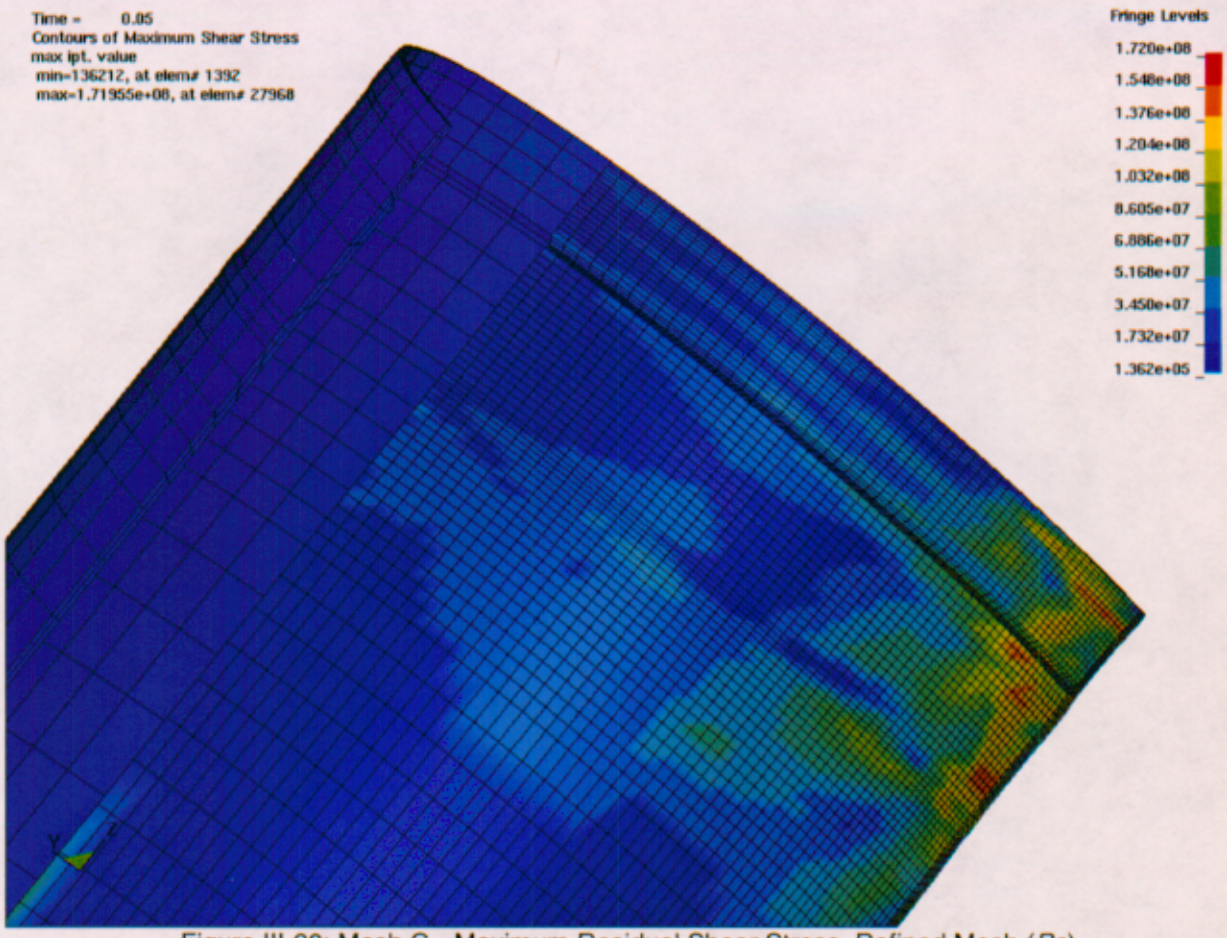

Figure III-20: Mesh G - Maximum Residual Shear Stress, Refined Mesh (*Pa*)

ATTACHMENT V
NAME, SIZE, DATE AND TIME OF CREATION OF THE FILES CONTAINED IN ATTACHEMENT IV (CD)

Name	Size (kB)	Date	Time
gapCD2.zip - alf1v2			
d3hsp	18,049	11/18/02	03:25p
d3plot	7,647	11/18/02	03:25p
d3plot21	4,452	11/18/02	03:24p
nogapnoDT1SR2.k	8	11/18/02	03:25p
gapCD2.zip - alf5v4			
d3hsp	17,913	11/18/02	03:26p
d3plot	7,647	11/18/02	03:27p
d3plot21	4,452	11/18/02	03:27p
nogapnoDT5SR4.k	8	11/18/02	03:26p
gapCD2.zip - geomalf1nogap			
extract_segments2.inp	1	11/18/02	03:29p
geomnogap1FA90.out	689	11/18/02	03:29p
geomnogapFA90.inp	64	11/18/02	03:29p
ngeom3.inc	4,307	11/21/02	02:00p
README.TXT	1	11/21/02	01:59p
gapCD2.zip - geomalf5nogap			
extract_segments2.inp	1	11/18/02	03:29p
geomnogap5.inp	64	11/18/02	03:29p
geomnogap5.out	689	11/18/02	03:29p
ngeom3.inc	4,307	11/21/02	02:01p
README.TXT	1	11/21/02	01:59p
geometry horizontal CD2.zip - Mesh F - horiz 8 deg			
bcgeom3.inc	1	11/6/02	02:21p
egeom3.inc	5,870	11/6/02	02:21p
extract_segments2.inp	2	11/6/02	02:21p
ngeom3.inc	5,707	11/6/02	02:21p
se3isco.inc	6	11/6/02	02:21p
se3isfi.inc	18	11/6/02	02:21p
se3osco.inc	12	11/6/02	02:21p
se3osfi.inc	57	11/6/02	02:21p
standhoriz8bot.inp	65	11/6/02	02:21p
standhoriz8bot.out	750	11/6/02	02:21p
sym3.inc	38	11/6/02	02:21p
geometry horizontal CD2.zip - Mesh G - horiz 1 deg			
bcgeom3.inc	1	11/6/02	02:21p
egeom3.inc	5,870	11/6/02	02:21p
extract_segments2.inp	2	11/6/02	02:21p
ngeom3.inc	5,707	11/6/02	02:21p
se3isco.inc	6	11/6/02	02:21p
se3isfi.inc	18	11/6/02	02:21p
se3osco.inc	12	11/6/02	02:21p
se3osfi.inc	57	11/6/02	02:21p
standhoriz1bot.inp	65	11/6/02	02:21p
standhoriz1bot.out	749	11/6/02	02:21p
sym3.inc	38	11/6/02	02:21p
geometry horizontal CD2.zip - Mesh H - horizontal			
bcgeom3.inc	2	11/6/02	02:20p
egeom3.inc	5,896	11/6/02	02:20p
extract_segments2.inp	2	11/6/02	02:20p

Name	Size (kB)	Date	Time
geomstandhoriz5.inp	66	11/6/02	02:20p
geomstandhoriz5.out	751	11/6/02	02:20p
ngeom3.inc	5,736	11/6/02	02:20p
se3isco.inc	6	11/6/02	02:20p
se3isfi.inc	18	11/6/02	02:20p
se3osco.inc	12	11/6/02	02:20p
se3osfi.inc	57	11/6/02	02:20p
sym3.inc	39	11/6/02	02:20p
geometry vertical CD.zip - Mesh A - vertical			
bcgeom3.inc	2	9/27/02	04:40p
egeom3.inc	3,412	9/27/02	04:40p
extract_segments2.inp	1	9/27/02	04:40p
geomstandvert.inp	63	9/27/02	04:40p
geomstandvert.out	647	9/27/02	04:40p
ngeom3.inc	3,502	9/27/02	04:40p
symx.inc	20	9/27/02	04:40p
symxz.inc	1	9/27/02	04:40p
symz.inc	20	9/27/02	04:40p
geometry vertical CD.zip - Mesh B - 1 deg, v 1, 2, 4			
bcgeom3.inc	4	9/27/02	04:31p
egeom3.inc	4,112	9/27/02	04:31p
extract_segments2.inp	2	9/27/02	04:31p
geomstand1FA90.inp	64	9/27/02	04:31p
geomstand1FA90.out	700	9/27/02	04:31p
ngeom3.inc	4,307	9/27/02	04:31p
se3isco.inc	6	9/27/02	04:31p
se3isfi.inc	11	9/27/02	04:31p
se3osco.inc	13	9/27/02	04:31p
se3osfi.inc	37	9/27/02	04:31p
sym3.inc	31	9/27/02	04:31p
geometry vertical CD.zip - Mesh C - 1deg, v 6, 10, 20			
bcgeom3.inc	4	9/27/02	04:39p
egeom3.inc	6,818	9/27/02	04:39p
extract_segments2.inp	0	9/27/02	04:39p
geom1stand6msbis.inp	64	9/27/02	04:39p
geom1stand6msbis.out	788	9/27/02	04:39p
ngeom3.inc	6,884	9/27/02	04:39p
sym3.inc	40	9/27/02	04:39p
geometry vertical CD.zip - Mesh D - 5deg			
extract_segments2.inp	0	9/27/02	04:40p
geomstand5FA90.inp	64	9/27/02	04:40p
geomstand5FA90.out	698	11/21/02	02:01p
ngeom3.inc	4,307	9/27/02	04:40p
README.TXT	0	11/21/02	01:59p
geometry vertical CD.zip - Mesh E - 8 deg			
extract_segments2.inp	0	9/27/02	04:40p
geomstand8FA90.inp	64	9/27/02	04:40p
geomstand8FA90.out	689	11/21/02	02:02p
ngeom3.inc	4,307	9/27/02	04:40p
README.TXT	0	11/21/02	01:59p

Name	Size (kB)	Date	Time
geometry vertical CD.zip - Mesh J - 5 deg, v 20			
bcgeom3.inc	3	11/21/02	02:07p
egeom3.inc	6,818	11/21/02	02:07p
extract_segments2.inp	1	11/21/02	02:07p
geom5stand20ms.inp	64	11/21/02	02:07p
geom5stand20ms.out	783	11/21/02	02:07p
ngeom3.inc	6,884	11/21/02	02:07p
sym3.inc	40	11/21/02	02:07p
geometry vertical CD.zip - Mesh K - 8 deg, v 20			
bcgeom3.inc	4	11/21/02	02:08p
egeom3.inc	6,818	11/21/02	02:08p
extract_segments2.inp	1	11/21/02	02:08p
geom8stand20ms.inp	64	11/21/02	02:08p
geom8stand20ms.out	783	11/21/02	02:08p
ngeom3.inc	6,884	11/21/02	02:08p
sym3.inc	40	11/21/02	02:08p
mesh refinementCD.zip - horizontal drops\geom mesh G - 1deg			
bcgeom3.inc	1	11/6/02	02:24p
egeom3.inc	11,146	11/6/02	02:24p
extract_segments2.inp	2	11/6/02	02:24p
geomrefbot1ax4.inp	66	11/6/02	02:24p
geomrefbot1ax4.out	796	11/6/02	02:24p
ngeom3.inc	10,213	11/6/02	02:24p
se3isco.inc	6	11/6/02	02:23p
se3isfi.inc	18	11/6/02	02:23p
se3osco.inc	12	11/6/02	02:23p
se3osfi.inc	90	11/6/02	02:23p
sym3.inc	48	11/6/02	02:23p
mesh refinementCD.zip - horizontal drops\geom mesh H - horizontal			
bcgeom3.inc	2	11/6/02	02:23p
egeom3.inc	11,172	11/6/02	02:23p
extract_segments2.inp	2	11/6/02	02:23p
geomrefhorizax4.inp	66	11/6/02	02:23p
geomrefhorizax4.out	799	11/6/02	02:23p
ngeom3.inc	10,241	11/6/02	02:23p
se3isco.inc	6	11/6/02	02:23p
se3isfi.inc	18	11/6/02	02:23p
se3osco.inc	12	11/6/02	02:23p
se3osfi.inc	90	11/6/02	02:23p
sym3.inc	48	11/6/02	02:23p
mesh refinementCD.zip - horizontal drops\run mesh G - 1deg			
d3hsp	42,993	11/6/02	02:28p
d4plot	19,296	11/6/02	02:28p
d4plot51	11,043	11/6/02	02:28p
horizrefbotalf1v4.k	8	11/6/02	02:28p
mesh refinementCD.zip - horizontal drops\run mesh H - horiz			
d3hsp	43,112	11/6/02	02:27p
d4plot	19,345	11/6/02	02:28p
d4plot21	11,071	11/6/02	02:27p
horrefax4alf0v6.k	9	11/6/02	02:27p
mesh refinementCD.zip - vertical drops\geom mesh A - vertical			
bcgeom3.inc	2	11/6/02	02:34p
egeom3.inc	7,892	11/6/02	02:34p
extract_segments2.inp	1	11/6/02	02:34p
geomvertref9total.inp	64	11/6/02	02:34p
geomvertref9total.out	688	11/6/02	02:34p
ngeom3.inc	7,330	11/6/02	02:34p
symx.inc	29	11/6/02	02:34p
symxz.inc	1	11/6/02	02:34p
symz.inc	29	11/6/02	02:34p
mesh refinementCD.zip - vertical drops\geom mesh C - 1deg6ms			
bcgeom3.inc	4	11/6/02	02:37p
egeom3.inc	9,467	11/6/02	02:37p
extract_segments2.inp	1	11/6/02	02:37p
geom1ref6msbis.inp	64	11/6/02	02:37p
geom1ref6msbis.out	827	11/6/02	02:37p
ngeom3.inc	9,173	11/6/02	02:37p
sym3.inc	47	11/6/02	02:37p
mesh refinementCD.zip - vertical drops\geom mesh D - 5deg			
bcgeom3.inc	4	11/6/02	02:38p
egeom3.inc	5,587	11/6/02	02:38p
extract_segments2.inp	2	11/6/02	02:38p
geomref5FA90.inp	64	11/6/02	02:38p
geomref5FA90.out	13	11/6/02	02:38p
ngeom3.inc	5,621	11/6/02	02:38p
se3isco.inc	6	11/6/02	02:38p
se3isfi.inc	12	11/6/02	02:38p
se3osco.inc	13	11/6/02	02:38p
se3osfi.inc	49	11/6/02	02:38p
sym3.inc	35	11/6/02	02:38p
mesh refinementCD.zip - vertical drops\run mesh A - vertical			
d3hsp	30,529	11/6/02	02:41p
d3plot	13,588	11/6/02	02:41p
d3plot21	7,717	11/6/02	02:41p
ref9totvert4.k	6	11/6/02	02:41p
mesh refinementCD.zip - vertical drops\run mesh C - 1deg6ms			
d3hsp	37,979	11/6/02	02:44p
d4plot	16,712	11/6/02	02:44p
d4plot51	9,562	11/6/02	02:44p
ref1SR6.k	6	11/6/02	02:44p
mesh refinementCD.zip - vertical drops\run mesh D - 5deg			
d3hsp	23,341	11/15/02	08:59a
d3hsp2	15	11/15/02	08:59a
d3plot	10,119	11/15/02	09:00a
d3plot21	5,845	11/15/02	09:00a
ref5SR4noDT.k	8	11/15/02	08:59a
SD5 - end impacts 100 C.zip - 1deg\alf1v1			
d3hsp	17,883	11/13/02	10:53a
d3plot	7,647	11/13/02	10:53a
d3plot21	4,452	11/13/02	10:53a
stand1SR1.k	8	11/13/02	10:53a
SD5 - end impacts 100 C.zip - 1deg\alf1v2			
d3hsp	17,883	11/13/02	10:55a
d3plot	7,647	11/13/02	10:55a
d3plot21	4,452	11/13/02	10:55a
stand1SR2.k	8	11/13/02	10:55a
SD5 - end impacts 100 C.zip - 1deg\v10			

Name	Size (kB)	Date	Time
d3hspalf1v10new	28,344	10/3/02	02:31p
d4plot	12,333	10/3/02	02:37p
d4plot51	7,109	10/3/02	02:37p
stand1SR10NEW.k	6	10/3/02	02:31p
SD5 - end impacts 100 C.zip - 1deg\v4			
d3hspalf1v4	17,884	10/1/02	03:15p
d3plot	7,647	10/1/02	03:38p
d3plot51	4,452	10/1/02	03:38p
stand1SR4.k	8	10/1/02	03:15p
SD5 - end impacts 100 C.zip - 1deg\v6			
d3hspalf1v6new	28,344	10/3/02	02:31p
d4plot	12,333	10/3/02	02:38p
d4plot51	7,109	10/3/02	02:37p
stand1SR6NEW.k	6	10/3/02	02:31p
SD5 - end impacts 100 C.zip - 5deg\alf5v1			
d3hsp	18,020	11/13/02	10:57a
d4plot	7,647	11/13/02	10:57a
d4plot21	4,452	11/13/02	10:57a
stand5SR1.k	8	11/13/02	10:57a
SD5 - end impacts 100 C.zip - 5deg\alf5v10			
d3hsp	18,020	11/13/02	10:59a
d4plot	7,647	11/13/02	10:59a
d4plot21	4,452	11/13/02	10:59a
stand5SR10.k	8	11/13/02	10:59a
SD5 - end impacts 100 C.zip - 5deg\alf5v2			
d3hsp	18,020	11/13/02	10:58a
d4plot	7,647	11/13/02	10:58a
d4plot21	4,452	11/13/02	10:58a
stand5SR2.k	8	11/13/02	10:58a
SD5 - end impacts 100 C.zip - 5deg\alf5v4			
d3hsp	17,883	11/13/02	11:00a
d3plot	7,647	11/13/02	11:00a
d3plot21	4,452	11/13/02	11:00a
stand5SR4.k	8	11/13/02	11:00a
SD5 - end impacts 100 C.zip - 5deg\alf5v6			
d3hsp	17,884	11/13/02	10:54a
d3plot	7,647	11/13/02	10:54a
d3plot51	4,452	11/13/02	10:54a
stand5SR6.k	8	11/13/02	10:54a
SD5 - end impacts 100 C.zip - 8deg\alf8v1			
d3hsp	17,883	11/13/02	11:02a
d3plot	7,647	11/13/02	11:02a
d3plot21	4,452	11/13/02	11:02a
stand8SR1.k	8	11/13/02	11:02a
SD5 - end impacts 100 C.zip - 8deg\alf8v10			
d3hsp	17,883	11/13/02	11:04a
d3plot	7,647	11/13/02	11:03a
d3plot21	4,452	11/13/02	11:03a
stand8SR10.k	8	11/13/02	11:04a
SD5 - end impacts 100 C.zip - 8deg\alf8v2			
d3hsp	17,883	11/13/02	10:56a
d3plot	7,647	11/13/02	10:56a
d3plot21	4,452	11/13/02	10:56a
stand8SR2.k	8	11/13/02	10:56a
SD5 - end impacts 100 C.zip - 8deg\alf8v4			
d3hsp	17,883	11/13/02	11:03a
d3plot	7,647	11/13/02	11:03a
d3plot21	4,452	11/13/02	11:03a

Name	Size (kB)	Date	Time
stand8SR4.k	8	11/13/02	11:02a
SD5 - end impacts 100 C.zip - 8deg\alf8v6			
d3hsp	17,883	11/13/02	11:01a
d3plot	7,647	11/13/02	11:01a
d3plot21	4,452	11/13/02	11:01a
stand8SR6.k	8	11/13/02	11:00a
SD5 - end impacts 100 C.zip - vertical\v1			
d3hspvert1	14,467	10/1/02	03:16p
d3plot	6,224	10/1/02	03:16p
d3plot51	3,594	10/1/02	03:16p
STANDvert1.k	6	10/1/02	03:16p
SD5 - end impacts 100 C.zip - vertical\v10			
d3hspvert10	14,467	9/27/02	03:43p
d3plot	6,224	10/1/02	03:24p
d3plot51	3,594	10/1/02	03:24p
STANDvert10.k	6	9/27/02	03:43p
SD5 - end impacts 100 C.zip - vertical\v2			
d3hspvert2	14,467	10/1/02	03:11p
d3plot	6,224	10/1/02	03:10p
d3plot51	3,594	10/1/02	03:10p
STANDvert2.k	6	10/1/02	03:11p
SD5 - end impacts 100 C.zip - vertical\v4			
d3hspvert4	14,467	9/27/02	04:13p
d3plot	6,224	10/1/02	03:25p
d3plot51	3,594	10/1/02	03:24p
STANDvert4.k	6	9/27/02	04:13p
SD5 - end impacts 100 C.zip - vertical\v6			
d3hspvert6	14,583	9/27/02	04:29p
d3plot	6,224	10/1/02	03:32p
d3plot51	3,594	10/1/02	03:32p
STANDvert6.k	6	9/27/02	04:29p
SD6 - end impacts 150C.zip - 1deg\alf1v1			
d3hsp	17,883	11/13/02	11:26a
d3plot	7,647	11/13/02	11:26a
d3plot21	4,452	11/13/02	11:26a
stand1SR1.k	8	11/13/02	11:26a
SD6 - end impacts 150C.zip - 1deg\alf1v2			
d3hsp	17,883	11/13/02	11:32a
d3plot	7,647	11/13/02	11:31a
d3plot21	4,452	11/13/02	11:31a
stand1SR2.k	8	11/13/02	11:32a
SD6 - end impacts 150C.zip - 1deg\v10			
d3hspalf1v10	28,067	9/27/02	04:15p
d3plot	12,333	10/1/02	03:25p
d3plot51	7,109	10/1/02	03:25p
stand1SR10NEW.k	6	9/27/02	04:15p
SD6 - end impacts 150C.zip - 1deg\v20			
d3hsp	28,067	11/21/02	04:07p
d4plot	12,333	11/21/02	04:08p
d4plot51	7,109	11/21/02	04:08p
stand1SR20.k	6	11/21/02	04:07p
SD6 - end impacts 150C.zip - 1deg\v4			
d3hspalf1v4	18,022	9/27/02	04:29p
d3plot	7,647	10/1/02	03:33p
d3plot51	4,452	10/1/02	03:33p
stand1SR4.k	8	9/27/02	04:29p
SD6 - end impacts 150C.zip - 1deg\v6			
d3hspalf1v6	28,067	9/27/02	04:15p

Name	Size (kB)	Date	Time
d3plot	12,333	10/1/02	03:25p
d3plot51	7,109	10/1/02	03:25p
stand1SR6NEW.k	6	9/27/02	04:15p
SD6 - end impacts 150C.zip - 5deg\alf5v1			
d3hsp	17,883	11/13/02	11:34a
d3plot	7,647	11/13/02	11:34a
d3plot21	4,452	11/13/02	11:34a
stand5SR1.k	8	11/13/02	11:34a
SD6 - end impacts 150C.zip - 5deg\alf5v10			
d3hsp	17,883	11/13/02	11:35a
d3plot	7,647	11/13/02	11:35a
d3plot21	4,452	11/13/02	11:35a
stand5SR10.k	8	11/13/02	11:35a
SD6 - end impacts 150C.zip - 5deg\alf5v2			
d3hsp	17,883	11/13/02	11:27a
d3plot	7,647	11/13/02	11:28a
d3plot20	4,452	11/13/02	11:28a
stand5SR2.k	8	11/13/02	11:27a
SD6 - end impacts 150C.zip - 5deg\alf5v4			
d3hsp	17,883	11/13/02	11:29a
d3plot	7,647	11/13/02	11:29a
d3plot21	4,452	11/13/02	11:29a
stand5SR4.k	8	11/13/02	11:29a
SD6 - end impacts 150C.zip - 5deg\alf5v6			
d3hsp	17,883	11/13/02	11:37a
d3plot	7,647	11/13/02	11:37a
d3plot21	4,452	11/13/02	11:37a
stand5SR6.k	8	11/13/02	11:37a
SD6 - end impacts 150C.zip - 5deg\v20			
d3hsp	28,072	11/21/02	04:09p
d4plot	12,333	11/21/02	04:09p
d4plot21	7,109	11/21/02	04:09p
stand5SR20.k	6	11/21/02	04:09p
SD6 - end impacts 150C.zip - 8deg\alf8v1			
d3hsp	17,883	11/13/02	11:38a
d3plot	7,647	11/13/02	11:38a
d3plot21	4,452	11/13/02	11:38a
stand8SR1.k	8	11/13/02	11:38a
SD6 - end impacts 150C.zip - 8deg\alf8v10			
d3hsp	17,883	11/13/02	11:33a
d3plot	7,647	11/13/02	11:33a
d3plot21	4,452	11/13/02	11:33a
stand8SR10.k	8	11/13/02	11:33a
SD6 - end impacts 150C.zip - 8deg\alf8v2			
d3hsp	17,883	11/13/02	11:36a
d3plot	7,647	11/13/02	11:35a
d3plot21	4,452	11/13/02	11:35a
stand8SR2.k	8	11/13/02	11:36a
SD6 - end impacts 150C.zip - 8deg\alf8v4			
d3hsp	18,020	11/13/02	11:39a
d3plot	7,647	11/13/02	11:39a
d3plot21	4,452	11/13/02	11:39a
stand8SR4.k	8	11/13/02	11:39a
SD6 - end impacts 150C.zip - 8deg\alf8v6			
d3hsp	17,884	11/13/02	11:30a
d3plot	7,647	11/13/02	11:30a
d3plot51	4,452	11/13/02	11:30a
stand8SR6.k	8	11/13/02	11:30a

Name	Size (kB)	Date	Time
SD6 - end impacts 150C.zip - 8deg\v20			
d3hsp	28,074	11/21/02	04:10p
d4plot	12,333	11/21/02	04:10p
d4plot21	7,109	11/21/02	04:10p
stand8SR20.k	6	11/21/02	04:10p
SD6 - end impacts 150C.zip - vertical\alf0v10			
d3hspalf0v10	14,581	11/13/02	11:41a
d4plot	6,224	11/13/02	11:40a
d4plot21	3,594	11/13/02	11:40a
STANDvert10.k	6	11/13/02	11:41a
SD6 - end impacts 150C.zip - vertical\v2			
d3hspvert2	14,391	10/3/02	02:36p
d4plot	6,224	10/3/02	02:36p
d4plot51	3,594	10/3/02	02:36p
STANDvert2.k	5	10/3/02	02:36p
SD6 - end impacts 150C.zip - vertical\v20			
d3hsp	14,474	11/21/02	04:08p
d4plot	6,224	11/21/02	04:08p
d4plot21	3,594	11/21/02	04:08p
STANDvert20.k	6	11/21/02	04:08p
SD6 - end impacts 150C.zip - vertical\v4			
d3hspvert4	14,391	10/3/02	02:36p
d4plot	6,224	10/3/02	02:36p
d4plot51	3,594	10/3/02	02:36p
STANDvert4.k	5	10/3/02	02:36p
SD6 - end impacts 150C.zip - vertical\v6			
d3hspvert6	14,467	9/27/02	04:18p
d3plot	6,238	9/27/02	04:18p
d3plot51	3,605	9/27/02	04:18p
STANDvert6.k	6	9/27/02	04:18p
SD7 - side impacts 150C.zip - 1deg\v10			
d3hspalf1v10	24,044	11/6/02	02:08p
d4plot	10,625	11/6/02	02:09p
d4plot21	6,187	11/6/02	02:09p
horizalf1v10.k	8	11/6/02	02:08p
SD7 - side impacts 150C.zip - 1deg\v2			
d3hspalf1v2	24,044	11/6/02	02:07p
d3plot	10,625	11/6/02	02:07p
d3plot21	6,187	11/6/02	02:07p
horizalf1v2.k	8	11/6/02	02:07p
SD7 - side impacts 150C.zip - 1deg\v20			
d3hsp	24,259	12/4/02	07:33a
d3hsp2	9	12/4/02	07:33a
d4plot	10,625	12/4/02	07:33a
d4plot21	6,187	12/4/02	07:33a
horizalf1v20.k	9	12/4/02	07:33a
SD7 - side impacts 150C.zip - 1deg\v4			
d3hspalf1v4	24,235	11/22/02	10:16a
d4plot	10,625	11/22/02	10:15a
d4plot51	6,187	11/22/02	10:15a
horizalf1v4.k	8	11/22/02	10:16a
SD7 - side impacts 150C.zip - 1deg\v6			
d3hsp2alf1v6	9	11/22/02	10:18a
d3hspalf1v6	24,230	11/22/02	10:18a
d4plot	10,625	11/22/02	10:19a
d4plot21	6,187	11/22/02	10:18a
horizalf1v6.k	8	11/22/02	10:17a
SD7 - side impacts 150C.zip - 8deg\v10			

Name	Size (kB)	Date	Time
d3hspalf8v10	24,050	11/6/02	02:15p
d3plot	10,625	11/6/02	02:15p
d3plot21	6,187	11/6/02	02:15p
horizalf8v10.k	8	11/6/02	02:15p
SD7 - side impacts 150C.zip - 8deg\v2			
d3hsp	24,050	11/22/02	10:28a
d3plot	10,625	11/22/02	10:29a
d3plot21	6,187	11/22/02	10:28a
horizalf8v2.k	8	11/22/02	10:28a
SD7 - side impacts 150C.zip - 8deg\v20			
d3hsp	24,264	12/4/02	07:34a
d4plot	10,625	12/4/02	07:34a
d4plot21	6,187	12/4/02	07:34a
horizalf8v20.k	9	12/4/02	07:34a
SD7 - side impacts 150C.zip - 8deg\v4			
d3hspalf8v4	24,245	11/6/02	02:13p
d3plot	10,625	11/6/02	02:13p
d3plot21	6,187	11/6/02	02:13p
horizalf8v4.k	8	11/6/02	02:13p
SD7 - side impacts 150C.zip - 8deg\v6			
d3hspalf8v6	24,245	11/6/02	02:03p
d3plot	10,625	11/6/02	02:04p
d3plot21	6,187	11/6/02	02:04p
horizalf8v6.k	8	11/6/02	02:03p
SD7 - side impacts 150C.zip - horizontal\v1			
d3hspalf0v1	24,165	11/6/02	01:50p
d4plot	10,672	11/6/02	01:50p
d4plot21	6,216	11/6/02	01:50p
horizalf0v1.k	9	11/6/02	01:50p
SD7 - side impacts 150C.zip - horizontal\v10			
d3hspalf0v10	24,166	11/6/02	01:56p
d3plot	10,672	11/6/02	01:57p
d3plot51	6,216	11/6/02	01:57p
horizalf0v10.k	9	11/6/02	01:56p
SD7 - side impacts 150C.zip - horizontal\v2			
d3hspalf0v2	24,362	11/6/02	02:01p
d3plot	10,672	11/6/02	02:01p
d3plot51	6,216	11/6/02	02:01p
horizalf0v2.k	9	11/6/02	02:01p
SD7 - side impacts 150C.zip - horizontal\v20			
d3hsp	24,380	12/4/02	07:35a
d4plot	10,672	12/4/02	07:35a
d4plot21	6,216	12/4/02	07:34a
horizalf0v20.k	9	12/4/02	07:35a
SD7 - side impacts 150C.zip - horizontal\v4			
d3hsp	24,362	11/22/02	10:26a
d3plot	10,672	11/22/02	10:26a
d3plot51	6,216	11/22/02	10:26a
horizalf0v4.k	9	11/22/02	10:26a
SD7 - side impacts 150C.zip - horizontal\v6			
d3hspalf0v6	24,166	11/6/02	01:53p
d3plot	10,672	11/6/02	01:53p
d3plot51	6,216	11/6/02	01:53p
horizalf0v6.k	9	11/6/02	01:53p
SD8 - end impacts 200C revA.zip - 1deg\alf1v1			
d3hsp	18020	12/18/02	01:03p
d4plot	7647	12/18/02	01:03p
d4plot21	4452	12/18/02	01:03p

Name	Size (kB)	Date	Time
stand1SR1.k	8	12/18/02	01:03p
SD8 - end impacts 200C revA.zip - 1deg\alf1v10			
d3hspalf1v10	28342	11/21/02	04:35p
d4plot	12333	11/21/02	04:34p
d4plot21	7109	11/21/02	04:34p
stand1SR10.k	6	11/21/02	04:35p
SD8 - end impacts 200C revA.zip - 1deg\alf1v2			
d3hsp	18020	11/21/02	04:14p
d4plot	7647	11/21/02	04:14p
d4plot21	4452	11/21/02	04:14p
stand1SR2.k	8	11/21/02	04:14p
SD8 - end impacts 200C revA.zip - 1deg\alf1v20			
d3hsp	28065	11/21/02	04:39p
d4plot	12333	11/21/02	04:39p
d4plot21	7109	11/21/02	04:39p
stand1SR20.k	6	11/21/02	04:39p
SD8 - end impacts 200C revA.zip - 1deg\alf1v4			
d3hsp	17883	11/21/02	04:22p
d4plot	7647	11/21/02	04:22p
d4plot21	4452	11/21/02	04:22p
stand1SR4.k	8	11/21/02	04:22p
SD8 - end impacts 200C revA.zip - 1deg\alf1v6			
d3hsp	28344	12/18/02	01:03p
d4plot	12333	12/18/02	01:05p
d4plot51	7109	12/18/02	01:05p
stand1SR6.k	6	12/18/02	01:03p
SD8 - end impacts 200C revA.zip - 5deg\alf5v1			
d3hsp	17883	11/21/02	04:29p
d4plot	7647	11/21/02	04:29p
d4plot21	4452	11/21/02	04:29p
stand5SR1.k	8	11/21/02	04:29p
SD8 - end impacts 200C revA.zip - 5deg\alf5v10			
d3hsp	18020	11/21/02	04:18p
d4plot	7647	11/21/02	04:18p
d4plot21	4452	11/21/02	04:18p
stand5SR10.k	8	11/21/02	04:18p
SD8 - end impacts 200C revA.zip - 5deg\alf5v2			
d3hsp	18020	12/18/02	01:06p
d4plot	7647	12/18/02	01:06p
d4plot21	4452	12/18/02	01:05p
stand5SR2.k	8	12/18/02	01:06p
SD8 - end impacts 200C revA.zip - 5deg\alf5v20			
d3hsp	28071	11/21/02	04:40p
d4plot	12333	11/21/02	04:40p
d4plot21	7109	11/21/02	04:40p
stand5SR20.k	6	11/21/02	04:40p
SD8 - end impacts 200C revA.zip - 5deg\alf5v4			
d3hsp	18020	11/21/02	04:18p
d4plot	7647	11/21/02	04:18p
d4plot21	4452	11/21/02	04:18p
stand5SR4.k	8	11/21/02	04:18p
SD8 - end impacts 200C revA.zip - 5deg\alf5v6			
d3hsp	18020	11/21/02	04:36p
d4plot	7647	11/21/02	04:36p
d4plot21	4452	11/21/02	04:36p
stand5SR6.k	8	11/21/02	04:35p
SD8 - end impacts 200C revA.zip - 8deg\alf8v1			
d3hsp	18020	11/21/02	04:19p

Name	Size (kB)	Date	Time
d4plot	7647	11/21/02	04:19p
d4plot21	4452	11/21/02	04:19p
stand8SR1.k	8	11/21/02	04:19p
SD8 - end impacts 200C revA.zip - 8deg\alf8v10			
d3hsp	18018	11/21/02	04:38p
d3hsp2	9	11/21/02	04:37p
d4plot	7647	11/21/02	04:38p
d4plot21	4452	11/21/02	04:38p
stand8SR10.k	8	11/21/02	04:37p
SD8 - end impacts 200C revA.zip - 8deg\alf8v2			
d3hsp	17883	11/21/02	04:25p
d4plot	7647	11/21/02	04:25p
d4plot26	4452	11/21/02	04:25p
stand8SR2.k	8	11/21/02	04:25p
SD8 - end impacts 200C revA.zip - 8deg\alf8v20			
d3hsp	28074	11/21/02	04:44p
d4plot	12333	11/21/02	04:43p
d4plot21	7109	11/21/02	04:43p
stand8SR20.k	6	11/21/02	04:43p
SD8 - end impacts 200C revA.zip - 8deg\alf8v4			
d3hsp	18020	12/18/02	01:06p
d4plot	7647	12/18/02	01:06p
d4plot21	4452	12/18/02	01:06p
stand8SR4.k	8	12/18/02	01:06p
SD8 - end impacts 200C revA.zip - 8deg\alf8v6			
d3hspalf8v6	18020	11/21/02	04:37p
d4plot	7647	11/21/02	04:37p
d4plot21	4452	11/21/02	04:36p
stand8SR6.k	8	11/21/02	04:37p
SD8 - end impacts 200C revA.zip - vertical\v10			
d3hsp	14465	11/21/02	04:32p
d4plot	6224	11/21/02	04:32p
d4plot21	3594	11/21/02	04:32p
STANDvert10.	6	11/21/02	04:32p
SD8 - end impacts 200C revA.zip - vertical\v2			
d3hsp	14467	11/21/02	04:41p
d4plot	6224	11/21/02	04:41p
d4plot51	3594	11/21/02	04:41p
STANDvert2.k	6	11/21/02	04:41p
SD8 - end impacts 200C revA.zip - vertical\v20			
d3hsp	14474	11/21/02	04:33p
d4plot	6224	11/21/02	04:33p
d4plot21	3594	11/21/02	04:32p
STANDvert20.	6	11/21/02	04:33p
SD8 - end impacts 200C revA.zip - vertical\v4			
d3hsp	14465	11/21/02	04:42p
d4plot	6224	11/21/02	04:43p
d4plot21	3594	11/21/02	04:43p
STANDvert4.k	6	11/21/02	04:42p
SD8 - end impacts 200C revA.zip - vertical\v6			
d3hsp	14465	11/21/02	04:33p
d4plot	6224	11/21/02	04:33p
d4plot21	3594	11/21/02	04:33p
STANDvert6.k	6	11/21/02	04:33p
SD9 - side impacts 200C.zip - 1deg\v1			
d3hsp	24,044	11/22/02	10:41a
d3plot	10,625	11/22/02	10:41a
d3plot21	6,187	11/22/02	10:41a

Name	Size (kB)	Date	Time
horizalf1v1.k	8	11/22/02	10:41a
SD9 - side impacts 200C.zip - 1deg\v10			
d3hspalf1v10	24,240	11/22/02	10:47a
d4plot	10,625	11/22/02	10:47a
d4plot21	6,187	11/22/02	10:47a
horizalf1v10.k	8	11/22/02	10:47a
SD9 - side impacts 200C.zip - 1deg\v2			
d3hsp	24,044	11/22/02	10:44a
d3plot	10,625	11/22/02	10:43a
d3plot21	6,187	11/22/02	10:43a
horizalf1v2.k	8	11/22/02	10:43a
SD9 - side impacts 200C.zip - 1deg\v20			
d3hsp	24,259	12/4/02	04:23p
d4plot	10,625	12/4/02	04:23p
d4plot21	6,187	12/4/02	04:23p
horizalf1v20.k	9	12/4/02	04:23p
SD9 - side impacts 200C.zip - 1deg\v4			
d3hsp	24,240	11/22/02	10:44a
d3plot	10,625	11/22/02	10:45a
d3plot21	6,187	11/22/02	10:45a
horizalf1v4.k	8	11/22/02	10:44a
SD9 - side impacts 200C.zip - 1deg\v6			
d3hspalf1v6	24,240	11/22/02	10:46a
d4plot	10,625	11/22/02	10:46a
d4plot21	6,187	11/22/02	10:46a
horizalf1v6.k	8	11/22/02	10:46a
SD9 - side impacts 200C.zip - 8deg\v10			
d3hsp	24,050	11/22/02	10:49a
d3plot	10,625	11/22/02	10:50a
d3plot21	6,187	11/22/02	10:50a
horizalf8v10.k	8	11/22/02	10:49a
SD9 - side impacts 200C.zip - 8deg\v2			
d3hsp	24,050	11/22/02	10:48a
d3plot	10,625	11/22/02	10:48a
d3plot21	6,187	11/22/02	10:48a
horizalf8v2.k	8	11/22/02	10:48a
SD9 - side impacts 200C.zip - 8deg\v20			
d3hsp	24,071	12/4/02	04:24p
d4plot	10,625	12/4/02	04:24p
d4plot21	6,187	12/4/02	04:24p
horizalf8v20.k	9	12/4/02	04:24p
SD9 - side impacts 200C.zip - 8deg\v4			
d3hsp	24,050	11/22/02	10:51a
d3plot	10,625	11/22/02	10:51a
d3plot21	6,187	11/22/02	10:51a
horizalf8v4.k	8	11/22/02	10:51a
SD9 - side impacts 200C.zip - 8deg\v6			
d3hsp	24,050	11/22/02	10:52a
d3plot	10,625	11/22/02	10:52a
d3plot21	6,187	11/22/02	10:52a
horizalf8v6.k	8	11/22/02	10:52a
SD9 - side impacts 200C.zip - horizontal\v1			
d3hsp	24,171	11/22/02	10:53a
d4plot	10,672	11/22/02	10:53a
d4plot21	6,216	11/22/02	10:53a
horizalf0v1.k	9	11/22/02	10:53a
SD9 - side impacts 200C.zip - horizontal\v10			
d3hsp	24,171	11/22/02	10:59a

Name	Size (kB)	Date	Time
d3plot	10,672	11/22/02	11:00a
d3plot21	6,216	11/22/02	10:59a
horizalf0v10.k	9	11/22/02	10:59a
SD9 - side impacts 200C.zip - horizontal\v2			
d3hsp	24,171	11/22/02	10:40a
d3plot	10,672	11/22/02	10:40a
d3plot21	6,216	11/22/02	10:40a
horizalf0v2.k	9	11/22/02	10:40a
SD9 - side impacts 200C.zip - horizontal\v20			
d3hsp	24,386	12/4/02	04:26p
d4plot	10,672	12/4/02	04:26p
d4plot21	6,216	12/4/02	04:26p

Name	Size (kB)	Date	Time
horizalf0v20.k	9	12/4/02	04:26p
SD9 - side impacts 200C.zip - horizontal\v4			
d3hsp	24,171	11/22/02	10:53a
d4plot	10,672	11/22/02	10:54a
d4plot21	6,216	11/22/02	10:54a
horizalf0v4.k	9	11/22/02	10:53a
SD9 - side impacts 200C.zip - horizontal\v6			
d3hsp	24,171	11/22/02	10:56a
d4plot	10,672	11/22/02	10:56a
d4plot21	6,216	11/22/02	10:55a
horizalf0v6.k	9	11/22/02	10:56a

ATTACHMENT VI
SELECTED STRESS FIELD PLOTS

This attachment presents the residual 1st principal stress field in a few cases studied in this calculation.

For each of the cases presented, the first figure shows the extent of the damage (red elements) in the vertical direction of the outer shell, and the second figure shows a detailed stress field in the OS-bottom lid junction. Part of the trunnion collar sleeve is added in the first figure to illustrate the vertical (axial) extension of damage. It should be noted that, for each angle and velocity, the first and the second figure present the same results, with a different focus and different stress fringe levels. In all cases, the maximum 1st principal stress is indicated in the upper left corner of the picture.

All cases are end impacts at 150 ℃. The corner showed is the corner on the impacted side.

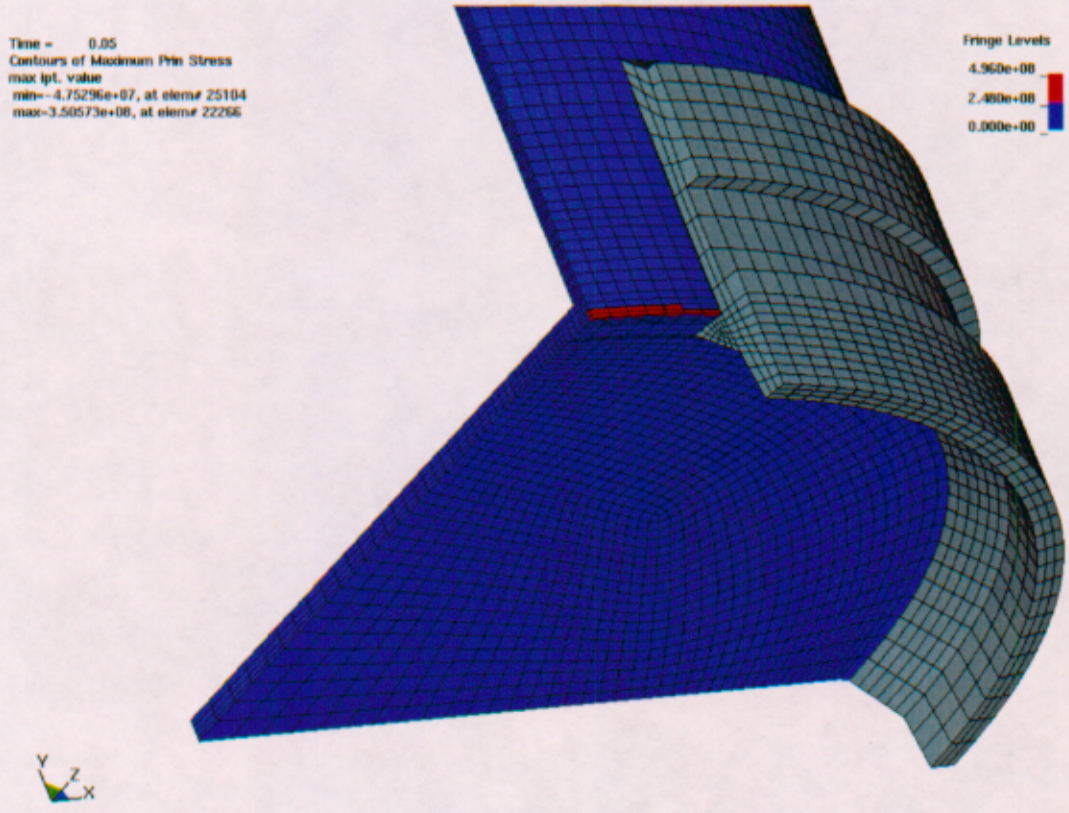

Figure VI-1: Stress in Outer shell, α=1°, v=1 *m/s*, Global View (*Pa*)

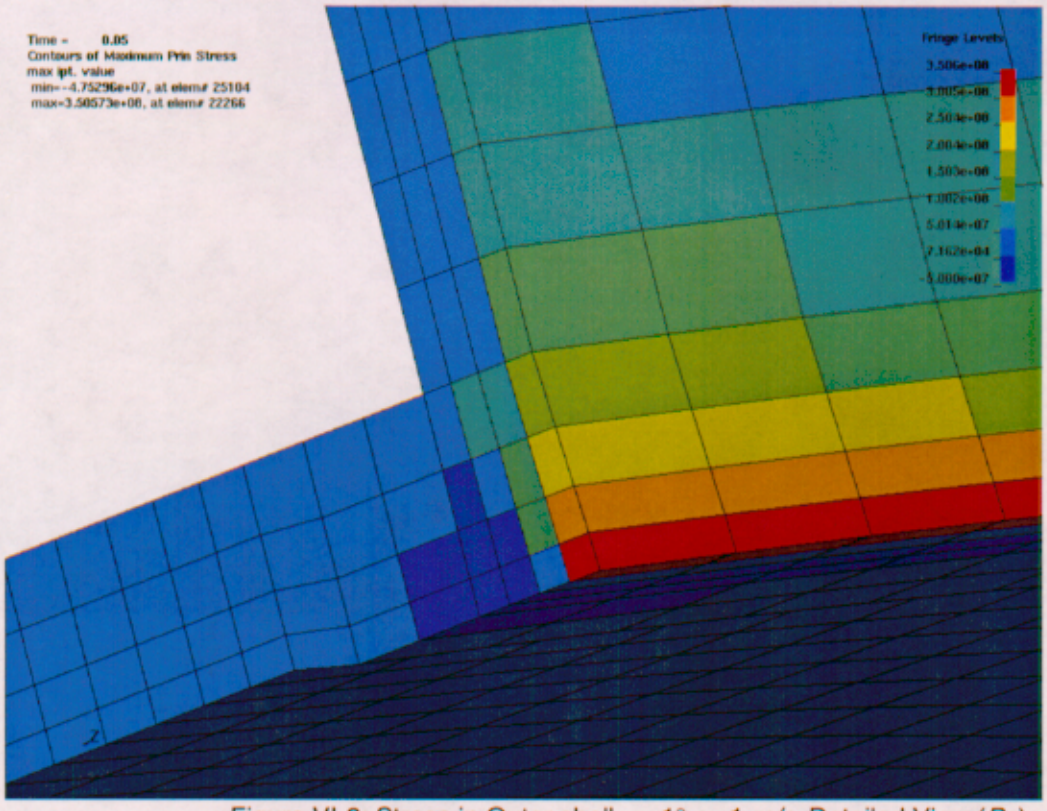

Figure VI-2: Stress in Outer shell, α=1°, v=1 *m/s*, Detailed View (*Pa*)

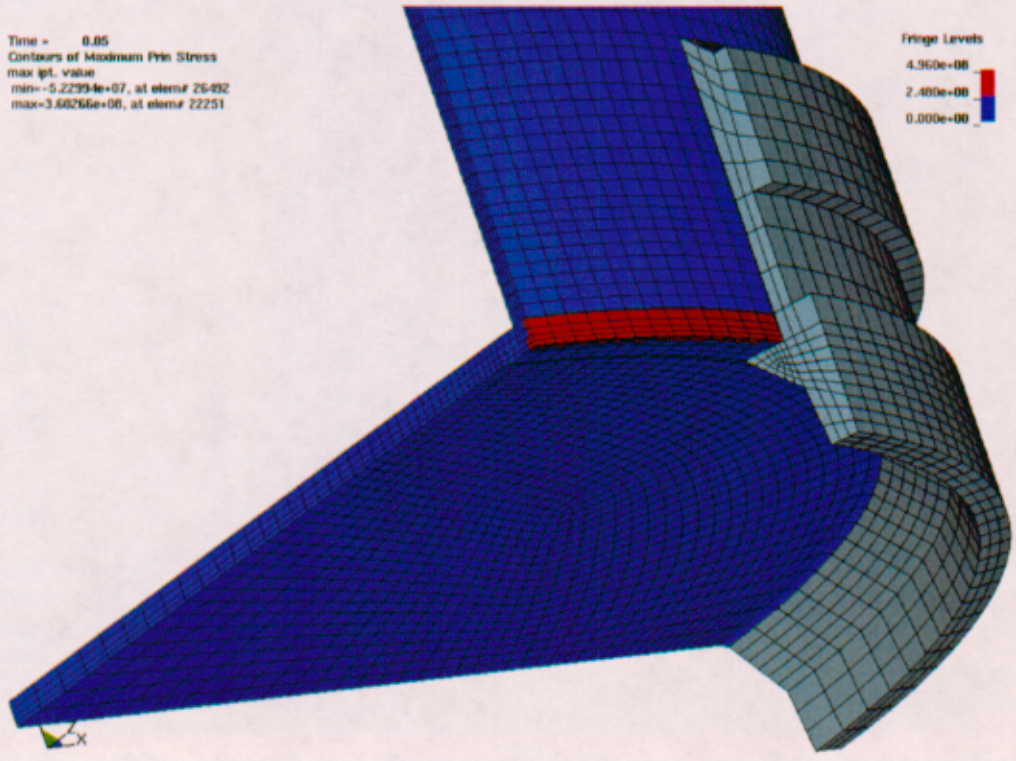

Figure VI-3: Stress in Outer shell, α=1°, v=2 *m/s*, Global View (*Pa*)

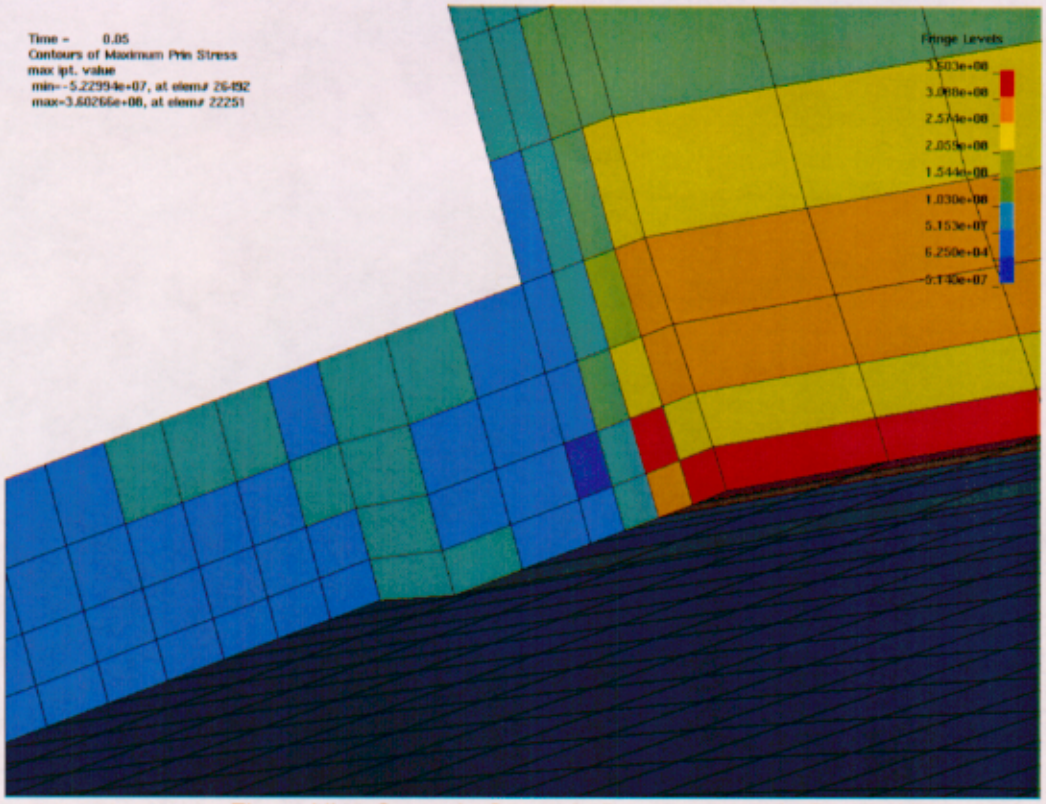

Figure VI-4: Stress in Outer shell, α=1°, v=2 *m/s*, Detailed View (*Pa*)

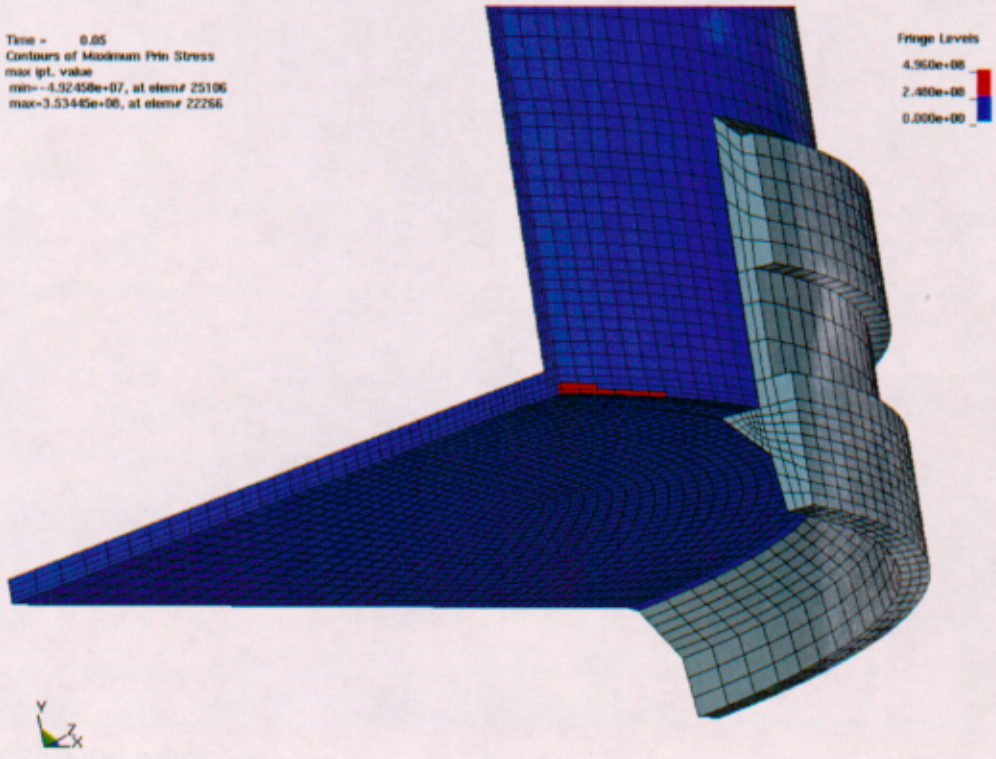

Figure VI-5: Stress in Outer shell, α=5°, v=1 *m/s*, Global View (*Pa*)

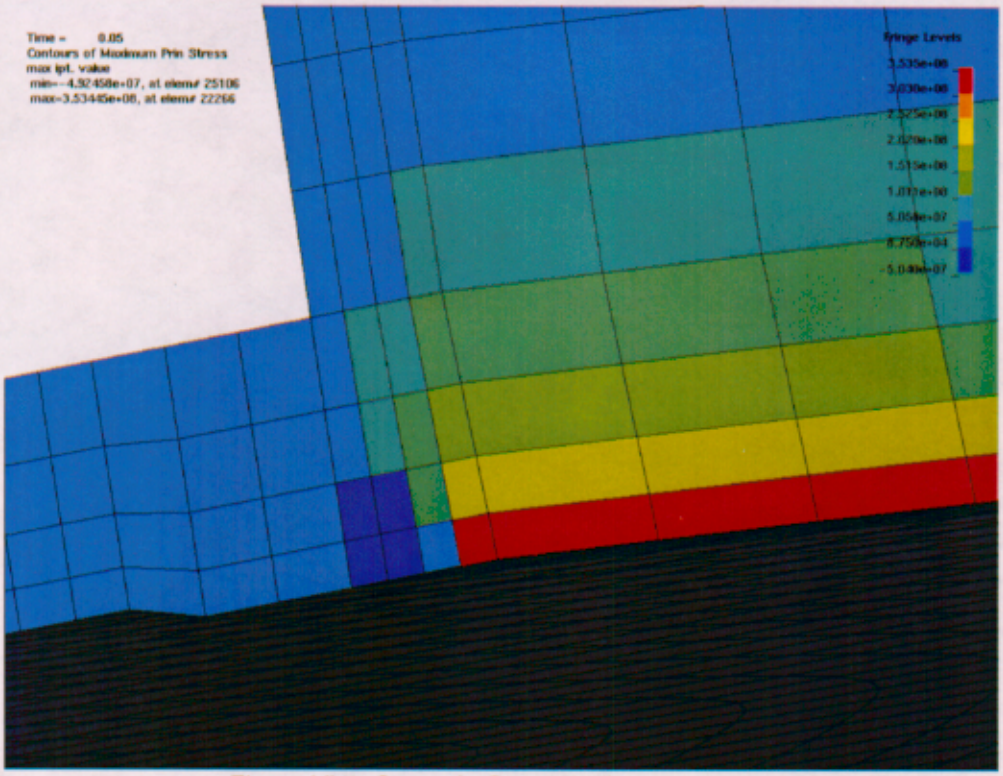

Figure VI-6: Stress in Outer shell, α=5°, v=1 *m/s*, Detailed View (*Pa*)

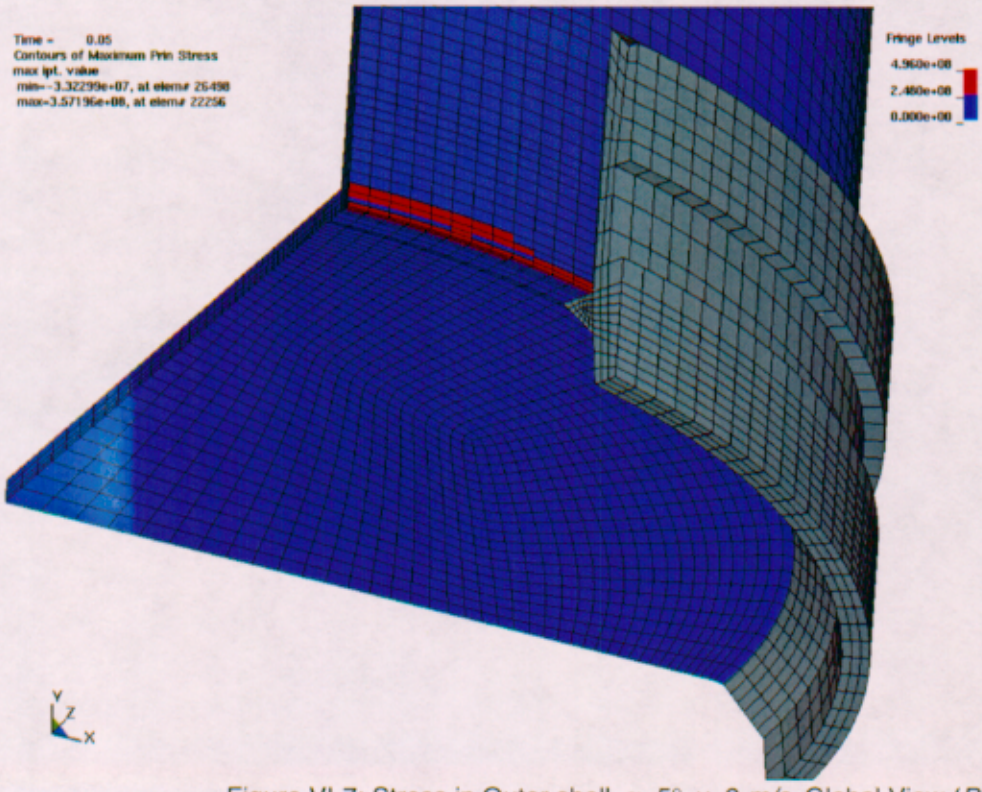

Figure VI-7: Stress in Outer shell, α=5°, v=2 *m/s*, Global View (*Pa*)

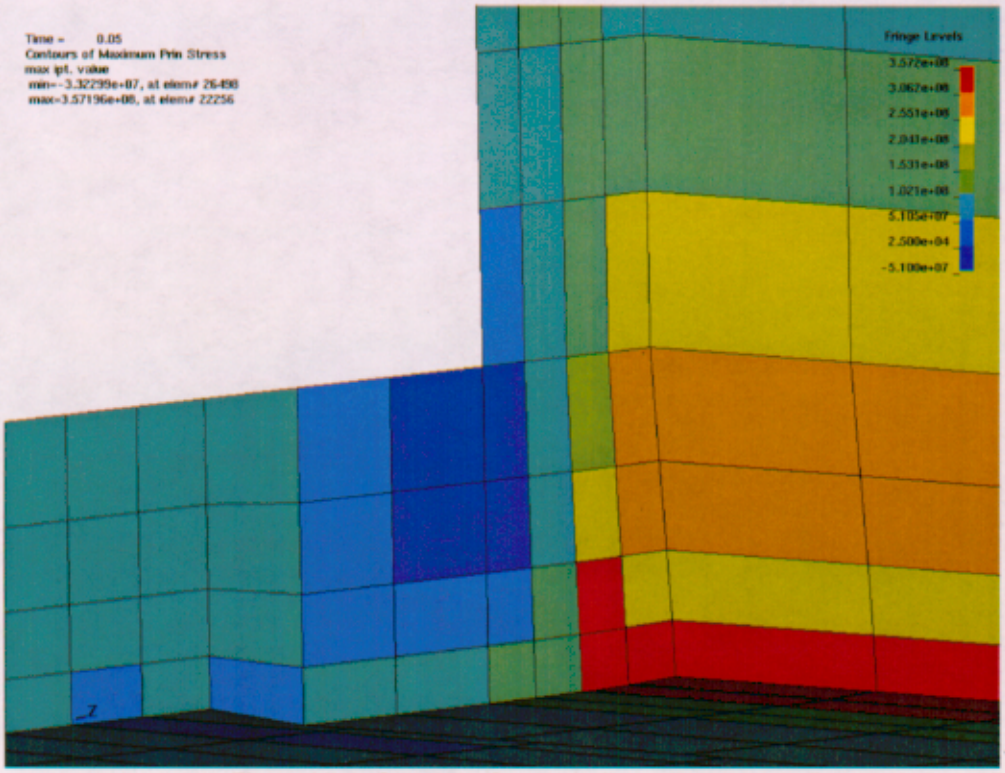

Figure VI-8: Stress in Outer shell, α=5°, v=2 *m/s*, Detailed View (*Pa*)

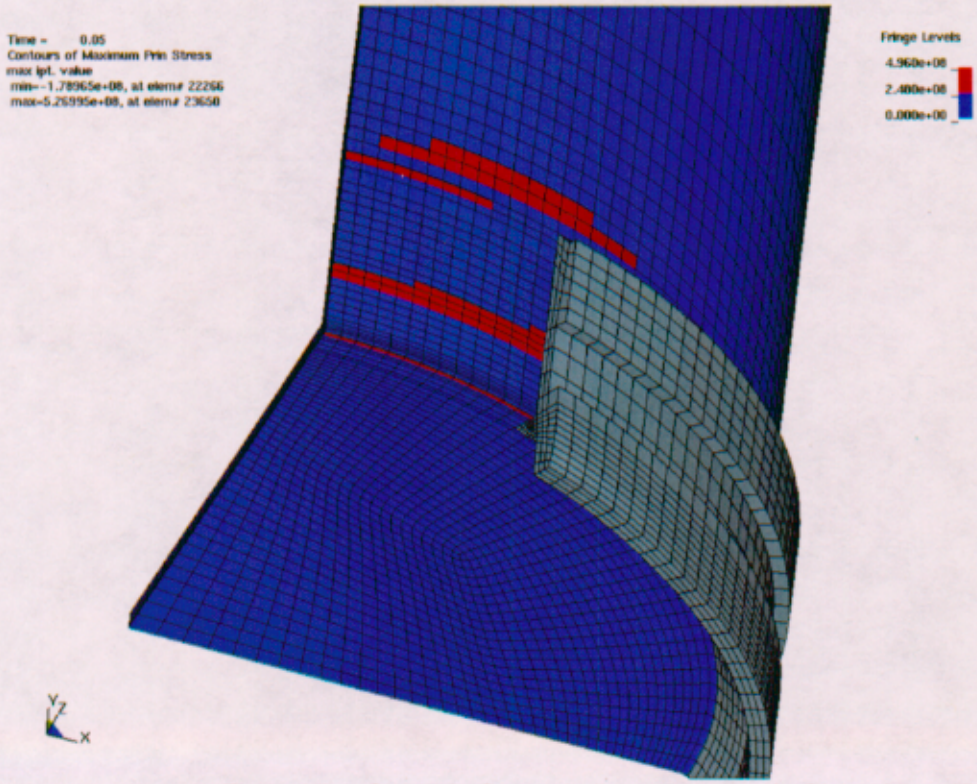

Figure VI-9: Stress in Outer shell, α=8°, v=6 *m/s*, Global View (*Pa*)

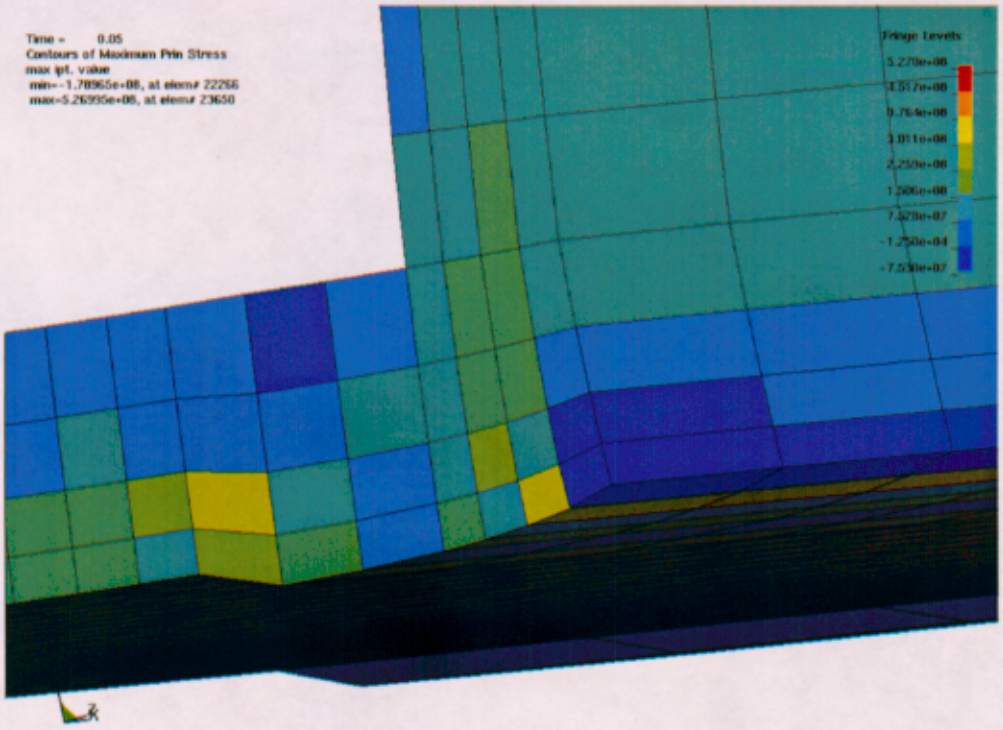

Figure VI-10: Stress in Outer shell, α=8°, v=6 *m/s*, Detailed View (*Pa*)